Title
Stockpile Drying Of Freshly Harvested Almonds

Author
Mayanja, Ismael Kilinya

Publication Date
2021

Peer reviewed|Thesis/dissertation

Stockpile Drying Of Freshly Harvested Almonds

By

ISMAEL KILINYA MAYANJA

THESIS

Submitted in partial satisfaction of the requirements for the degree of

MASTER OF SCIENCE

in

Biological Systems Engineering

in the

OFFICE OF GRADUATE STUDIES

of the

UNIVERSITY OF CALIFORNIA

DAVIS

Approved:

Irwin R. Donis-Gonzalez, Chair

Patrick H. Brown

Farzaneh Khorsandi

Committee in Charge

2021

Abstract

Pest and human pathogen infestation, irrigation management, and visible dust generation during conventional almond harvesting challenge current harvest practices. Early, off-ground harvesting is a potential solution. However, almonds harvested early contain high moisture, making them susceptible to postharvest quality deterioration if not properly dried. Thus, this research proposes stockpile drying of almonds as an alternative. Stockpile drying eliminates sweeping and picking processes of conventional windrow drying, which emit significant dust. It reduces pest and human pathogen infestation by permitting early harvesting, and doesn't interfere with irrigation timing, since it is not conducted in the almond orchard. A stockpile of 4,155 kg was dehydrated with a Stockpile Heated and Ambient air Dryer (SHAD), which uses a combination of heated and ambient air to achieve dehydration. Almonds were dehydrated for 11 days from an average dry basis moisture content (MC_{db}) equal to 12.6 % to a desired storage MC_{db} of around 6 %. However, there was non-uniformity of moisture observed throughout the stockpile attributed to the inability of the SHAD to properly distribute and deliver the drying air to the almonds. To address this, an air distributor containing 12 outlets, arranged in 4 rows with 3 outlets each was developed to enhance air distribution in the stockpile. The effect of using an air distributor as an additional component of the SHAD was evaluated with 'Nonpareil'(Np), 'Winter'(Wi), and 'Monterey'(Mo) varieties of stockpile weight equal to 4,763 kg, 2,585 kg, and 6,849 kg, respectively. All experiments were directly compared with conventional windrow drying. Drying of almonds with a combination of SHAD and air distributor achieved desirable MC_{db} (< 6 %) across all varieties in a shorter time (maximum of 7 days), compared to the previous experiment without an air distributor (11 days). On the other hand, the conventional windrow drying took longer with drying periods (up to 13.63 days), and the desired final MC_{db} was only reached during the 'Mo' experiment. Further, the

addition of the air distributor improved the specific moisture extraction rate, moisture extraction rate, and coefficient of performance by a percentage increase of 125%, 249%, and 255%, respectively. Thus, the SHAD with an air distributor can be used to directly dehydrate almonds outdoors in stockpiles and can replace conventional windrow drying of almonds.

To my father, Hajji Hassan Mayanja, thank you for your infinite love and support. And to my mother, Faridah Mayanja, you will always be my muse though you are no longer part of this world. This is dedicated to you, Mom and Dad.

ACKNOWLEDGEMENT

Firstly, I would like to thank my major advisor, Dr. Irwin Donis Gonzalez for entrusting me to undertake the project. Thank you for your encouragement and mentorship, indeed you have been a strong foundation to my research and life. Dr. Gail Bornhost, my minor supervisor for her advice especially in fulfilling the requirements towards my degree program.

I extend my appreciation to Dr.Michael Coates,co-principle investigator of the project, for his continued guidance and support which was fundamental to the structuring and accomplishment of the project deliverables. Dr. Franz Niederholzer for sharing his almond field experience and supplying the almond samples which were used for this project.

My gratitude goes to the thesis committee members; Dr. Patrick H. Brown and Dr. Farzaneh Khorsandi for their profound input, which helped improve the overall structure and content of the thesis.

I wish to convey my appreciation to Andy Cobb, whose fabrication expertise was pertinent in developing the physical prototypes of the project and to my fellow students; Laudia Anokye-Bempah, Lucine Grigoryan, Alice Mei-Wong Dien, Lucia Felix, and Carlos Humberto Orozco who assisted in field set-up of equipment and laboratory testing of the almond samples.

I thank the faculty and staff of the Department of Biological and Agricultural Engineering (BAE) for their assistance, and kindness, which provided a conducive atmosphere to conduct my research efficiently.

I am grateful to the Almond Board of California, for their financial support which was crucial to the existence and success of the project.

I am indebted to my father and eight siblings; Khassim, Abdul Karim, Hakim, Latwifah, Fahad, Wasswa, Kato and Madinah for their moral support and unconditional love that energized me throughout my degree program. Thank you, Mayanja family.

Lastly, I thank Allah the Almighty God, for His exceptional love, care, assistance and for providing me with the gift of health throughout my career.

TABLE OF CONTENTS

LIST OF FIGURES

LIST OF TABLES

CONVERSIONS FROM INTERNATIONAL SYSTEM OF UNITS (SI) TO UNITED STATES CUSTOMARY (US) UNITS

Conversion table from SI to US units			
Meters (m)	1 m	Feet (‘)	3.28’
Millimeters (mm)	1 mm	Inches (“)	0.039”
Hectares (Ha)	1 Ha	Acres	2.47 acres
Kilograms (Kg)	1 Kg	Pounds (Ib)	2.204 Ib
Grams (g)	1 g	Ounces (Oz)	0.035 Oz
Celsius (^{o}C)	O ^{o}C	Fahrenheit (^{o}F)	32 ^{o}F

CHAPTER 1

INTRODUCTION

1.1 Almonds

Almonds (*Prunus dulcis (*Miller) D.A. Webb) belong to the Rosaceae family, which includes many edible and economically important fruits such as peaches, raspberries, and apples (Potter et al., 2007; Verma, 2014). The almond tree is a deciduous tree with a height range of 4 to 10 m and an approximate trunk diameter of 300 mm. Almond leaves are lanceolate with dimensions in the range of 40 to 130 mm length, 12 to 40 mm breadth, and a petiole length of about 25 mm (Verma, 2014).

The almond fruit is a drupe that contains a thick fleshy exocarp, called the hull (Yetunde and Udofia, 2015). The leathery grey-green coated hull encloses a hard shell (hardened endocarp) containing a seed. Differently to other prunus, the seed is the edible component of the almond, making it durable and a relatively nonperishable food item (Esfrahlan et al., 2010; Verma, 2014), if properly dehydrated and stored. Figures 1.1a, b, and c show the percentage mass (including moisture) of all the almond fruit components at harvest, an almond fruit illustration, and the estimated dry basis moisture content (MC_{db}) of different components of almonds at harvest, respectively.

1.2 Origin of almonds

Browicz and Zohary, (1996) suggested that almonds were domesticated in Levant countries, which include: Lebanon, Syria, Iraq, Palestine, and Jordan. This was based on both botanical evidence that almonds were derived from wild forms of *Prunus dulcis* abundant in Levant countries and Archaeological evidence from Bronze Age sites, dated to the late part of the 3rd millennium BC. However, the most prominent evidence is that almonds originated from the arid mountainous

regions of Central Asia, based on the presence of their wild ancestors, such as *Amygdalus fenzliana* (Ladizinsky et al., 1999; Martínez-Gómez et al., 2007; Gradziel et al 2011). The latter is supported by Zeinalabedini et al (2010), who based on genetic sequencing, which showed that *A. fenzlinas* is the probable ancestor of the modern cultivated almond.

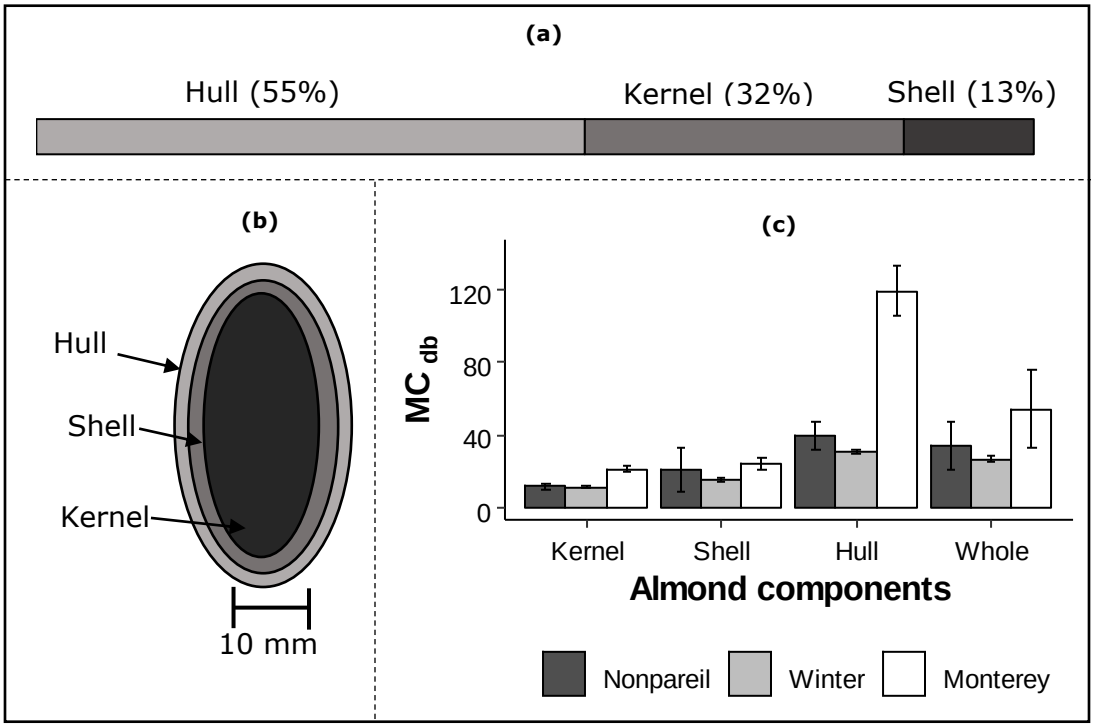

Figure 1.1:(a). Percentage mass (including moisture) of almond components at harvest; (b) Schematic representation of main components of almonds (Dingke and Fielke, 2014). Typical dimensions of a whole almond at harvest: length: 25.74 to 40.89 mm; width: 16.13 to 29.20 mm; thickness: 12.69 to 37.32 mm (Dingke and Fielke, 2014); (c) Approximate dry basis moisture content (MCdb) of different almond components at harvest recorded for 2021/2022 season from NICKELS soil laboratory Orchards (Arbuckle, California).

1.3 History of almonds in California

European varieties of almonds were the first to be planted in California in 1853 (Wickson,1889). However, they were irregular bearers because of the difference in climatic conditions from their place of origin. Subsequent trial variety testing identified the most bearing varieties and respective bearing locations (Geisseler and Horwath, 2016). In 1886, A.T. Hatch from Suisun Valley, the largest almond planter in California at the time, showcased 192 almond varieties, of which four

varieties were outstanding and selected for propagation: 'IXL','Ne-Plus Ultra', 'Nonpareil' and, 'El Supremo' (Wickson, 1889). Currently, 'Nonpareil' is the most grown almond variety in California (CDFA, 2020). Then in the early 1900s, cross-pollination with compatible and more climatic favorable varieties was established, which led to the growth of the almond cultivated land (Geisseler and Horwath, 2016; Wickson, 1921). By the 1920s, about 20,000 acres of almonds were cultivated, which grew to 100,000 acres in the 1960s (Traynor, 2017). The almond acreage quadrupled to 400,000 bearing acres by 1985 and 525,000 acres by 2001. This unprecedented increase in almond acreage was attributed to the development of value-added products such as snacks, and the increase in the irrigated area of San-Joaquin valley (Johnston, 2003). California's acreage has been increasing gradually and is currently (2020) estimated at 1,530,000 acres constituting of 1,180,000 bearing and 350,000 acres non-bearing acres (CDFA, 2020).

1.4 Almond nutritional and health attributes

Almonds are a nutrient-dense food (Richardson et al., 2009), where 100 grams is estimated to constitute 4.41g, 21.15g, 49.93g, 21.55g, and 2.97g of water, protein, total fat, carbohydrates, and ash respectively (USDA,2015). Further, the total fats of almonds are composed of 12.44g (25%) of polyunsaturated fatty acids (PUFA) and 31.55g (63%) of monounsaturated fatty acids (MUFA), which are considered to reduce the risk of heart disease (Niramitmahapanya et al., 2011; USDA, 2015). Also, total fats constitute 3.8g (8 %) saturated fatty acids, which are the lowest of all nuts (Richardson et al., 2009). Berryman et al (2015) indicated that consuming 42.5g of Almonds per day lowers levels of low-density lipoprotein cholesterol (Phung et al., 2009), maintains levels of high-density lipoprotein cholesterol, and reduces obesity. Consumption of almonds also increases the plasma concentration of polyphenols, raises total antioxidant potential in plasma, and reduces lipid peroxidation (Torabian et al., 2009). A study was carried out on 27 hyperlipidemic men and

women which concluded that consumption of almonds as a snack in the diet reduces the risk of coronary heart disease (Jenkins et al., 2002).

Other health attributes of almonds conducted by other studies include lowering postprandial glycemia, insulinemia, and oxidative stress (Jenkins et al., 2006); Improving the immune surveillance of the peripheral blood mononuclear cells towards viral infections (Arena et al., 2010); and a potential source of prebiotics, by increasing bifidobacteria and Eubacterium retractable populations and concentrations of butyrate (Mandalari et al., 2008).

1.5 World production of almonds and comparison with California

Almonds are the number one produced nut in the World, accounting for 31% of World nut production, followed by walnuts (21%), cashews (17%), pistachios (14%), and hazelnuts (12%). In the 2019/2020 season, almond production increased by 7% from the previous season and has a 26% increase for the past decade, as shown in Figure 1.2. California (USA) is the largest producer of almonds in the world with an estimate of 77 % of almonds produced (INC, 2020). Over 30 almond varieties are grown in California. 'Nonpareil' is the largest variety planted representing total planted acreage of 39% because they are easily blanched, have a smooth kernel allowing easy, blemish-free processing. 'Monterey' (15%) is the second most grown followed by 'Butte' (9%) and, 'Carmel' (8%) as shown in Figure 1.3 (CDFA, 2020). Bolling et al. (2010) stated that almond varieties have unique polyphenol profiles and the polyphenol content as the composition of almond skins. The major physical classification of almond varieties is based on shell hardness. This includes soft ('Nonpareil', 'Carmel', 'Independence', 'Aldrich'), semi-hard ('Butte', 'Fritz'), and hard shells ('Monterey', 'Padre') (ABC, 2020).

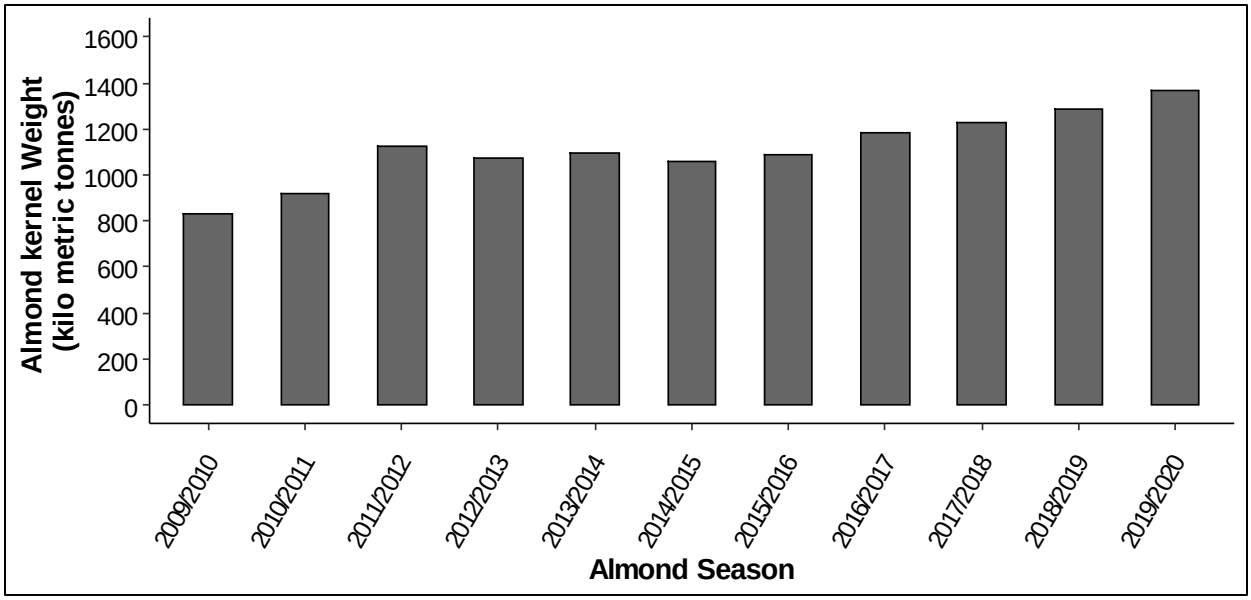

Figure 1.2: World almond production for the past decade (INC, 2020).

Australia is the second-largest producer of almonds accounting for 8% of the world market share (CDFA, 2020). The first planting of almonds in Australia was conducted in 1836 in Kangaroo Island and spread to Adelaide plains in the early 1900s, along the Murray River in the 1960s, and Sunraysia region in the 1970s. The total acreage of planted almonds has increased from 8,762 acres in 2000 to 131,000 acres in 2019, representing a 15-fold increase in 2 decades. Similar to California, 'Nonpareil' is the largest planted variety in Australia accounting for 46%, followed by Carmel (24%), Monterey (11%), and Price (8%) (ABA, 2020).

Spain accounts for 6% of the world market share (CDFA, 2020). Spanish almond production has steadily increased over the last 4 seasons reaching over 78,000 Metric Tonnes in 2019/2020 (INC,2020). The most widely produced almond varieties in Spain are 'Marcona' and 'Desmayo Largueta' (Socias et al., 2015). Turkey and Italy both account for 1% of the world share each. And the rest of the world accounts for the remaining 1%.

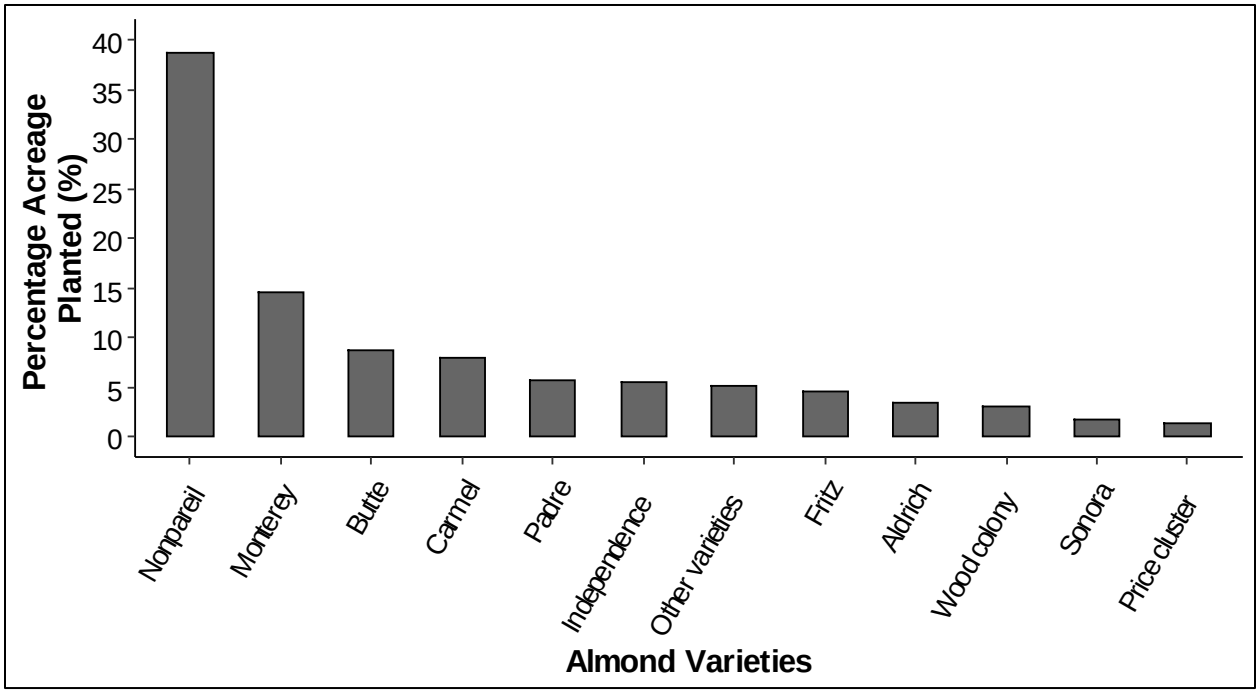

Figure 1.3: Almond varieties cultivated in California.

The USA is the world leader in almond exports, exporting 534,128 metric tonnes of shelled almonds to the European Union (49%) and Asia (27%). Further, the USA accounted for 25.7 % of almond consumption in 2018, followed by India (7.6 %), Germany (5.2 %), Spain (5.1 %), Vietnam (4.6 %), and China (3.9 %) (INC, 2020)

1.6 Almond growth life cycle

Mediterranean climate consists of mild winters with a rainy season and hot summers, which are vital to the growth of the almond. In California, the almond tree is dormant during the Winter (November to January). Thereafter, a vegetative growth phase is observed, and flower buds begin to swell towards to prepare for bloom. White and light pink flowers from the almond tree buds appear around February to mid-March, when pollination takes place (Verma, 2014; ABC, 2017). Almonds fully develop during the Spring (March to June). Almond hulls split open during the summer (July) exposing the kernel and allowing Almonds to partially dry in the tree (ABC, 2017).

The central valley is the most productive place for almonds, mainly attributed to California's almond favorable climate, soils, and irrigation supply.

1.7 Almond current harvest and drying practices

Shaking of almonds is the first step in the harvesting of almonds, which is initiated when almonds are nearing 100% hull split (Connell et al., 1996). Shaking is performed by a mechanical shaker. The working principle of the shaker is to vibrate the tree, at around 1 m height, so that the binding force between the almond fruit and the tree is broken, allowing the almonds to drop on the ground (Kepner et al.,1987). The shaking process takes about 3 seconds (s) and can vary depending on the variety. The use of mechanical shakers allows for a large-scale production, within a reasonable timeframe. However, one drawback is the damage caused on the trunks because of vigorous shaking, causing the bark to tear from the tree and therefore, further infestation with pathogens such as *Ceratocystis fimbriata*, and also resulting on insect infestation, including the Nitidulid bettle, *Carpopophilus freeman*, and the American plum borer (*Euzophera semifuneralis*). This impacts the tree's health and reduces its longevity. The damage to the trunks can be mitigated by proper maintaining of shaking equipment, and proper training of mechanical shaker operators (Connell et al., 2005).

Almonds are then left to dry on the orchard floor for up to 21 days, where they dry from a typical 10% to 20% kernel dry basis moisture content (MC_{db}) to an industry storage standard of 6% MC_{db} or less. Drying is imperative as it increases almond shelf life and reduces their susceptibility to developing molds, rancidity (Chilka and Ranade, 2018), and concealed damage (Reil et al., 1996).

The dried almonds are then swept into a windrow, parallel to the almond tree rows by a large mechanical sweeper that uses a cylindrical sweeper head with rubber or metal tines, and a blower that often generates significant dust (Faulkner and Capered, 2012). Almonds are then picked up

from the windrows on the orchard floor by mechanical pickers with considerable dust and transported to the hulling and shelling facility as described in Figure 1.4. According to Buchner et al., (2019), the estimated operation cost for harvesting, sweeping and picking-up almonds in an acre of land is $ 128, $ 72, and $ 48 respectively.

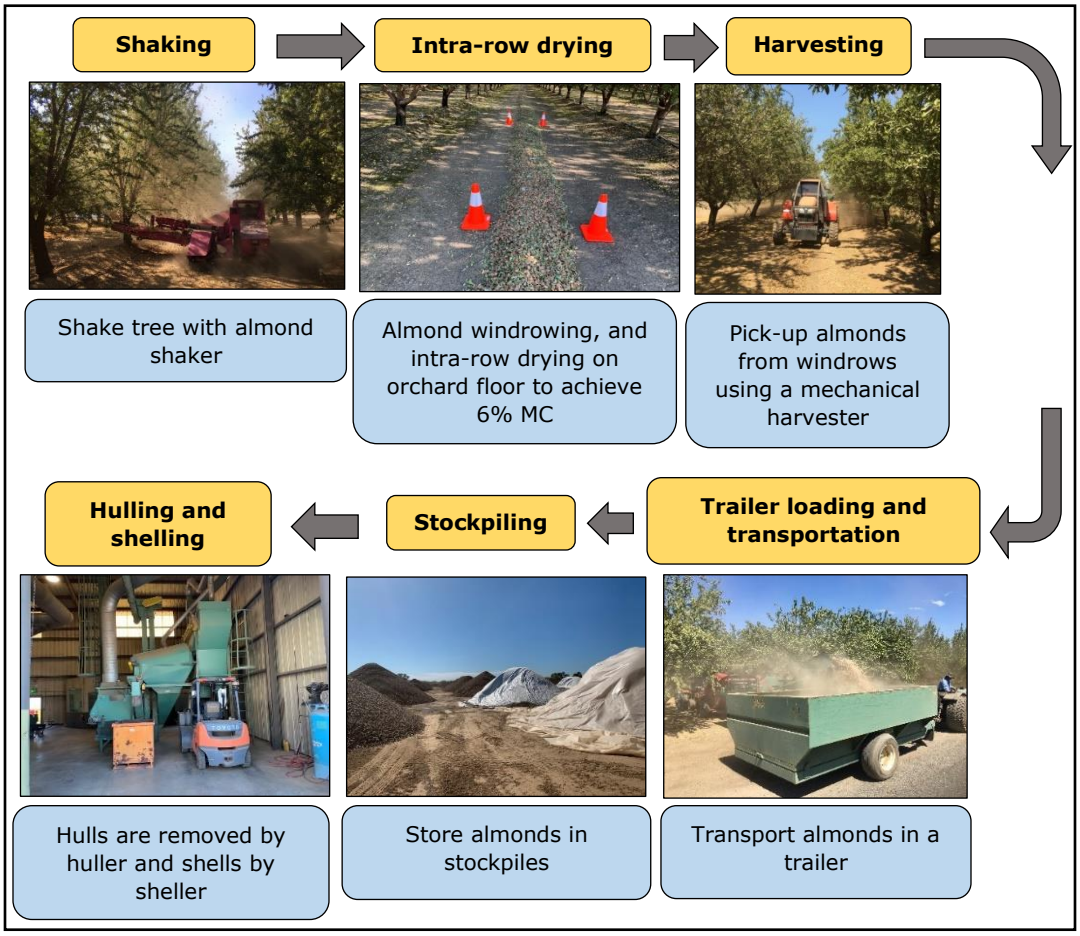

Figure 1.4: Flow diagram showing post-harvest handling steps currently applied by almond growers in the United States

On the other hand, a minority of almond growers in California dry almonds with a combination of natural windrow drying for about 3 to 7 days and mechanical drying in an almond bin stadium dryer, using heated air at 50 ^{o}C for about 2 days. Figure 1.5 exemplifies typical kernel MC_{db} from measurements performed during the 2019/2020 harvesting season when using a combination of windrow and bin drying. Dehydrating almonds in bins are associated with uniform drying and

ensure better almond quality since drying conditions can be controlled. Also, almonds are hulled before dehydrated in bins which permits drying larger volumes in comparison to windrow drying. Additionally, drying of almonds in bins is not affected with weather conditions such as rain, and wind gusts. However, drying almonds with a combination of windrow drying and bin drying is not broadly popular, since it involves a second stage of drying (bin drying), demanding additional labor and a high initial investment cost.

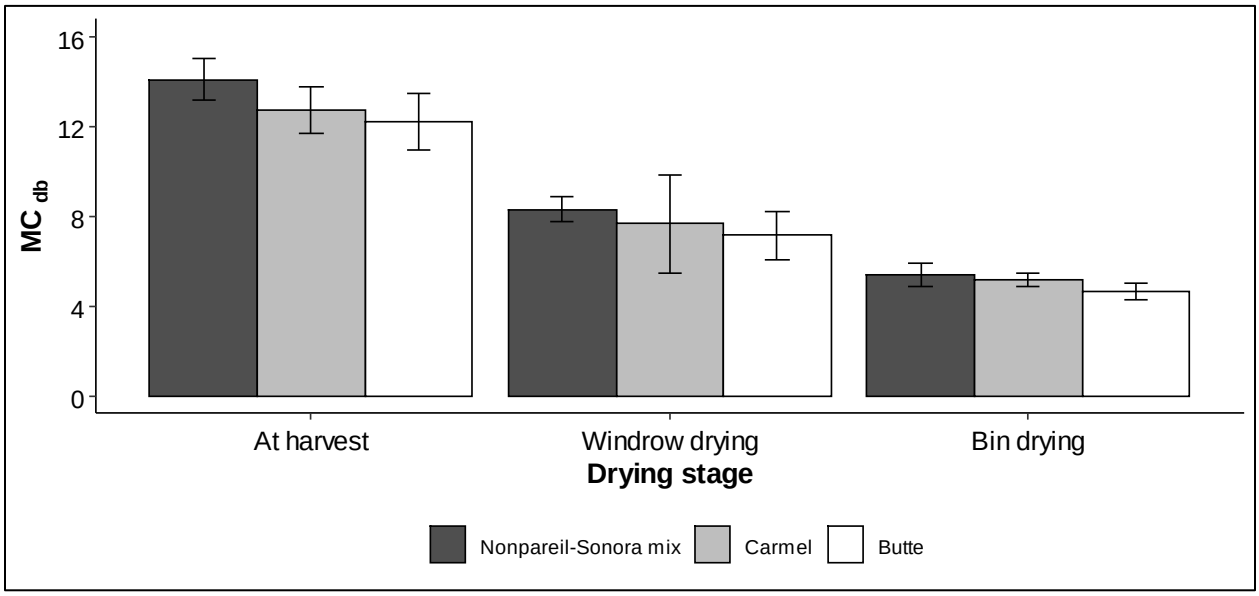

Figure 1.5: Kernel MCdb recorded in 2019 of almond dried by both windrow and bin drying.

1.8 Problem statement

Conventional almond harvesting is associated with pest and human pathogen infestation, irrigation management, and visible dust generation, which affect current harvest timing and method.

Windrow drying (current drying almond drying technique) involves dust emission processes such as pickup process that generates dust as the pickup machine removes dirt, dust, leaf, and other trash from the windrow materials using a suction fan that discharges into the almond orchard (Downey et al., 2008). More specifically, CARB (2017) reported that shaking, sweeping, and

pickup of almonds from the ground accumulates nearly 14.15 kg of microscopic dust particles (PM_{10}) when 1 acre of almonds is harvested, which translates to 16.7 million kg of PM_{10}. Based on 2019 California acreage of approximately 1,180,000 acres (CDFA, 2020). In 2019, the Almond Board of California (ABC) set a goal to reduce 50% of dust accumulated during the almond harvest by 2025 (ABC, 2020). Reducing dust in the almond industry can range from addressing the steps that create most of the visible dust such as sweeping into windrows and pick-up, all the way to dust-less (no soil contact) harvesting, challenging every step in the harvesting process**.** Also, the existing natural process of sun-drying almonds in the orchard is compromised if it rains or during periods of high humidity. The previous calls for the need for a high-volume mechanical method of drying, which if appropriately developed, will potentially lead to overall improvements in efficiency and cost reduction for the almond industry.

Additionally, Birds (mainly scrub jays) and rodents consume the nuts (Perry et al., 1989), and infestation of navel orange worm (NOW) (*Amyelois transitella*) (Johnson, 2013), which is the most common almond pest (Markle et al, 2016). In addition to a loss in revenue, the NOW leads to kernel damage, webbing, and frass, which degrade almond quality, and increasing the likelihood for mycotoxins development, including Aflatoxin B (Schatzki and Ong, 2001). Also, exposing almonds to the orchard ground, and water due to irrigation may lead to quality degradation and contamination with microorganisms including human pathogens, such as *Salmonella Enteritidis* (Martha et al, 2012).

Further, delays in postharvest irrigation, which is a common practice due to the conventional windrow drying method can lead to significant yield loss. Previous research demonstrated that postharvest almond irrigation is one of the most important water applications that depend on

preharvest irrigation practices, can reduce next season's yield by as much as 77% (Goldhamer and Viveros, 2000).

Early, off-ground harvesting is a potential solution but requires additional mechanical drying. Harvesting almonds 2 to 3 weeks before the typical harvest date has no perceptible effect on kernel quality. In addition, the early harvest of almonds can help mitigate the damage of pests, including the NOW (Curtis et al., 1984; Cornel et al, 1989). However, almonds harvested at an early stage contain high moisture (around 30% MC_{db} or more), which makes them prone to the development of molds and insect attack if conventionally sun-dried on the orchard ground. Therefore, an alternative drying technique would be beneficial to the almond industry. Nonetheless, the implementation and adoption of alternative drying methods are hindered by the lack of feasible mechanical dryers, which need to be further evaluated.

1.9 Objectives of this study

A common practice during almond harvest is to stockpile almonds in the open, outside, and adjacent to the orchard or huller, after drying. However, moist almonds cannot be stockpiled since they are susceptible to degradation, as previously described. Therefore, the objectives of this study were to:

i) Develop aeration parameters for stockpile drying of almonds to dehydrate in-hull almonds from different initial moisture contents (10 – 25 % kernel MCdb) to proper hulling and storage dry condition at or below 6% MCdb (chapter 2).

ii) Develop an air distribution system to enhance uniformity of the aeration parameters in the almonds stockpile (Chapter 3)

iii) Compare almond drying conditions and results between current windrow drying, and the newly developed stockpile dryer. Comparison will be based on final kernel MCdb, drying time, and quality parameters including mold content, decay injury, insect damage, internal cavities, color, and rancidity (Oils stability induction time, peroxide value, and free fatty acid content) (Chapter 4).

References

Arena A, Bisignano C, Stassi G, Mandalari G, Wickham MS, Bisignano G. Immunomodulatory and antiviral activity of almond skins. Immunol Lett. 2010 Aug 16;132(1-2):18-23. doi: 10.1016/j.imlet.2010.04.010. Epub 2010 May 11. PMID: 20438761.

ABA. Almond Board of Australia (2020). Australian Almonds. Retrieved from https://australianalmonds.com.au/wp-content/uploads/2020/08/2020_Almond_Insights.pdf

ABC. Almond Board of California. (2020). Almond Varieties and Selections Evaluation of National and International Varieties or Selections Under Development.

ABC. Almond Board of California. (2017). Almond Lifecyle. Retrieved from https://www.almonds.com/why-almonds/almond-lifecycle

Berryman, C.E., A.G. Preston, W. Karmally, R.J. Deckdelbaum and P. M. Kris-Etherton, 2011. Effects of almond consumption on the reduction of LDL-cholesterol: a discussion of potential mechanisms and future research directions". Nutrition Reviews, 69(4): 171-85.

Bolling, B., Dolnikowski, G., Blumberg, J., Chen, C-Y.O., 2010. Polyphenol content and antioxidant activity of California almonds depend on cultivar and harvest year. Food Chemistry 122, 819–825.

Browicz, K., Zohary, D. The genus Amygdalus L. (Rosaceae): Species relationships, distribution and evolution under domestication. Genet Resour Crop Evol 43, 229–247 (1996). https://doi.org/10.1007/BF00123275

Buchner.R.P., Niederholzer.F., Jarvis-Shean.K.S., Lightle, D. M., Symmes.E.J., D. A., Milliron.L., Steward.D. (2019). Sample Costs To Establish an Orchard and Produce Almonds. University of California Agriculture and Natural Resources Cooperative Extension Agricultural Issues Center.Retrieved from https://coststudyfiles.ucdavis.edu/uploads/cs_public/67/b7/67b72c81-5ce0-4462-a396-fbb62ce8564e/2019sacvalleyalmonds.pdf

CARB. (2017). Agricultural harvest operations. California Air Resources Board: Emission Inventory Source Category. Retrieved from https://ww3.arb.ca.gov/ei/areasrc/fullpdf/full7-5_2017.pdf

CDFA. (2020). California almond acreage report. California Department of Food and Agriculture. Retrieved from https://www.nass.usda.gov/Statistics_by_State/California/Publications/Specialty_and_Other_Releases/Almond/Acreage/202004almac.pdf

Chilka, A. G., & Ranade, V. V. (2018). Drying of almonds I: Single particle. Indian Chem. Eng., 60(3), 232-254. https://doi.org/10.1080/00194506.2017.1333464

Connell, J.H., J.M. Labavitch, G.S. Sibbett, W.O. Reil, W.W. Barnett, C. Heintz. 1989. Early harvest of almonds to circumvent late infestation by navel orangeworm. J. Amer. Soc. Hort. Sci. 114(4):595-599

Connell, J. H., Sibbett, G. S., Labavitch, J. M., & Freeman, M. W. (1996). Preparing for harvest. In W. Micke (Ed.), Almond production manual (UC ANR Publ. No 3364) (pp. 254-259). Oakland: University of California Agricultural and Natural Resources.

Connell J.H., van Steenwyk R.A., Gubler W.D. Almond trunk injury treatment following bark damage during shaker harvest. In : Oliveira M.M. (ed.), Cordeiro V. (ed.). XIII GREMPA Meeting on Almonds and Pistachios . Zaragoza : CIHEAM, 2005. p. 199-202

Curtis, C. E., Curtis, R. K., Andrews, K. L. (1984). Progression of Navel Orangeworm (Lepidoptera: Pyralidae) Infestation and Damage of Almonds on the Ground and on the Tree During Harvest. Environmental Entomology, 13(1), 146–149. https://doi.org/10.1093/ee/13.1.146

Dingke, Z., & Fielke, J. (2014). Some physical properties of Australian nonpareil almonds related to bulk storage. Int. J. Agric. Biol. Eng., 7(5), 116-122.

Downey, D., Giles, D. K., & Thompson, J. F. (2008). In situ transmissiometer measurements for real-time monitoring of dust discharge during orchard nut harvesting. JEQ, 37(2), 574-581. https://doi.org/10.2134/jeq2006.0423

Esfahlan, A. J., Jamei, R., Esfahlan, R. J. (2010). The importance of almond (Prunus amygdalus L.) and its by-products. Food Chemistry, 120(2), 349–360. https://doi.org/10.1016/j.foodchem.2009.09.063

Faulkner, W. B., & Capareda, S. C. (2012). Effects of sweeping depth on particulate matter emissions from almond harvest operations. Atmospheric Pollution Res., 3(2), 219-225. https://doi.org/10.5094/APR.2012.024

Goldhamer, D. A., Viveros, M. (2000). Effects of preharvest irrigation cutoff durations and postharvest water deprivation on almond tree performance. Irrigation Science, 19(3), 125–131. https://doi.org/10.1007/s002710000013

Gradziel, T.M. (2011). Origin and dissemination of almond. In: Horticultural Reviews (edited by J. Janick). Pp. 23– 81. Hoboken: John Wiley & Sons, Inc.

Geisseler, D., Horwath, W. R. (2016). Almond Production in California. Fertilizer Research and Education Program, 1–3. Retrieved from https://apps1.cdfa.ca.gov/FertilizerResearch/docs/Almond_Production_CA.pdf

INC. (2020). Nuts and dried fruits. Statistical yearbook 2019/2020. International Nut, and Dried Fruit Council. Retrieved from https://www.nutfruit.org/files/tech/1587539172_INC_Statistical_Yearbook_2019-2020.pdf

Jenkins DJ, Kendall CW, Josse AR, Salvatore S, Brighenti F, Augustin LS, Ellis PR, Vidgen E, Rao AV. Almonds decrease postprandial glycemia, insulinemia, and oxidative damage in healthy individuals. J Nutr. 2006 Dec;136(12):2987-92. doi: 10.1093/jn/136.12.2987. PMID: 17116708.

Jenkins, D. J. A., Kendall, C. W. C., Marchie, A., Parker, T. L., Connelly, P. W., Qian, W., … Spiller, G. A. (2002). Dose response of almonds on coronary heart disease risk factors: Blood lipids, oxidized low-density lipoproteins, lipoprotein(a), homocysteine, and pulmonary nitric

oxide: A randomized, controlled, crossover trial. Circulation, 106(11), 1327–1332. https://doi.org/10.1161/01.CIR.0000028421.91733.20

Johnston, W.E., 2003. Cross sections of a diverse agriculture: profiles of California's agricultural production regions and principal commodities. In Siebert, J. (Ed.) California Agriculture: Dimensions and Issues. pp. 29-55.

Kepner, R. A., R. Bainer and E. L. Barger, 1987. Farm Machinery, CBS Publishers and Distributors, Daya Basti, Delhi.

Ladizinsky, G. On the Origin of Almond. Genetic Resources and Crop Evolution 46, 143–147 (1999). https://doi.org/10.1023/A:1008690409554

Mandalari G, Nueno-Palop C, Bisignano G, Wickham MS, Narbad A. Potential prebiotic properties of almond (Amygdalus communis L.) seeds. Appl Environ Microbiol. 2008 Jul;74(14):4264-70. doi: 10.1128/AEM.00739-08. Epub 2008 May 23. PMID: 18502914; PMCID: PMC2493170.

Markle, J. C., Niederholzer, F. J. A., Zalom, F. G. (2016). Evaluation of spray application methods for navel orangeworm control in almonds. Pest Management Science, 72(12), 2339–2346. https://doi.org/10.1002/ps.4279

Martha A.K, Harbir. K, Luxin. W, Michelle D.D, LINDA J. H; Survival of Salmonella, Escherichia coli O157:H7, and Listeria monocytogenes on Inoculated Almonds and Pistachios Stored at −19, 4, and 24°C. J Food Prot 1 August 2012; 75 (8): 1394–1403. doi: https://doi.org/10.4315/0362-028X.JFP-12-023

Martínez-Gómez P., Sánchez-Pérez R., Dicenta F., Howad W., Arús P., Gradziel T.M. (2007) Almond. In: Kole C. (eds) Fruits and Nuts. Genome Mapping and Molecular Breeding in Plants, vol 4. Springer, Berlin, Heidelberg. https://doi.org/10.1007/978-3-540-34533-6_11

Moreira, R. G., & Bakker-Arkema, F. W. (1989). Moisture desorption model for nonpareil almonds. J. Agric. Eng. Res., 42(2), 123-133. https://doi.org/10.1016/0021-8634(89)90045-0

Niramitmahapanya, S., Harris, S. S., Dawson-Hughes, B. (2011). Type of dietary fat is associated with the 25-hydroxyvitamin D 3 increment in response to vitamin D supplementation. Journal of Clinical Endocrinology and Metabolism, 96(10), 3170–3174. https://doi.org/10.1210/jc.2011-

1518

Perry, E., Sibbett, G. S. (1998). Harvesting and Storing Your Home Orchard ' s Nut Crop : 8005, 1–9. Retrieved from http://homeorchard.ucdavis.edu/8005.pdf

Phung, O. J., Makanji, S. S., White, C. M., Coleman, C. I. (2009). Almonds Have a Neutral Effect on Serum Lipid Profiles: A Meta-Analysis of Randomized Trials. Journal of the American Dietetic Association, 109(5), 865–873. https://doi.org/10.1016/j.jada.2009.02.014

Potter, D., Eriksson, T., Evans, R. C., Oh, S., Smedmark, J. E., Morgan, D. R.,... Campbell, C. S. (2007). Phylogeny and classification of Rosaceae. Plant Systematics Evolution, 266(1), 5-43. https://doi.org/10.1007/s00606-007-0539-9

Richardson, D. P., Astrup, A., Cocaul, A., Ellis, P. (2009). The nutritional and health benefits of almonds: a healthy food choice. Food Science & Technology Bulletin: Functional Foods, 6(4), 41–50. https://doi.org/10.1616/1476-2137.15765

Reil, W., Labavitch, J., & Holberg, D. (1996). Harvesting. In W. Micke (Ed.), Almond production manual (UC ANR Publ. No.3364) (pp. 260-264). Oakland: University of California, Agricultural and Natural Resources.

Torabian, S., Haddad, E., Rajaram, S., Banta, J. and Sabate, J. (2009) Acute Effect of Nut Consumption on Plasma Total Polyphenols, Antioxidant Capacity and Lipid Peroxidation. Journal of Human Nutrition and Dietetics, 22, 64-71.
http://dx.doi.org/10.1111/j.1365-277X.2008.00923.x

Traynor, J (2017) A History of Almond Pollination in California, Bee World, 94:3, 69-79, DOI: 10.1080/0005772X.2017.1353273

Schatzki, T. F., Ong, M. S. (2001). Dependence of aflatoxin in almonds on the type and amount of insect damage. Journal of Agricultural and Food Chemistry, 49(9), 4513–4519. https://doi.org/10.1021/jf010585w

Socias, R., Kodad, O., Alonso, M. (2015). The introduction of new almond cultivars in spanish almond growing, 50(11), 1726–1728.

U.S. Department of Agriculture, Agricultural Research Service, Nutrient Data Labratory. USDA National Nutrient Database for Standard Reference, Release 28. Version Current: September 2015. http://www.ars.usda.gov/nea/bhnrc/ndl.

Wickson, E.J. 1889. The California fruits and how to grow them. 1st Edition. Dewey & Co. Pacific Rural Press, San Francisco, CA

Wickson, E.J. 1921. The California fruits and how to grow them. 9th Edition. Pacific Rural Press, San Francisco, CA

Verma, M. K. (2014). Almond production technology. Training manual on teaching of post-graduate courses in horticulture (fruit science). 274-280. Retrieved from https://www.researchgate.net/publication/282365926

Yetunde, A. E., & Udofia, U. S. (2015). Nutritional and sensory properties of almond (Prunus amygdalu Var. Dulcis) seed milk. World J. Dairy Food Sci., 10(2), 117-121.

Zeinalabedini, M., Khayam-Nekoui, M., Grigorian, V., Gradziel, T.M., Martínez-Gómez, P., 2010. The origin and dissemination of the cultivated almond as determined by nuclear and chloroplast SSR marker analysis. Scientia Horticulturae 125, 593–601. doi:10.1016/j.scienta.2010.05.007

CHAPTER 2

DEVELOPMENT OF A STOCKPILE HEATED AND AMBIENT AIR DRYER (SHAD) FOR FRESHLY HARVESTED ALMONDS

Abstract

Pest and human pathogen infestation, irrigation management, and dust generation during conventional almond harvesting are challenging current harvest timing and method. Early, off-ground harvesting is a potential solution. However, almonds harvested early contain high moisture, making them susceptible to postharvest quality deterioration, if not properly dried. Therefore, an appropriate mechanical drying technique would be beneficial to the almond industry. The study aimed at developing a stockpile heated, and ambient air dryer (SHAD) to determine the feasibility of dehydrating almonds (Var. 'Monterey'). A stockpile containing 4,155 kg of almonds was created and almonds were dehydrated from their initial 12.6% almond kernel dry-basis moisture content (MC_{db}) to final MC_{db} of 6.04%. Drying was achieved as a combination of heated air at a temperature of 55°C in the drying plenum with airflow of 0.078 m^3/s per m^3 of fresh almonds, and ambient air at 18.47 ^oC. After drying, almond quality parameters were measured, including damage by molds or decay, insect injury, and presence of internal cavities. Drying energy consumption, cost, and performance indicators were also determined. The differences in MC_{db} between the bottom, middle, and top layers of the almond stockpile were significant ($p \leq 0.05$). Post-hoc Tuckey test was conducted which indicated that the MC_{db} in the top layer was significantly lower than that in the middle and bottom layers. Results showed that damage by molds or decay, insect injury, and internal cavities were 1.81%, 0%, and 1.77%, respectively, after drying. Therefore, the overall almond quality was not compromised. The drying process cost $11.65 per tonne of the initial weight of almonds with a Specific Moisture Extraction Rate (SMER) of 0.64 kg/kWh, Moisture Extraction Rate (MER) of 1.02 kg/h, and a Coefficient of Performance (COP) of 1.33. Comparison with other dryers in the literature shows that SMER and MER were within limits. However, a low COP was observed.

Keywords. *Dust, Energy, Postharvest, Stockpile drying, Tree nuts.*

1.0 Introduction

Pest and human pathogen infestation, irrigation management, and dust generation during conventional almond harvesting are challenging current harvest timing and method. Early, off-ground harvesting and dehydrating almonds in a stockpile is a potential solution. This allows harvesting before the pest and human pathogen attack, permits timely irrigation since drying is not conducted in the almond orchard, and eradiates sweeping and picking process of windrow drying which cause significant dust.

A stockpile is normally referred to as a large quantity of goods or produce held in one place either for temporary storage or reserve (Simpson and Weiner, 1989). It is a common practice of rice and corn farmers to stockpile the grain before loading it to the bins for drying and storage. On contrary, almond growers prefer to store almonds in stockpiles rather than using bins due to the infrastructure requirement, high initial cost, and maintenance involved in the bins. However, moist (freshly harvested) almonds cannot be stockpiled since they are more susceptible to mold growth and the development of aflatoxins due to the favorable conditions for fungal growth (Ding et al., 2015; Kumar et al., 2021). Therefore, almonds are first dehydrated in windrows then transferred to the stockpiles for storage. Drying large quantities of almonds in a stockpile with a negligible risk to post harvest quality deterioration is only possible with aeration. This involves passing large volumes of air through the almond mass using a fan normally referred as mechanical aeration (Calderon, 1972). One form of mechanized aeration is passing ambient air to the almonds, this involves using solar heat in terms of thermal energy to directly dry the almonds (Wang et al., 2016). However, ambient aeration is unreliable due to its limitation to only daytime, uncertainty, and variability due to weather such as in rainy days. Heated mechanized aeration is the other form of aeration, which involves the use of heated air generated by the heater then passed to the almonds

to achieve dehydration (Kunze, 1979; Overhults et al, 1973; Waewsak et al., 2006). Heated mechanized aeration is reliable, not limited to daytime but incurs a higher operating cost of either gas, fuel or electricity depending on the power mechanism used. Thus, there is a need for a stockpile aeration system that leverages the solar heat when available and supplements it with heated air

Therefore, the objective of this study was to develop an outdoor stockpile heated and ambient air dryer (SHAD) to determine the feasibility of dehydrating almonds (Var. '*Monterey*') in a stockpile adjacent to a commercial almond orchard. To assess this concept, an almond stockpile containing an initial mass of 4,155 kg was built and dehydrated from its initial 12.6 ± 1.6% MC_{db} to the desired storage conditions equal to or less than 6% MC_{db}. Kernel damage by molds or decay, insect injury, and the presence of internal cavities were the quality parameters tested for both freshly harvested and dried almond samples. Then the energy efficiency, energy cost, and dryer performance indicators of the stockpile dryer were calculated and compared with other dryers.

2.0 Materials and methods

2.1 Sample preparation

Fresh '*Monterey*' almonds were harvested from Nickels Soil Laboratory (Arbuckle, Calif.) nearing 100% hull split and swept into a windrow by a Flory Model 7630 sweeper (Flory Industries, Salida, Calif.). Almonds were picked up using a Flory 480 PTO harvester (Flory Industries, Salida, Calif.) powered by a Kubota M108 tractor (Kubota Tractor Co., Grapevine, Tex.) and transferred to a conveyor cart (Jesse Manufacturing Co., Chico, Calif.). Immediately after pickup, experimental samples were collected from the conveyor cart using a plastic container, which carried about 2 kg of almonds and were placed in a labeled sample mesh bag. Almond collection was repeated to yield a total of 42 samples. Twelve samples were immediately transported to the Postharvest

Engineering Laboratory at the University of California (UC) Davis (Davis, Calif.) to test for initial moisture content and quality parameters. A wireless data logger (El-USB-2, Lascar Electronics Co., Erie, Pa.) that recorded temperature (T), relative humidity (RH), and dew point temperature every 5 min was placed in each of the remaining samples (30). These were used to monitor the drying process within the stockpile. Each data logger was roughly placed in the center of each sample mesh bag and fully covered with almonds to shield it from the environment.

2.2 Drying Equipment (Portable Infield Almond Dryer)

A mobile stand-alone drying system used for the stockpile drying experiment was built at the Biological and Agricultural Engineering (BAE) fabrication shop at UC Davis (Figs. 2.1a and b). The drying system consists of the following components: 1) a 9.72 hp dual powered (propane and gasoline) generator (Model 100297, Champion Global Power Equipment, Santa Fe Springs, Calif.); 2) a 2 hp propane heated vane axial fan with a 457.20 mm diameter outlet (Sukup Manufacturing Co., Sheffield, Iowa); 3) a 2.13 m × 1.52 m × 0.30 m air distribution plenum built from 28.70 mm thickness plywood; 4) a 1.22 m height × 1.83 m carbon steel diamond-shaped expanded metal A-frame with 3.05 mm (0.12 in.) overall thickness, openings of 42.93 mm × 14.22 mm, strand thickness of 4.06 mm, and strand width of 3.05 mm ; 5) high temperature rigid 304 stainless steel duct hoses of 152.40 mm diameter to connect the fan to the plenum, and the plenum to the A-frame. A pressure sensor (Series MS Magnesense, Dwyer Instruments Inc, Michigan City, Ind.) was used to record pressure in the drying plenum.

A rechargeable battery operated weather station (Fig. 2.1c) with a 5 W solar panel, held by a 2.99 m tripod (U30-NRC-SYS-C, Onset Computer Corp, Bourne, Mass.) was placed adjacent to the drying system to monitor environmental conditions during the experiment, consisting of the following: 1) a T/RH sensor (S-THB-M002, Onset Computer Corp.) covered by a solar radiation

shield (RS3, Onset Computer Corp.); 2) a wind speed sensor (S-WSB-M003, Onset Computer Corp.); 3) a wind direction sensor (S-WDA-M003); 4) a solar radiation sensor (S-LIB-M003); 5) a data logger (HOBO U30 NRC, Onset Computer Corp.) to store the data from the weather station sensors at 5-min intervals.

2.3 Drying stockpile and sample distribution

Almonds were deposited directly from the conveyer cart onto the A-frame until a stockpile height of about 0.30 m was achieved to form the bottom layer, 10 replicates of almond mesh bags containing T/RH sensors were placed on the partial almond stockpile. The procedure was repeated to form the middle and top layers, with a partial stockpile height of 1.22 and 2.13 m, respectively, as shown in Figure 2.1d. The conveyer cart contained an inbuilt weighing scale that was used to record the almond stockpile mass that amounted to 4,155 kg at a height, width, and length equal to 2.13 m × 3.05 m × 3.66 m, respectively. Corrugated French pipes of size 0.09 m × 3.05 m were used to demarcate the stockpile perimeter and keep it intact. Almonds were dried for 11 days until the desired storage moisture content of about 6% MC_{db} was achieved (USDA, 2019).

Drying was achieved by a combination of heated air at 55 ± 5.29 °C recorded in the drying plenum with airflow of 0.078 ± 0.02 m^3/s per m^3 of fresh almonds, and ambient air at a temperature and relative humidity of 18.47 ± 5.43 °C and 31.74 ± 13.77%, respectively. After drying, 30 mesh bag samples of almonds were retrieved from the stockpile and immediately transported to the Postharvest engineering laboratory at UC Davis to test for final moisture content and quality parameters.

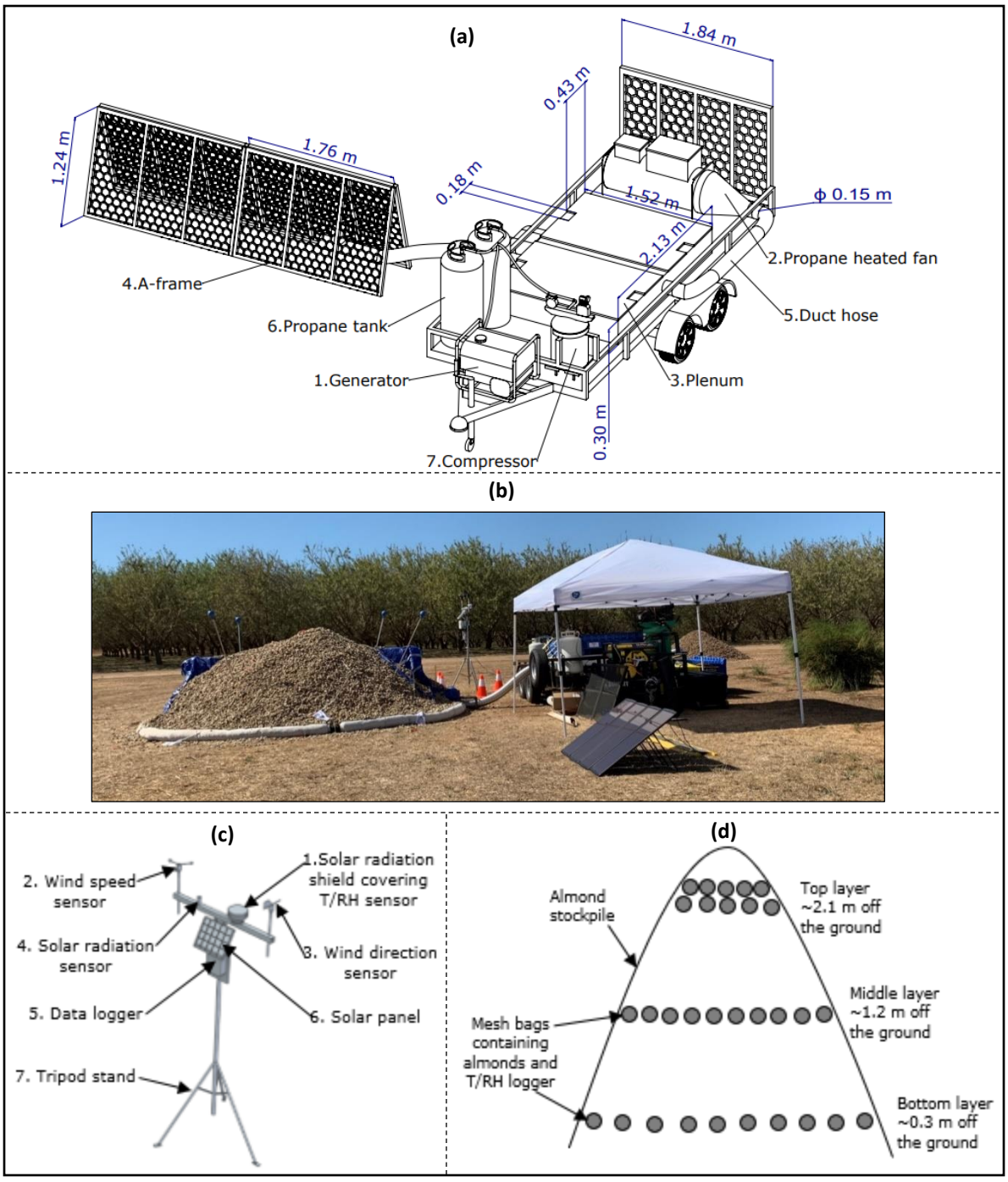

Figure 2.1. (a) Schematic representation of stockpile dryer showing main components. (b) Picture showing stockpile dryer, taken at NICKELS Soil Laboratory Orchards (Arbuckle, California). (c) Schematic representation of the weather station kit and the main components. (d) Schematic representation of stockpile of almonds showing three layers of almonds.

2.4 Sample Moisture Content Determination

Five almonds were randomly selected from each sample mesh bag. Hulls were manually removed (hulling), and then kernels were extracted after the shell was cracked with a hammer (shelling). Almond kernels were then placed in a 70 mm diameter aluminum crimpled-walled weighing dish (Cole-Parmer Instrument Co., Vernon Hills, Ill.). Dry basis moisture content expressed as a percentage was determined using the oven drying method for 24 h at an oven temperature of 105°C as described by AOAC (1990).

2.5 Quality Parameters

Ten almonds were randomly selected from each sample mesh bag to visually quantify any damage by molds or decay, insect injury, and presence of internal cavities. The number of defective almonds was counted and expressed as a percentage of the total sample (10) per tested quality parameter, as specified in the shipping point and market inspection instructions almonds manual (USDA, 1998). The procedure was repeated for all the 30 mesh bags and an average was calculated. The presence of split cotyledons after cutting the kernels in half with a knife shows internal cavities (Coates, 2018). Moldy almonds were denoted when visible on the kernel. The white or grey mold that could easily be rubbed off with fingers was ignored and decay was recorded when the kernel was completely or partially decomposed (USDA, 1998; Kader, 2013). The presence of insect, web, frass, or evidence of insect feeding was counted as insect injury (USDA, 1998; Schatzki and Ong, 2001).

2.6 Energy Usage During Drying

The total energy utilized by the SHAD is the sum of the electrical and propane energy consumed by the heater and fan. Electrical usage (E_1) expressed in kWh (converted from Wh by a factor of 1000) is computed using equation 1 (Motevali et al., 2011; Muralidhara, 2017).

$$E_1 = dp \times q \times t \quad (1)$$

where dp is the total pressure within the plenum (Pa); q is the fan-delivered airflow (m^3/s), which was calculated from the fan performance curve; and t is the drying time (h).

Propane energy usage (E2) by the heated fan is computed using:

$$E_2 = N \times P \quad (2)$$

where N is the amount of propane used by the heater; and P is the amount of energy in 1 L of propane gas, equal to 25,503 kJ (Elgas, 2019).

Total energy consumption E_t (kJ) is given by equation 3, after converting E_1 from kWh to kJ, where 1 kWh is equal to 3,600 kJ.

$$E_t = E_1 + E_2 \quad (3)$$

Specific energy required to removed 1000 kg (a tonne) of water from the almond stockpile (E_{tn}) is calculated using:

$$E_{tn} = \frac{E_t}{W} \times 1000 \quad (4)$$

where W is the mass of water removed from the almonds (271 kg); and factor 1000 denotes a tonne of water in the almonds.

2.7 Energy Cost

The energy cost required to dry a tonne of the initial weight of almond stockpile (C_{tn}) is calculated using:

$$C_{tn} = \frac{C_p + C_e}{m_a} \times 1000 \quad (5)$$

where Cp is the total propane cost ($0.63 per L of propane) (EIA, 2019); Ce is the total electricity cost ($0.16 per 1 kWh) (EIA, 2020); ma is the initial weight of almonds (4,155 kg); factor 1000 denotes a tonne of fresh almonds (before drying).

2.8 Dryer Performance Indicators

2.8.1 Specific Moisture Extraction Rate (SMER)

SMER (kg/kWh) describes the effectiveness of energy used during drying (Prasertsan and Saen-Saby, 1998), calculated using (Stawreberg and Nilsson, 2010, Liu et al., 2018):

$$SMER = \frac{W}{E_t} \qquad (6)$$

E_t is converted from kJ to kWh, where 1 kWh is equal to 3,600 kJ.

2.8.2 Moisture Extraction Rate (MER)

MER (kg/h) measures the dryer capacity (Prasertsan and Saen-Saby, 1998), calculated using (Liu et al., 2018):

$$MER = \frac{W}{t} \qquad (7)$$

2.8.3 Coefficient of Performance (COP)

COP is used to evaluate the efficiency of the propane heated fan. COP is a dimensionless value expressed as the ratio of energy produced to the energy used by the propane-heated fan, calculated using (Oktay and Hepbasli, 2003; Yahya, 2016):

$$COP = \frac{\sum Q}{E_t} \qquad (8)$$

where ∑Q (kJ) is the total dissipated energy.

Earle and Earle, (2004) indicated that *Q* is calculated as the sum of the energy required to raise the temperature of the almonds and the latent heat used to remove water from the almonds, as shown in:

$$Q = m_a \times C_a (T_1 - T_2) + W \times C_v \quad (9)$$

where Ca is the specific heat capacity of the almonds taken as 2.2 kJ/kgK (ASHRAE, 2010); T1 and T2, expressed in K, are the initial and final temperatures of the almonds.

During drying, the heater automatically turned on and off, controlling the airflow, pressure buildup, and saving energy usage. Equation 9 was modified into equation 10 to account for the total energy ($\sum_{t=1}^{t} Q$) required to raise the temperature of the almonds during the entire drying period, as quantified by temperature sensors in each almond sample.

$$\sum_{t=1}^{t} Q = m_a' \, C_a' \sum_{t=1}^{t} (T_1 - T_2) + W' \, C_v \quad (10)$$

where $\sum_{t=1}^{t} (T_1 - T_2)$ is the sum of temperature rise during the entire drying period; and Cv is the water latent heat of vaporization at 55° C (328K) taken as 2,369.63 kJ/kg (Osborne et al., 1939).

2.9 Data Analysis

All data visualization and analysis were developed in SAS Enterprise 7.1. A split-plot design was used for this experiment, where the stockpile (plot) was partitioned into three subplots: bottom, middle and top layers. Analysis-of-Variance (ANOVA) was conducted on both MC_{db} and quality parameters to determine whether the differences were statistically significant between each layer. When a significant main effect was found, a post hoc test using Tukey's Honest Significant

Difference (HSD) test was conducted to ascertain where the difference of the means lies in the layers at a 95% confidence level ($p \leq 0.05$). In addition, mean data of temperature and RH within each mesh bag sample were graphed against time (days) for each stockpile layer (bottom, middle, and top) to visualize their trend and relationship.

3.0 Results and Discussion

3.1 Moisture Content and Quality Parameters

After 11 days of drying, the mean MC_{db} for the bottom, middle, and top layers were 7.12 ± 2.64%, 6.42 ± 3.27%, and 4.59 ± 0.73%, respectively, as shown in Figure 2.2a. ANOVA test showed that MC_{db} was significantly different between the stockpile layers (p-value < 0.01, F-value = 8.67, 2 degrees-of-freedom). Post hoc Tukey's honestly significant difference (HSD) test was conducted, which showed that the MC_{db} in the bottom and middle layers were not statistically different. It is hypothesized that the significant difference between the MC_{db} in the stockpile layers can partly be attributed to the non-uniform distribution of air during the drying process.

Quality parameter testing for almonds before drying showed that internal cavities, decay or mold damage, and insect injury were 0%. After drying, the almond stockpile was 96.12 ± 3.59% free from quality concerns or defects. Internal cavities and decay or mold damage contributed 1.77 ± 2.66%, and 1.81 ± 2.57%, respectively (Fig. 2.2b). No evidence of insect injury was observed, so this factor was excluded for further analysis. ANOVA showed that the differences of the quality parameters were not significant between the stockpile layers (p-value = 0.93, F-value = 0.26, 5 degrees-of-freedom), therefore a post hoc test was not conducted. Mold or decay can potentially be attributed to sections within the stockpile, which did not receive sufficient air due to the potential lack of proper air distributed through the stockpile. Coates (2018) indicated that internal cavities are caused by a fast-drying rate, where the outer surface of the almond solidifies before

the center leading to kernel splitting. USDA (1998) reports that decay or mold damage and insect injury have a 5% tolerance during grading while live insects have 0% tolerance, hence the quality parameter results are low and not concerning.

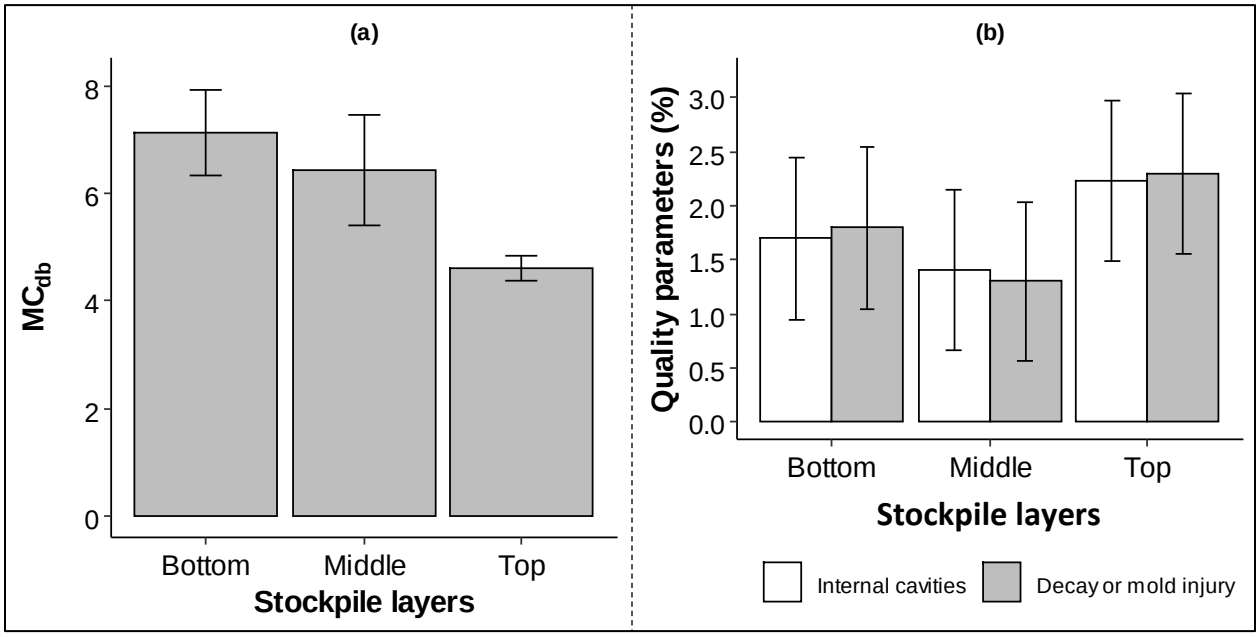

Figure 2.2. (a) Bar plot showing moisture content with stockpile layer. Bar plots followed by the same letter are not significantly different at p = 0.05 (ANOVA) (Tukey's Honest Significant Difference). (b) Bar plots showing quality parameters (%) per stockpile layer. Error bars indicate standard error.

3.2 Ambient Conditions

The stockpile was assumed to receive the same treatment of ambient conditions throughout, which are as follows: average ambient temperature of 18.47 ± 5.43°C and RH of 31.74 ± 13.77% recorded by T/RH sensor; average wind speed of 1.61 ± 2.03 m/s and gust speed of 2.78 ± 2.81 m/s recorded by wind speed sensor; average wind direction of 133.30 ± 65.42 ∅ recorded by wind direction sensor, and average solar radiation of 197.47 ± 262.19 W/m^2 recorded by a solar radiation sensor.

3.3 Drying Conditions

The initial RH for the almond stockpile was 70.38 ± 2.87%. At the end of the drying period, the top layer yielded the lowest RH (26.25%) in comparison to the middle (52.95%) and bottom layers (58.40%) as shown in Figure 2.3a. Additionally, a low rate of change in RH was recorded for the bottom (0.58% per day) and middle layers (0.26% per day) of the stockpile, which was not the case for the top layer (5.91% per day). Differences in RH can be partly attributed to the differences in the distribution and air delivery from the fan. Figure 2.3b shows the temperature profile. The fan ran throughout the entire experiment, but the heater automatically turned on and off depending on the ambient conditions accounting for 28% of the drying time. The large temperature gap, between the plenum temperature (especially when the heater is on) and the almonds temperature, is an indication that the system had low efficiency in achieving the desired drying temperature.

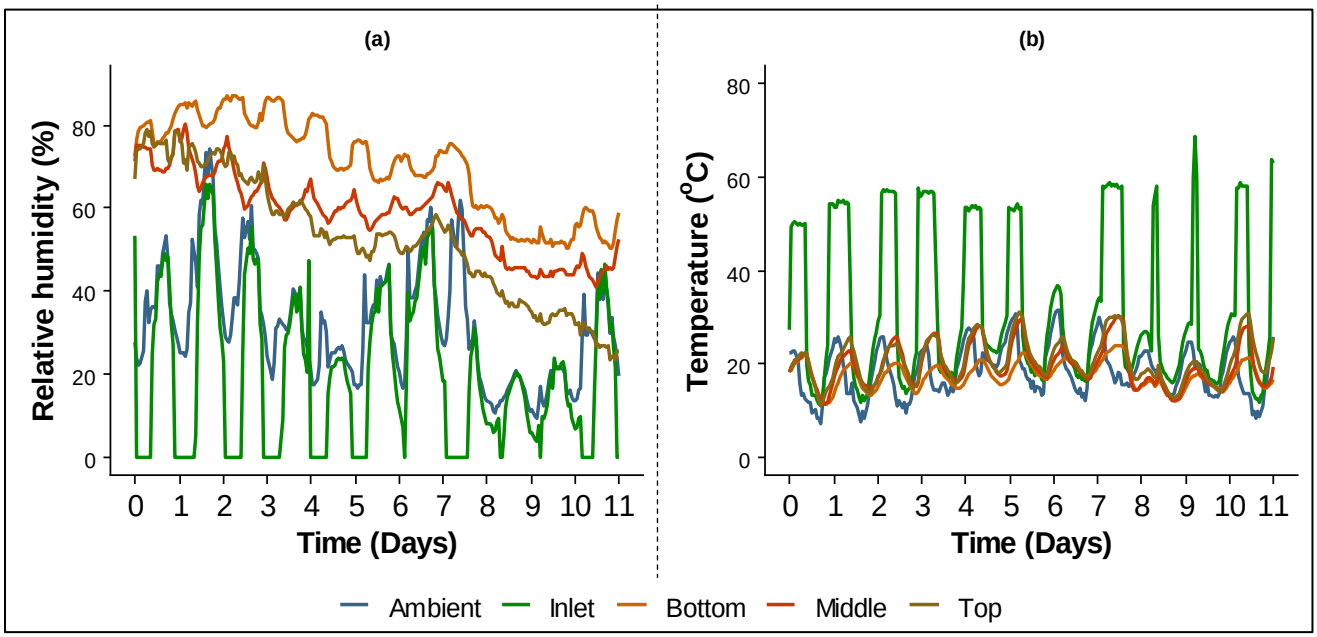

Figure 2.3. (a) Relative humidity profile, (b) temperature profile.

3.4 Energy Usage During Drying

An average pressure (*dp*) of 308.48 ± 74.1 Pa was recorded in the drying plenum, indicating that the fan delivered air to the stockpile at an airflow (*q*) equal to 1.86 ± 0.45 m^3/s. Electrical energy consumption (E_1) equaled 545,328 kJ, propane energy usage (E_2) equaled 978,809.36 kJ, and therefore the total energy consumption (E_t) during the whole drying process. An average pressure (*dp*) of 308.48 ± 74.1 Pa was recorded in the drying plenum, indicating that the fan delivered air to the stockpile at an airflow (*q*) equal to 1.86 ± 0.45 m^3/s. Electrical energy consumption (E_1) equaled 545,328 kJ, propane energy usage (E_2) equaled 978,809.36 kJ, and therefore the total energy consumption (E_t) during the whole drying process was 1,524,137.36 kJ. The specific energy required to remove a tonne of water from the almond stockpile (E_{tm}) was 5,623,290 kJ/kg of water.

3.5 Energy Cost

Propane (C_p) and electricity costs (C_e) of $ 24.18 and $24.24, respectively, were calculated, achieving a total drying cost of $48.42 ($C_p + C_e$). The total cost required to dry a tonne of almonds is $11.65.

3.6 Dryer Performance Indicators

Drying in this experiment was achieved as a combination of using both heated and ambient air to attain a SMER, MER, and COP of 0.64 kg/kWh, 1.02 kg/h, and 1.33, respectively. Perera and Rahman (1997) indicated that SMER of Heated Air Dryers (HAD) is in the 0.12 to 1.28 kg/kWh range. Further, Pal and Khan (2010) reported that drying sweet pepper with a HAD at 45°C yielded a SMER of 0.93 kg/kWh and MER of 0.22 kg/h, increasing the drying temperature to 55°C provided a SMER of 1.06 kg/kWh and MER of 0.37 kg/h. Therefore, the SMER of the SHAD is within the range of existing HAD, while a higher MER was recorded in this study.

A comparison of SHAD used in this experiment with other types of dryers shows that SMER (Fig. 2.4a) and MER (Fig. 2.4b) values are within the appropriate range. However, comparisons show that a low COP (Fig. 2.4c) was generated. Kitanovski et al. (2009) reported that a low COP indicates that the system has low efficiency. In the case of the SHAD, non-uniform distribution of warm air in the stockpile and heat lost due to sections of the A-frame not fully covered by the almond stockpile forced longer drying periods, which partly contributed to a low COP.

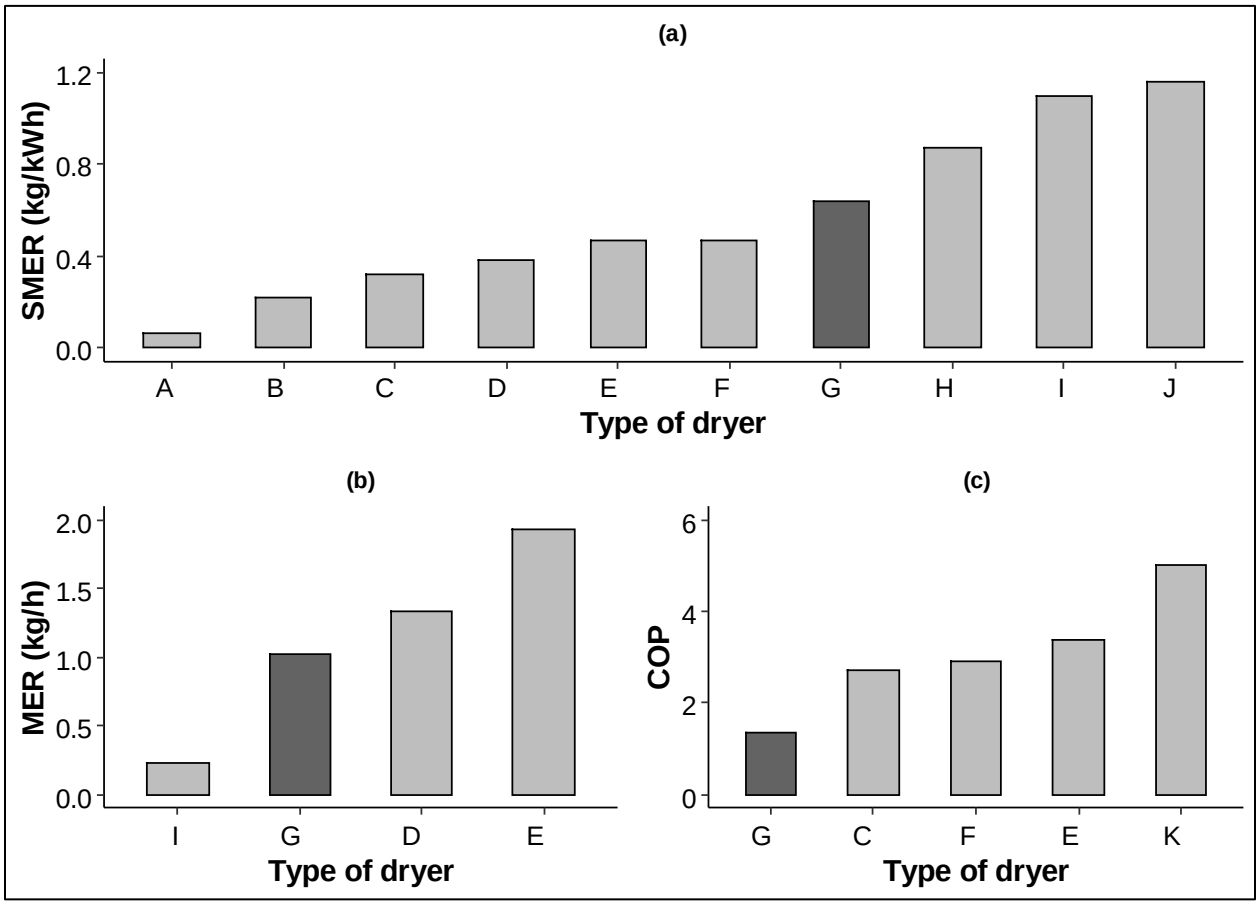

Figure 2.4. (a). Bar plot comparing SMER of different dryers. (b) Bar plot comparing MER of different dryers. (c) Bar plot comparing COP of different dryers. [A] Closed system heat pump dryer for ginger at 50°C (Chapchaimoh et al., 2016), [B] Convection solar dryer for bitter gourd (Vijayan et al., 2016), [C] Heat pump dryer for tomato slices at 45°C (Coşkun et al., 2017), [D] Solar dryer for cassava at 40°C (Yahya et al., 2016), [E] Solar assisted heat pump dryer for cassava at 45°C (Yahya et al., 2016), [F]Solar assisted heat pump for mushrooms at 45°C (Şevik et al., 2013), [G] Stockpile heated and ambient air dryer for almonds at 55°C (this study), [H] Solar dryer for chili at 50°C (Mohanraj and Chandrasekar, 2009), [I] Heat pump dryer for sweet pepper at 40°C (Pal and Khan, 2010), [J] Heat pump assisted hybrid photovoltaic thermal solar dryer for saffron at 45°C (Mortezapour et al., 2012), **[**K] Heat pump for mint leaves at 45°C (Ceylan and Gürel, 2016).

Further studies will focus on improving air distribution within the stockpile during the drying process, this can be achieved by introducing an air distribution duct underneath the stockpile with channels diverting air to the entire stockpile. The concept is adapted from Das et al. (2001) where an air distribution duct was developed for an air recirculating tray dryer, and also Noyes (2006) suggested the use of multiple air ducts to distribute the air in silos. Further studies comparing the SHAD with the conventional windrow drying method need to be carried out in parallel. Altering the drying conditions, such as drying temperature and airflow will also be considered.

4.0 Conclusion

A SHAD was developed to directly dry almonds outdoors in stockpiles. The SHAD is intended to replace the conventional method of sun-drying almonds, which involves sweeping and picking processes that generate dust. The adaptation of the SHAD has the potential to reduce the drying time of almonds if the efficiency of the dryer is improved. Almond stockpile of 4,155 kg was dried with SHAD using a combination of heated and ambient air for 11 days. Almonds were dried from 12.6 ± 1.6% to 6.04 ± 2.21% MC_{db}, Tukey's HSD test showed that the bottom (7.12 ± 2.64% MC_{db}) and the middle layer (6.42 ± 3.27% MC_{db}) were in the same Tukey grouping in comparison to the top layer (4.59 ± 0.73% MC_{db}). This is attributed to the non-uniform distribution of air within the stockpile and air leakage, which led to warm air escaping rather than being forced through the stockpile.

Initial quality parameter tests showed that internal cavities, decay or mold damage, and insect injury were 0%. After drying, the stockpile was tested to be 96.12 ± 3.59% free from quality concerns, attributed to 1.77 ± 2.66% internal cavities, 1.81 ± 2.57% decay or mold damage, and there was no insect injury. The effect of quality parameters on the stockpile layer was found not to be significant ($p \leq 0.05$). Energy performance indicators showed a SMER of 0.64 kg/kWh, MER

of 1.02 kg/h, COP of 1.33, and the drying process cost $11.65 per tonne. Comparison with other commercial dryers showed that SMER and MER are within acceptable limits, however, a low COP was observed.

The major drawback is that there was a lack of appropriate air distribution through the stockpile. Work is ongoing to develop an air distributor to be placed underneath the A-frame to ensure that drying air is evenly distributed throughout the stockpile. Further studies will also include a parallel comparison of the SHAD drying method with the conventional windrow drying of almonds.

References

ABC. Almond Board of California. (2017). Almond Lifecyle. Retrieved from https://www.almonds.com/why-almonds/almond-lifecycle

AOAC. (1990). Official methods of analysis of the association of official analytical chemists (15th ed.). Association of Official Analytical Chemists.

ASHRAE. (2010). Handbook: Refrigeration (SI ed., Vol. 30329). American Society of Heating Refrigerating and Air-Conditioning Engineers Inc.

Calderon, M., 1972. Aeration of Grain - Benefits and Limitations. EPPO Bulletin 2, 83–94.. doi:10.1111/j.1365-2338.1972.tb02137.x

Ceylan, I., & Gurel, A. E. (2016). Solar-assisted fluidized bed dryer integrated with a heat pump for mint leaves. Appl. Thermal Eng., 106, 899-905. https://doi.org/10.1016/j.applthermaleng.2016.06.077.

Chapchaimoh, K., Poomsa-ad, N., Wiset, L., & Morris, J. (2016). Thermal characteristics of heat pump dryer for ginger drying. Appl. Thermal Eng., 95, 491-498. https://doi.org/10.1016/j.applthermaleng.2015.09.025

Coates, M. C. (2018). Defining and modeling the boundaries for mechanized dehydration to produce high quality almonds. PhD diss. University of South Australia, School of Engineering.

Coskun, S., Doymaz, Ä., Tunckal, C., & Erdogan, S. (2017). Investigation of drying kinetics of

tomato slices dried by using a closed loop heat pump dryer. Heat Mass Transfer, 53(6), 1863-1871. https://doi.org/10.1007/s00231-016-1946-7

Das, S., Das, T., Srinivasa Rao, P., & Jain, R. K. (2001). Development of an air recirculating tray dryer for high moisture biological materials. J. Food Eng., 50(4), 223-227. https://doi.org/10.1016/S0260-8774(01)00024-3

Ding, N., Xing, F., Liu, X., Selvaraj, J. N., Wang, L., Zhao, Y., ... & Liu, Y. (2015). Variation in fungal microbiome (mycobiome) and aflatoxin in stored in-shell peanuts at four different areas of China. Frontiers in microbiology, 6, 1055.

Earle, R. L., & Earle, M. D. (2004). Unit operations in food processing: web edition. The New Zealand.

EIA. (2019). Petroleum and other liquids. United States Energy Information and Administration. Retrieved from https://www.eia.gov/dnav/pet/hist/LeafHandler.ashx?n=PET&s=W_EPLLPA_PRS_NUS_DPG&f=W

EIA. (2020). Electric power monthly. United States Energy Information and Administration. Retrieved from https://www.eia.gov/electricity/monthly/epm_table_grapher.php?t=epmt_5_6_a

ELGAS. (2019). Propane BTU per gallon, propane BTU per cubic foot, propane therms to gallons: Propane gallons to pounds conversion - Full conversion chart. ELGAS. Retrieved from https://www.elgas.com.au/blog/1675-propane-conversion-values-pounds-gallons-btu-therms-ft-usa.

Kader, A. A. (2013). 2 - Impact of nut postharvest handling, de-shelling, drying and storage on quality. In L. J. Harris (Ed.), Improving the safety and quality of nuts (pp. 22-34). Woodhead Publ. https://doi.org/10.1533/9780857097484.1.22

Kitanovski, A., Gonin, C., Vuarnoz, D., Sari, O., & Egolf, P. W. (2009). A standardization of the coefficient of performance for magnetic refrigerators, heat pumps and energy conversion machines. Proc. 3rd Int. Conf. on Magnetic Refrigeration at Room Temperature, (pp. 1-9). Retrieved from http://infoscience.epfl.ch/record/215836

Kumar, A., Pathak, H., Bhadauria, S., & Sudan, J.. (2021). Aflatoxin contamination in food crops:

causes, detection, and management: a review. Food Production, Processing and Nutrition, 3(1). https://doi.org/10.1186/s43014-021-00064-y

Kunze, O. R, 1979. Fissuring of the Rice Grain After Heated Air Drying. Transactions of the ASAE 22, 1197–1201.. doi:10.13031/2013.35183

Liu, H., Yousaf, K., Chen, K., Fan, R., Liu, J., & Soomro, S. A. (2018). Design and thermal analysis of an air source heat pump dryer for food drying. Sustainability, 10(9), 3216. https://doi.org/10.3390/su10093216

Mohanraj, M., & Chandrasekar, P. (2009). Performance of a forced convection solar drier integrated with gravel as heat storage material for chili drying. J. Eng. Sci.Technol., 4(3), 305-314.

Moreira, R. G., & Bakker-Arkema, F. W. (1989). Moisture desorption model for nonpareil almonds. J. Agric. Eng. Res., 42(2), 123-133. https://doi.org/10.1016/0021-8634(89)90045-0

Mortezapour, H., Ghobadian, B., Minaei, S., & Khoshtaghaza, M. H. (2012). Saffron drying with a heat pump-assisted hybrid photovoltaic-thermal solar dryer. Drying Technol., 30(6), 560-566. https://doi.org/10.1080/07373937.2011.645261

Motevali, A., Minaei, S., Khoshtaghaza, M. H., & Amirnejat, H. (2011). Comparison of energy consumption and specific energy requirements of different methods for drying mushroom slices. Energy, 36(11), 6433-6441. https://doi.org/10.1016/j.energy.2011.09.024

Muralidhara, B. S. (2017). Unit-11 Conveying system-pneumatic. IGNOU.

Noyes, R. T. (2006). Development of a new low-energy environmentally compatible grain and seed drying and storage technology. Proc. 9th Int. Working Conf. on Stored Product Protection, (pp. 1285-1294).

Oktay, Z., & Hepbasli, A. (2003). Performance evaluation of a heat pump assisted mechanical opener dryer. Energy Convers. Manag., 44(8), 1193-1207. https://doi.org/10.1016/S0196-8904(02)00140-1

Overhults, Douglas G.; White, G. M.; Hamilton, H. E.; and Ross, I. J., "Drying Soybeans with Heated Air" (1973). Biosystems and Agricultural Engineering Faculty Publications. 134. https://uknowledge.uky.edu/bae_facpub/134

Osborne, N. S., Stimson, H. F., & Ginnings, D. C. (1939). Measurements of heat capacity and heat of vaporization of water in the range 0 degrees to 100 degrees C. J. Res. Natl. Bureau Standards, 23(2), 197. https://doi.org/10.6028/jres.023.008

Pal, U. S., & Khan, M. K. (2010). Performance evaluation of heat pump dryer. J. Food Sci. Technol., 47(2), 230-234. https://doi.org/10.1007/s13197-010-0031-3

Perera, C. O., & Rahman, M. S. (1997). Heat pump dehumidifier drying of food. Trends Food Sci. Technol., 8(3), 75-79. https://doi.org/10.1016/S0924-2244(97)01013-3

Prasertsan, S., & Saen-Saby, P. (1998). Heat pump drying of agricultural materials. Drying Technol., 16(1-2), 235-250. https://doi.org/10.1080/07373939808917401

Schatzki, T. F., & Ong, M. S. (2001). Dependence of aflatoxin in almonds on the type and amount of insect damage. J. Agric. Food. Chem., 49(9), 4513-4519. https://doi.org/10.1021/jf010585w

Sevik, S., Aktas, M., Dogan, H., & Kocak, S. (2013). Mushroom drying with solar assisted heat pump system. Energy Conversion Manag., 72, 171-178. https://doi.org/10.1016/j.enconman.2012.09.035

Simpson, J., & Weiner, E. (1989). The Oxford English Dictionary (20 Volume Set) (p. 22000). Oxford University Press, USA.

Stawreberg, L., & Nilsson, L. (2010). Modelling of specific moisture extraction rate and leakage ratio in a condensing tumble dryer. Appl. Therm. Eng., 30(14), 2173-2179. https://doi.org/10.1016/j.applthermaleng.2010.05.030

USDA. (1998). Shipping point and market shipping instructions for almonds. Washington, DC: USDA-Agricultural Marketing Service. Retrieved from https://www.ams.usda.gov/sites/default/files/media/Almond_Inspection_Instructions%5B1%5D.pdf

USDA. (2019). Commodity specification for shelled tree nuts. Washington, DC: USDA-Agricultural Marketing Service. Retrieved from https://www.ams.usda.gov/sites/default/files/media/CommoditySpecificationforShelledTreeNuts.pdf

Vijayan, S., Arjunan, T. V., & Kumar, A. (2016). Mathematical modeling and performance analysis of thin layer drying of bitter gourd in sensible storage based indirect solar dryer. Innovative Food Sci. Emerg. Technol., 36, 59-67. https://doi.org/10.1016/j.ifset.2016.05.014

Waewsak, J., Chindaruksa, S., Punlek, C. (2006). A mathematical modeling study of hot air drying for some agricultural products. Thammasat International Journal of Science and Technology, 11(1), 14–20.

Wang, R.Z., Xu, Z.Y., Ge, T.S., 2016. Introduction to solar heating and cooling systems, in:. pp. 3–12. doi:10.1016/b978-0-08-100301-5.00

Yahya, M., Fudholi, A., Hafizh, H., & Sopian, K. (2016). Comparison of solar dryer and solar-assisted heat pump dryer for cassava. Sol. Energy, 136, 606-613. https://doi.org/10.1016/j.solener.2016.07.049

CHAPTER 3

DESIGN, VALIDATION, AND OPTIMIZATION OF AN AIR-DISTRIBUTOR FOR AN ALMOND STOCKPILE HEATED AND AMBIENT AIR DRYER (SHAD) USING COMPUTATIONAL FLUID DYNAMICS (CFD) AND IN-FIELD MEASUREMENTS

Abstract

A Stockpile Heated and Ambient air Dryer (SHAD) was developed to replace the current conventional windrow drying of almonds, and its associated challenges including dust emission during harvest, almond pre and post-harvest pests infestation, and the potential of human pathogen cross-contamination. Previous experiments showed that the air supplied from the SHAD through the almond stockpile was unevenly distributed, thus reducing the SHAD's efficiency, increasing the drying time, and generating undesirable quality defects. Therefore, an air distributor containing 12 outlets, arranged in 4 rows with 3 outlets each was developed. This study focused on the optimization of air delivery from the air distributor by combining a Computational Fluid Dynamics (CFD) simulation model and in-field airflow measurements to validate and optimize the CFD model, and the air distributor performance. In-field airflow validation measurements showed that the percentage airflow distribution was 4.1, 30.8, 44.9, and 20.2% for the outlets in rows 1, 2, 3, and 4, respectively, when all outlets are open. This showed that almonds located in the region of row 1 would not receive sufficient air for proper drying. Thus, an optimized 3-row air distributor configuration was developed, which involved sealing off all outlets in row 1 to yield an airflow distribution percentage of 31.3%, 44.4%, and 24.3% for rows 2 through 4, subsequently. The 3-row air distributor configuration is desired, due to the typical almond stockpile cone-shape, where the middle and tallest section recieves the highest airflow (44.4%). Ultimately, the developed air distributor uniformly distributes airflow through an almond stockpile, hence improving the SHAD's efficiency.

Keywords. Airflow, optimization, CFD. Stockpile, cone-shape, multiple outlets,

1.0 Introduction

Chapter 2 focused on initial development of Stockpile heated and ambient air dryer (SHAD) as an alternative to the current convection windrow drying of almonds, and its associated challenges such as dust emission during harvest, pre and post-harvest pests infestation, and the potential of human pathogen cross-contamination. This involved supplying drying air to dehydrate almonds in a stockpile. However, results showed that drying air from the first-generation SHAD was unevenly distributed within the stockpile (Chapter 2; Mayanja et al., 2021). Thus, there is a need to design and fabricate an improved air distribution system to enhance SHAD's air distribution and efficiency.

Airflow is the movement of air between two points due to pressure difference, where air moves from a region of high to low pressure (RSES, 2008). Airflow is bound by three fundamental laws of physics (Wendt, 1992): 1) Conservation of mass, which states that the mass of air can't be created nor destroyed (Subramanian, 2011); 2) Conservation of energy, which states that the sum of all energy types (kinetic, potential, and internal energy) along the air stream is the same at each point (Qin and Duan, 2017); and 3) Conservation of momentum, which states that air movement can only be compelled by an external force, or fan in the case of the SHAD (Cengel and Cimbala, 2017). Further, airflow is categorized into laminar and turbulent flow. Laminar flow occurs when air is flowing in parallel layers without interference between the layers, while turbulent flow is characterized by irregular fluctuations or air mixing. (Qin et al., 2006; Cengel and Cimbala, 2017; Riveros and Riveros-Rosas, 2010).

Designing optimized systems to properly distribute the air in dryers is a complex, time-consuming, and costly process. Thus, Computational Fluid Dynamics (CFD), known as a computer-based airflow simulation, can reduce the challenges underlying the physical development of drying

systems (Versteeg and Malalasekera, 2007; Versteeg and Powell, 2010). CFD generally comprises three main steps: 1) Preprocessing, which defines the system's geometry (meshing), the definition of the airflow and boundary conditions, and underlying mathematical equations; 2) Solving stage, where the discretized equations are solved by the CFD model; and 3) Post-processing, which involves quantitative measurements and airflow result visualization (Versteeg and Malalasekera, 2007; SIEMENS, 2021).

The ventilation industry is one of the major applications of air distribution technology, where it is leveraged to optimize room heating or cooling (Nielsen, 2015; Nielsen, 2007; Gan, 1995; Awbi, 1998). Experimental and numerical studies have been conducted, which embarked on improving air distribution with multiple outlet plenums (Hassan et al., 2015). Thus, uniformity of air distribution to all sections of the stockpile can be achieved with the adoption of a multiple outlet air distributor. The basis of the SHAD air distributor is to uniformly distribute the supplied drying air through the almond stockpile to achieve dehydration under similar thermal conditions.

No studies exist where and air distributor has been evaluated as an addition to stockpile drying, in any agricultural products including almonds. Therefore, the purpose of this study was to model, design, fabricate, validate, and optimize a multiple-outlet air distributor for the almond SHAD. Steps conducted in this study are summarized in Figure 3.1, which involved developing a CFD model and its validation with in-field experimental data. In addition, an optimization step was conducted to maximize air distribution through the almond stockpile, based on the typical almond stockpile shape.

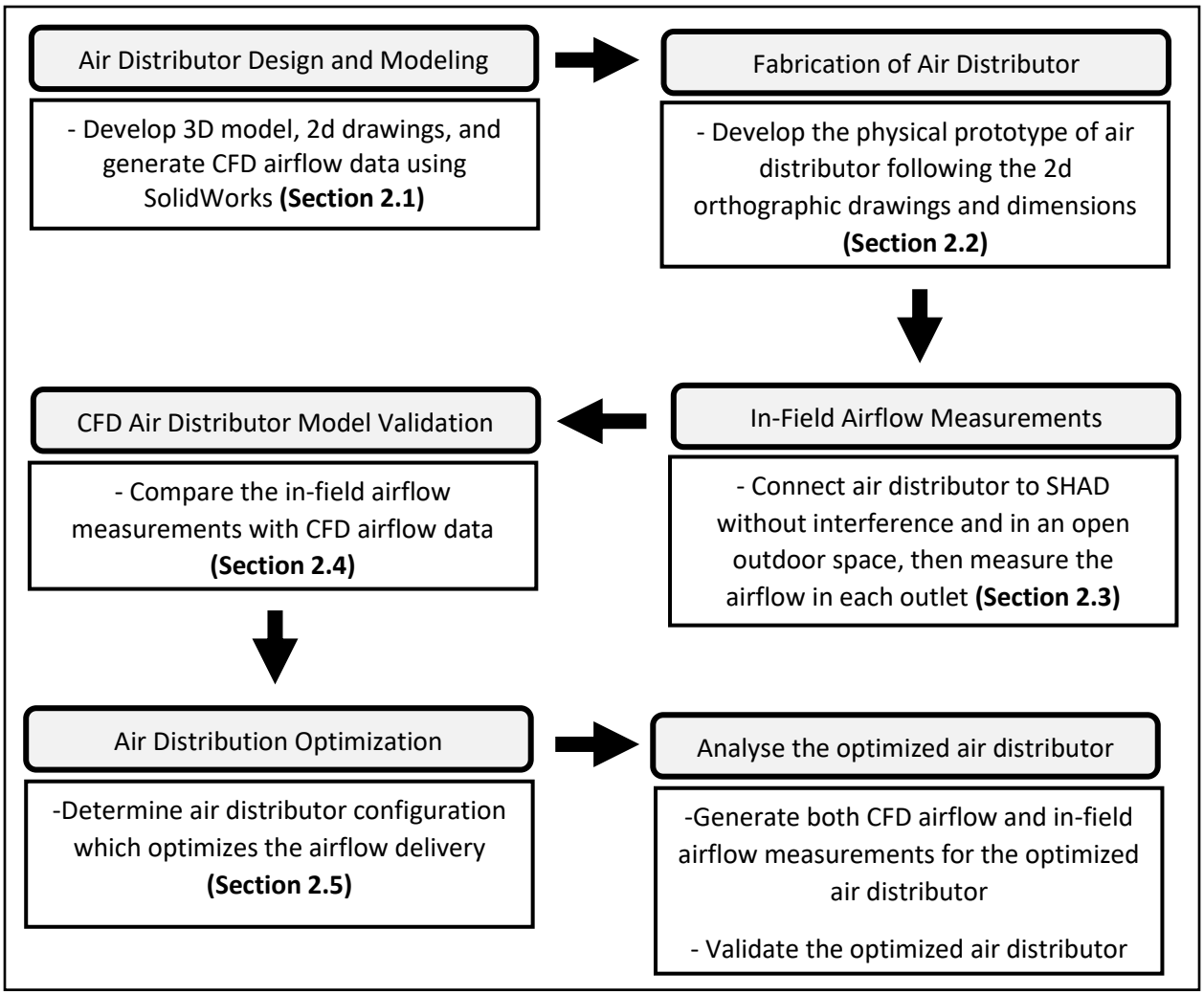

Figure 3.1. General steps followed to design, model, validate, and optimize the SHAD air-distributor

2.0 Materials and methods

2.1 Air distributor design and modeling

The three-dimensional (3D) design and simulations of the SHAD air distributor were performed using SolidWorks 2019 Service Pack (SP) 3.0 and its CFD simulation tool (Dassault Systèmes SolidWorks Corp, Waltham, MA, USA) using the parts, assembly, and drawing environments, as followed, and summarized in Figure 3.2:

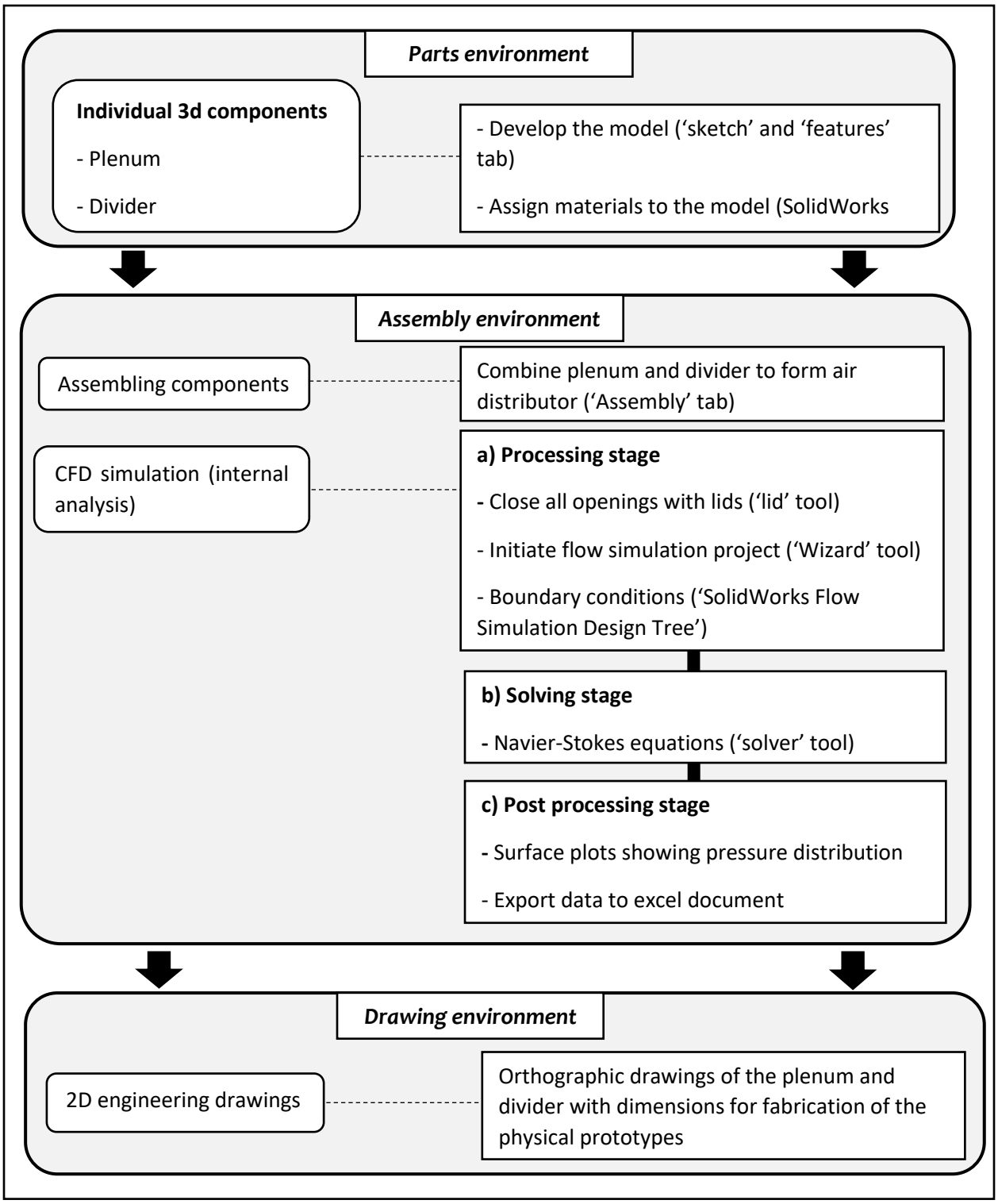

Figure 3.2: Flow chart showing the steps to develop the air distributor design and model.

2.1.1 Parts environment

Within SolidWorks, the SHAD's air distributor components or 'parts' are the model building blocks, and an assembly is comprised of one or multiple 'parts' (SolidWorks, 2015). First, the 'sketch' feature was applied to develop 2D sketches for each 'part', which are then transformed into independent 3D models using the 'features' element. The air distributor assembly consists of the combination of two 'parts', including the plenum and divider. The selected material for both 'parts' (plenum and divider) was 'cast carbon steel' (Lombard, 2018).

2.1.1.1 Plenum

The plenum is the component where the fan is connected to deliver the drying air before it is distributed through the almond stockpile. The role of the plenum is to laminarize the airflow by guaranteeing a similar pressure and temperature (T) along its length, before diffusing the air via the outlets (IRRI, 2021). There are two main types of plenums: 1) Extended plenum, which contains a main large duct with multiple outlets along its cross-section; and 2) Radial plenum, which doesn't contain a main duct, but rather individual outlets are connected to the main air supply or fan. In this study, an extended plenum of square cross-sectional shape was used, since it allows a higher airflow rate distribution with reduced airflow resistance and multiple outlets (Bhatia, 2001; Konzo, 1953; Jones, 2019). There are three main shapes of outlets connected to the plenum, including round, square, and rectangular outlets. Round outlets were used in this study, because of three reasons: 1) Offer the least resistance through the longitudinal air path, thereby requiring less fan power; 2) use the least amount of material; and 3) yield lower frequency noise, because of their curved surfaces (Bhatia, 2001). Twelve outlets in 4 rows with 3 on each side (left, right, and top) were placed on the plenum to uniformly distribute the drying air to the stockpile, as represented in Figure 3.3a.

2.1.1.2 Divider

Figure 3.3b shows a schematic representation of an air distributor with a uniform cuboid cross-section plenum. When air is forced through this type of plenum it results in a pressure increase along its longitudinal path, therefore forcing the majority of the air through the outlets furthest to the air inlet or fan (Bhatia, 2001). This results in insufficient airflow distribution to the outlets closer to the air inlet, and a lack of appropriate air distribution (RSES, 2009). Studies have shown that a tapered plenum will improve air delivery through multiple outlet rows (Fig 3.3c) (Hassan et al., 2015; Hassan et al., 2014). This is because pressure is inversely proportional to the area within the plenum (Cengel and Cimbala, 2017). Therefore, a three-sided tapered divider was placed within the plenum to gradually increase the pressure of the air through the plenum's longitudinal path. Hence, enhancing and uniformly distributing air through the outlets.

2.1.2 Assembly environment

The assembly environment within SolidWorks was used for two purposes: 1) To combine and arrange the two components or 'parts' into the air distributor assembly (plenum and divider) using the 'Assembly' feature, The divider was placed inside the plenum as schematically represented in Figures 3.3d and e. The distance between the divider and the plenum walls (left, right, and top) decreases lengthwise, creating and increase in pressure as the airflow moves through the plenum. and to conduct the CFD simulation (model generation, and analysis) with the 'flow simulation' feature.

2.1.2.1 CFD simulation

CFD model analysis is categorized into internal and external analyses. The internal analysis includes airflow within the air distributor model or the drying air flowing into the inlet and out

through the outlets. Alternatively, external analysis relates to the airflow surrounding the CFD model (SolidWorks, 2012), which was not considered in this application because the air distributor is surrounded by the almond stockpile. CFD analysis includes preprocessing, solving, and post-processing steps, which were applied as follows:

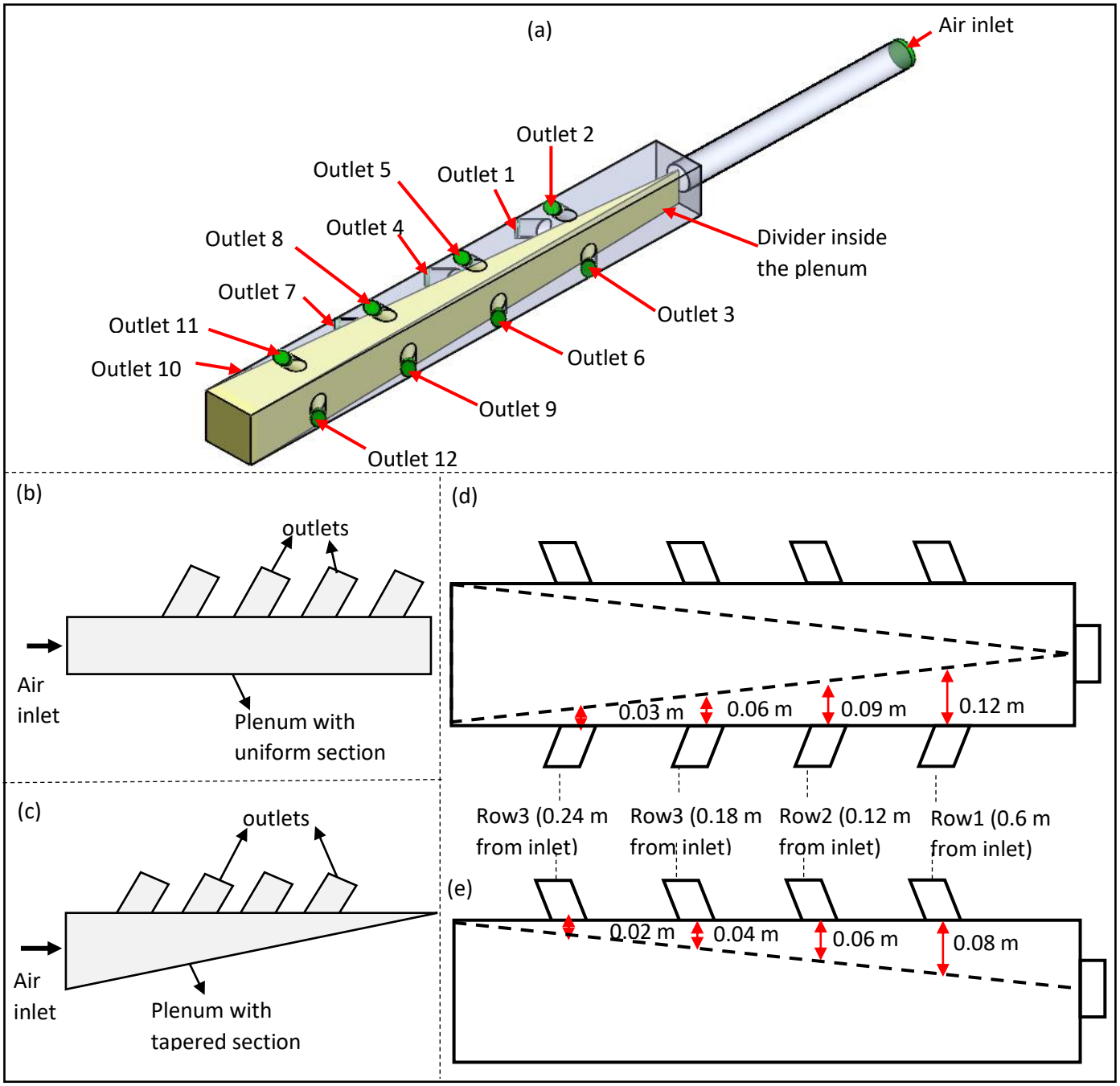

Figure 3.3. (a) The 3D design of the air distributor showing arrangement and numbering of outlets from 1 to 12 (grouped in 4 rows), and placement of divider inside the plenum and 13 lids on openings (1 inlet and 12 outlets). Color reference (Green for lids, grey for plenum, yellow for divider), Schematic representation of: (b) plenum with uniform longitudinal section, and (c) plenum with tapered longitudinal section. (d) Top view and (e) Side view of the air distributor showing the placement of the components and the distance between the divider and the outlets.

a) Preprocessing

Model openings must be closed before performing an internal analysis using the 'lid' tool. Lids are protrusions that cover openings. Lids allow defining the airflow boundary conditions (SolidWorks, 2011). In this study, 13 lids were placed on all the air distributor openings, consisting of 12 outlets and 1 inlet. The 'check geometry tool' was used to inspect for leakages in the model.

The flow simulation was performed with the SolidWorks 'wizard' tool, which allows the air distribution model and its parameters to be defined, including the model's name (i.e., Air distributor), unit system (i.e., International System of Units or SI), analysis type (i.e, Internal), and the type of fluid (i.e., Air). The SolidWorks Flow Simulation Design Tree (SFSDT) was created under the 'configuration manager' tab after the 'wizard' tool. SFSDT provides specifics of the model, data and allows for result visualization (SolidWorks, 2012). The 'Boundary condition' icon under the SFSDT was used to specify the flow conditions at each opening by selecting the inner face of the lids. The inlet airflow rate of 1.2 m^3/s, equal to the airflow provided by the fan, was selected as the inlet boundary condition. Then, the static atmospheric pressure (i.e., 101,325 Pa) was selected for the 12 outlets to simulate an open environment model (not a vacuum) (SolidWorks, 2012). The goal of this study was to obtain the CFD model airflow data for each outlet. Therefore, the 'volume flowrate' feature was selected as the surface goal for each of the 12 outlets, under the 'goals' icon in the SFSDT.

b) Solving stage

The solving stage ('run') is controlled by Solidworks and doesn't require user input. After the 3D model mesh has been automatically generated, the Navier-Stokes equations are solved. The Navier-Stokes differential equations are the basis of the CFD model and are governed by the mass, momentum, and energy conservation laws, as shown in Equations 1 to 3. In this study, these equations predict the air velocity in each outlet, and pressure changes through the geometry of the plenum (Jin and Webster, 2006; Sobachkin and Dumnov, 2013; Jonuskaite, 2017). Navier-Stokes equations derivatives, explicit definition of boundary conditions, and behavior with different fluids are described by Deissler, (1976); Inoue and Funaki, (1979); Bistafa, (2017); Drazin and Riley, (2006); Łukaszewicz and Kalita, (2016); Galdi, (2011).

$$\frac{\partial \rho}{\partial t} + \nabla . (\rho U) = 0 \quad \ldots\ldots\ldots\ldots\ldots\ldots \quad (1)$$

$$\frac{\partial \rho U}{\partial t} + \nabla . (\rho U \times U) = \nabla . \{-p\delta + \mu[\nabla U + (\nabla U)^T]\} + S_M \quad \ldots\ldots\ldots \quad (2)$$

$$\frac{\partial \rho h}{\partial t} + \nabla . (\rho U h) = \nabla . (\lambda \nabla T) + S_E \ldots\ldots\ldots\ldots\ldots\ldots \quad (3)$$

Where

ρ = *air* density (kg/m^3). ρ is 1.204 kg/m^3

U = *air* velocity vector (m/s)

μ = dynamic air viscosity (mPa. s). μ is 0.01825 mPa.s

S_M = momentum source (kg/m^2. s^2)

h = specific static enthalpy (J/kg).

λ = *air* thermal conductivity (W/m. K). λ is 0.02514 W/m. K

S_E = energy source (Kg/m. s^3)

c) Post processing

After solving the model, surface plots were generated to visualize the results. Surface plots reflecting the pressure distribution within the plenum with and without the divider were developed to study and justify the role of the divider, as discussed in Section 3.1. Also, outlet airflow data was exported by selecting the 'Results' icon, then 'Goal Plots' feature under the SFSDT.

2.1.3 Drawing Environment

The 2D engineering drawings are developed reflecting the dimensions of the air distributor. Dimension optimization for the air distributor was based on fixed and variable parameters. Fixed parameters were selected based on space available, applicability, and design feasibility, including: 1) The overall (including outlets) air distributor dimensions of 3 m long to dry properly sized stockpiles, and a width of 0.5 m, based on the available space within the SHAD A-frame; 2) Outlet dimensions, which were 0.1 diameter, 0.1 m length, and 0.6 m spacing from each other, sufficient to cover the length of the plenum. Variable parameters were optimized to provide the lowest deviation between the outlets' air delivery by applying the SolidWorks 'parametric' tool, which include the: 1) Angle of inclination of the outlets (θ); 2) longitudinal distance from both ends of the divider (y) (Fig 3.4a); and 3) vertical distance on the front end of the divider (x) (Fig 3.4b). The air distributor with angle $\theta = 45$, x = 0.2 m, and y = 3 m showed the lowest standard deviation of airflow for all the 12 outlets when a CFD simulation was run in comparison to alternative dimensions (Table 1). Appendices I and II show the dimensions and orthographic engineering drawings of the plenum and divider.

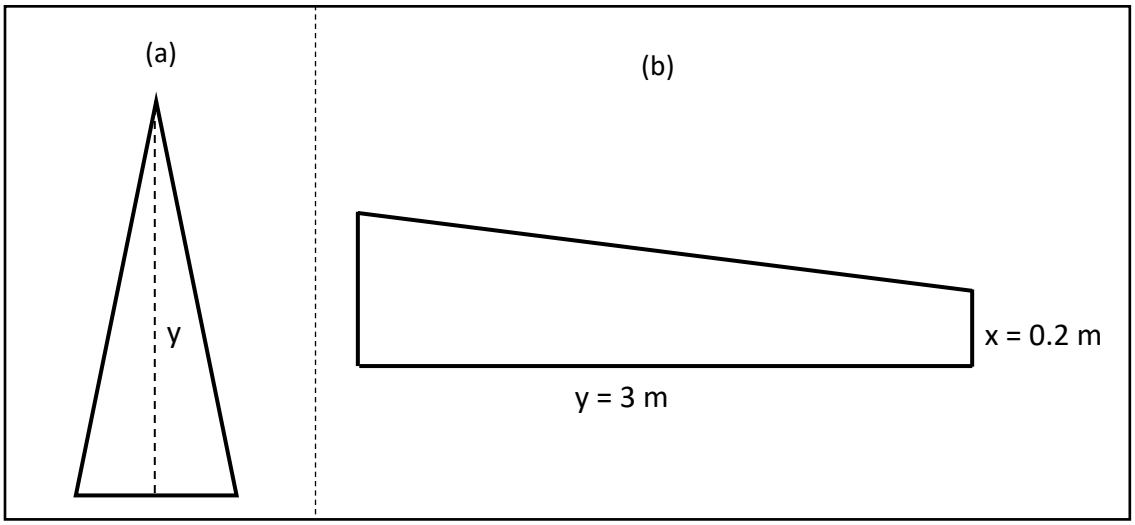

Figure 3.4. Schematic representation of the Divider showing the: (a) top, and (b) side views

Table 1: Variable parameters for the air distributor

Outlet angle of inclination	30	45	60	70	90	
(θ in degrees)	×	✓	×	×	×	
Divider Height	0.17	0.18	0.19	0.2	0.21	0.22
(x in m)	×	×	×	✓	×	×
Divider Length	2.5	2.6	2.7	2.8	2.9	3.0
(y in m)	×	×	×	×	×	✓

2.2 Fabrication and Placement of Air Distributor

The air distributor (Figs 3.5a, b, and c), comprising the plenum and divider, was built at the Biological and Agricultural Engineering (BAE) fabrication shop at UC Davis. Both components were fabricated from 18 GA carbon steel sheets.

2.3 In-Field Airflow Measurements

The air distributor was connected to the SHAD without interference and in an open outdoor space to measure the airflow in each outlet. The SHAD consists of a 1.49 kW (2 hp) propane heated vane

axial fan with a 457.2 mm diameter outlet (Sukup Manufacturing Co, Sheffield, IA, USA). The propane-heated fan was powered by a 12 kW (16 hp) generator (Model 100297, Champion Global power equipment, Santa Fe Springs, CA, USA). Two straight 304 stainless steel ducts of dimension 152.4 mm diameter, 1.5 m length, and one 152.4 mm diameter high temperature rigid 304 stainless steel hose were used to connect the outlet of the SHAD's fan to the inlet of the air distributor, as shown in Figure 3.5d.

Two pitot tube sensors were used to measure the delivered inlet airflow from the SHAD, and airflow outputs from each outlet. One pitot tube (DS 300 flow sensors, Dwyer Instrument Inc, Michigan City, IN, USA) was inserted in a 0.15 m pipe connecting the outlet of the fan to the air distributor, 2.2 m away from the fan to measure inlet airflow under approximate laminar flow (Cengel & Cimbala, 2017). The second pitot tube (PAFS-1010 flow sensors, Dwyer Instrument Inc, Michigan City, IN, USA) was inserted in a 0.1 m pipe connected to the air distributor outlets, 2.4 m away from the outlets to measure outlet output airflow without entry effects (laminar flow), as shown in Figure 3.5e. A pressure sensor (Series MS Magnesense, Dwyer Instruments Inc, Michigan City, IN, USA) was connected to each of the pitot tubes to record the static and total pressure at 5 second intervals. The difference between total and static pressures yields the velocity pressure (Pv). Airflow (Q) was calculated in m^3/s using Equations 4 and 5 (Cengel & Cimbala, 2017).

$$V = \sqrt{\frac{2P_v}{\rho}} \qquad (4)$$

$$Q = AV \qquad (5)$$

Where,

V = Velocity of airflow (m/s).

A = Pipe area (m^2). A = 0.018, and 0.008 m^2 for the inlet pipe and each of the outlets, respectively.

ρ = Air density (kg/m^3).

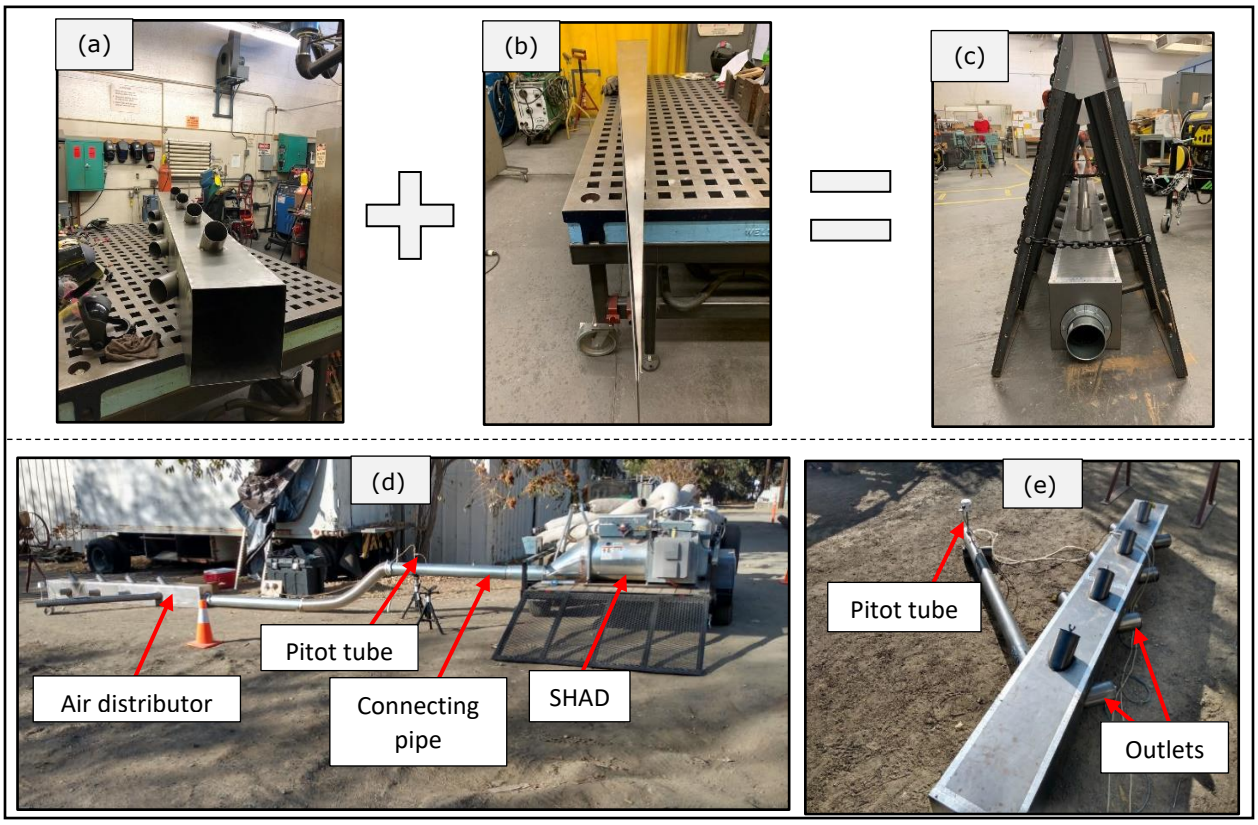

Figure 3.5. Picture showing (a) Plenum, (b) Divider, (c) Air distributor assembly (combination of plenum and divider) placed underneath the SHAD A-frame. (f). Set-up of the in-field experiment. (g) Air distributor with an embedded pitot tube.

An average heated drying T of 55.37 ºC and ambient drying T of 16.69 ºC measured by an embedded T sensor (HX94C, Omega Engineering Inc, Norwalk, CT, USA) were used to calculate the density of air ρ, as stated in Equation 6 (Dickerson et al., 1979).

$$\rho = \frac{P \times m}{n \times R \times T} \qquad (6)$$

Where,

P = Atmospheric pressure (101,325 Pa)

m = Air molar mass (0.02896 kg/mol)

n = Number of moles (taken as 1 to match units of molar mass)

R = Gas constant (8.3145 J/Kmol)

Percentage flow distribution (β) in the air distributor outlets was calculated using Equation 7 (Hassan et al., 2014), reflecting the airflow contribution of each outlet or group of outlets in relation to the inlet airflow.

$$\beta = \frac{Q_i}{Q} \times 100 \qquad (7)$$

Where,

i = Outlet number

β = Flow ratio for the ith outlet

Qi = Air flow rate of the ith outlet (m^3/s)

Q = Inlet airflow (m^3/s)

2.4 CFD Air Distributor Model Validation

The CFD model validation was performed by comparing the in-field airflow measurements with CFD model simulation output airflow data. The percentage Root Mean Square Error (%Error) was used to determine the variation between the in-field airflow and CFD airflow data, as shown in Equation 8 (Royapoor and Roskilly, 2015; Lee et al., 2020).

$$\%Error = \frac{\sqrt{\sum_{i=1}^{N_i} \frac{(M_i - S_i)^2}{N_i}}}{\frac{1}{N_i}\sum_{i=1}^{N_i} M_i} \times 100 \qquad (8)$$

Where;

i = Outlet number

Ni = Total number of outlets (12)

Si = Predicted CFD airflow for the ith outlet

Mi = Measured in-field airflow for the ith outlet

2.5 Air Distribution Optimization

Air distribution optimization was conducted to determine the optimum air distributor configuration and outlets that are likely to be sealed to properly distribute air through the almond stockpile. Optimization was performed by evaluating the changes in air distribution through subsequent sealing of outlets in Rows 1 through 4 with 152.4 mm diameter wingnut expansion plugs (McMaster-Carr Supply co, Santa Fe Springs, CA). Outlets in a sealed row that generate the lowest standard deviation (SD) of airflow, as calculated in Equation 9, from other open outlets are selected to achieve the optimized air distributor (Wan et al., 2014; Leys et al., 2013; Steven, 1979). In-field measurements for the optimized air distributor and its comparison with the CFD design were similarly generated as previously stated in sections 2.3 and 2.4.

$$SD = \sqrt{\frac{\sum Q_i^2 - \frac{(\sum Q_i)^2}{n}}{n-1}} \qquad (9)$$

Where

n = Total number of open outlets (n = 9)

Qi = Air flow rate of the ith outlet (m^3/s)

A useful air distributor should uniformly distribute the air through the outlets, based on a defined total airflow requirement. Most air distribution systems, such as building ventilation units (Mu et al., 2009; Lin et al., 2005), parallel flow heat exchangers (Wang et al., 2011; Camilleri et al., 2015), tray dryers (Misha et al., 2015), and bin dryers (Tórrez et al., 1998), aim at outputting the same amount of air through every outlet. On the contrary, the SHAD air distributor needs to consider

the cone shape of the almond stockpile. Due to the almond stockpile shape, it is desired that most of the airflow is delivered to the outlets in the middle section (Rows 2 and 3), as this is the section containing the most almonds.

3.0 Results and Discussion

3.1 Role of The Divider

Figure 3.6a and b show the surface plots that reflect the pressure distribution within the plenum with and without the divider, respectively. Air follows the path of least resistance (RSES, 2009). Thus, pressure builds up along the longitudinal path of the plenum rather than heading to the outlets in the absence of the divider. On contrary, the presence of the divider reduces the pressure buildup in the plenum and guides it to the outlets. (Allan, 2002; Hassan et al., 2014)

3.2 In-Field Airflow Measurements

Figure 3.6c shows the in-field airflow measurement results (line graph) when all the air distributor outlets are open and corresponding β-values (bar graph). Row 1 (outlets 1-3) yielded the lowest β-value of 4.1%. A low average β-value for outlets in Row 1 corresponds to lower pressure inside the plenum due to the largest lateral distance between the divider and the outlets. (Delele et al., 2013; Haroun and Raynal, 2013). A decrease in the lateral distance between the divider and outlets leads to an increase in β-value. Thus, the β-value for Outlets in Row 2 (Outlets 4-6), Row 3 (Outlets 7-9), and Row 4 (Outlets 10 – 12) were 30.8, 44.9, and 20.2%, where the middle section air distributor (Region of Row 2 and Row 3) outputs most of the airflow. Future work will explore an air distributor design with and increased overall length for larger stockpiles.

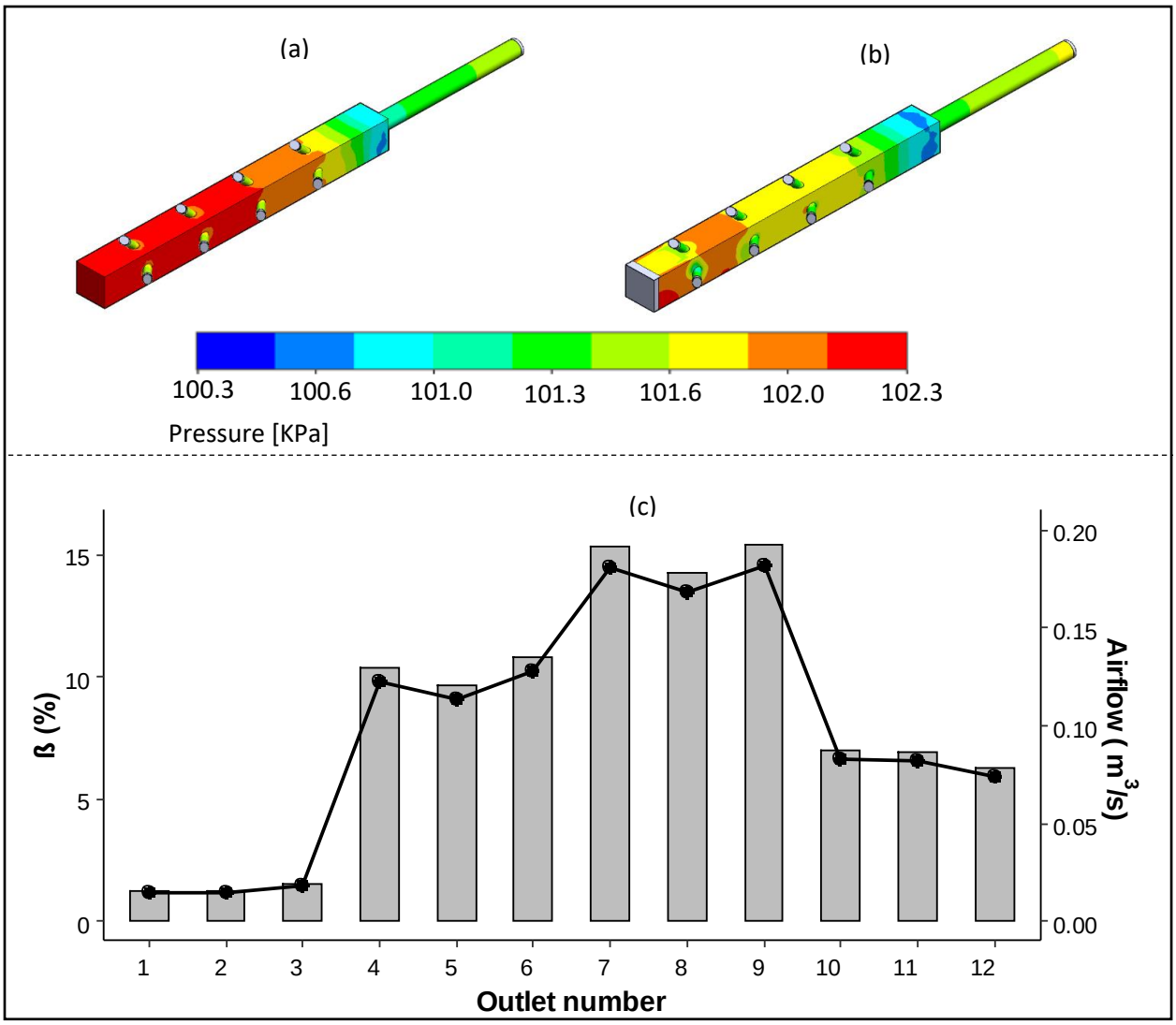

Figure 3.6. Surface plots showing the pressure distribution of the air distributor: (a) without divider, and (b) with divider. (c) Percentage airflow distribution (bar graph) and airflow rate (line graph) when all outlets are open.

3.3 Cfd Air Distributor Model Validation

Figure 3.7 shows the comparison between the airflow data obtained from the in-field airflow measurements and the CFD airflow data when all the outlets are open. The mean %Error was equal to 31.21%. Even though high, the discrepancy between the CFD model outputs and in-field measurements can be potentially attributed to iteration and grid convergence, discrepancies between the physical properties of the fabricated air distributor in comparison to the digital CFD model, placement of the divider within the plenum, and high variability of in-field measurements.

The highest %Error was observed in the airflow outputs for Row 1 (outlets 1-3). In addition, as previously stated in section 3.1, Row 1 outlets also produced the least amount of airflow. Therefore, there is a need to further optimize the design and consider implementing a 3-row, instead of a 4-row air distributor configuration (section 3.2).

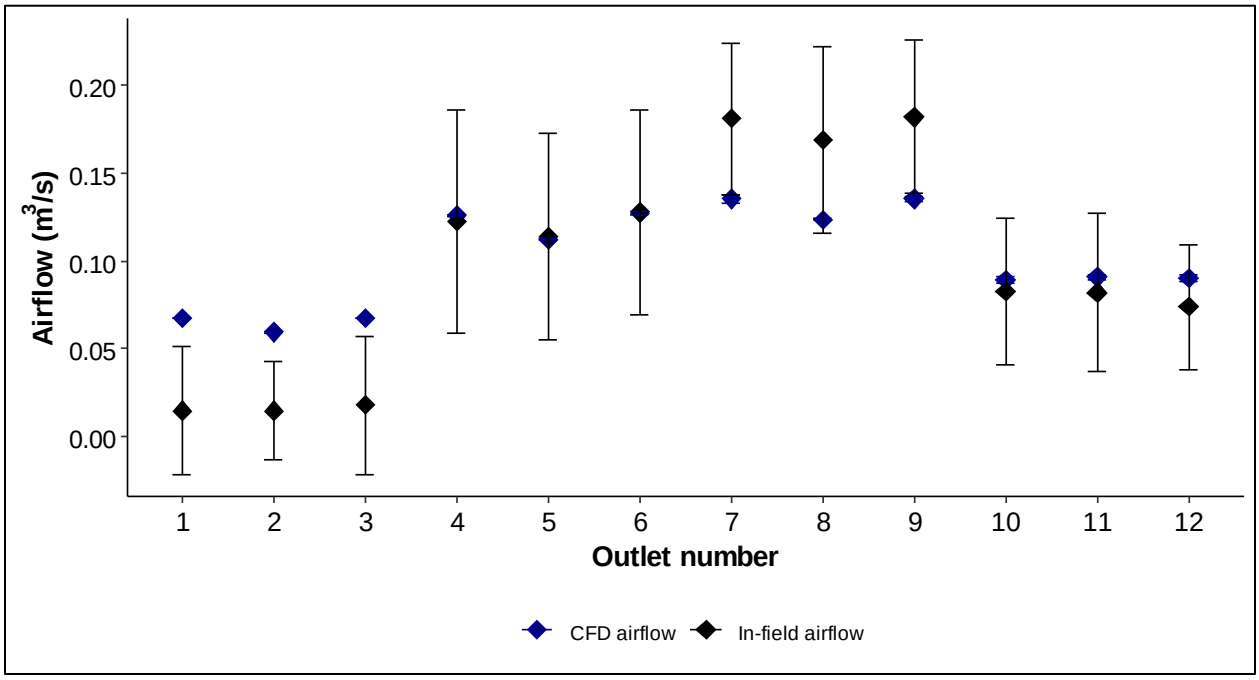

Figure 3.7. Airflow for CFD airflow and in-field airflow measurements, when all the outlets are open.

Other CFD modeling studies have yielded a wide range of error rates, partly based on model complexity, and environmental conditions that cannot be entirely included in the CFD design and simulation (Celik et al., (2007). On the low end (< 10 %Error); Sonthikun et al., (2016) reported a %Error of between 2.3 and 5.9% when simulating the temperature and airflow distribution of a solar biomass dryer; Fohimi et al., (2020) predicted the air ventilation and thermal comfort of an Atrium space with a %Error of less than 3%; Antony and Shyamkumar, (2016) simulated the air velocity of a fluidized bed dryer with a %Error of between 4.7 and 8.23%; and Zhang et al. (2016) predicted the air temperature and velocities for aeration of an indoor plant factor system with a %Error of 8.9% and 7.5%, respectively. Higher errors rates include studies by Ali et al., (2012)

who predicted the velocity and temperature of a ship's cabin air distributor with a %Error of 20.3% and 5.7%, respectively; Ameer et al., (2016) predicted air velocity distribution and ventilation effectiveness of wind towers with a %Error of 1.58 to 24.3%; and Lawrence and Maier, (2011) obtained a %Error of 4.4% and 23.1% at the center and periphery, respectively for airflow distribution in a maize silo with different grain mass configurations.

3.4 Air Distributor Optimization

Based on what was learned in section 3.2, a 3-row configuration air distributor was evaluated to divide stockpile air distribution into three sections (rows), rather than four. Figure 3.8 shows the air distributor in-field airflow measurement results (line graph) and corresponding β-values (bar graph) when outlets in rows 1 (a), 2 (b), 3 (c), and 4 (d) were subsequently sealed off. Sealing off outlets in row 1 yielded the lowest airflow SD on the open outlets (0.03 m^3/s), in comparison to sealing off rows 2 (0.06 m^3/s), 3 (0.04 m^3/s), and 4 (0.06 m^3/s). An air distributer partitioned into three sections yields β-values of 31.3, 44.4, and 24.3 %, as seen in Figure 3.9.

3.5 Optimized Model Validation

Figure 3.10 shows the comparison between the in-field measured airflows and the CFD-generated airflow data, based on the optimized air distributor design. The %Error of the optimized design was equal to 14.72 %, which is within an acceptable range in relation to other studies (Sonthikun et al., 2016; Fohimi et al., 2020; Shyamkumar, 2016; Zhang et al. 2016; Ali et al., 2012; Ameer et al., 2016; Maier, 2011). Proper air distribution to the stockpile can be achieved by either sealing off a selected group of outlets, as described in section 3.3, or through proper placement of the air distributor within the SHAD's A-frame. More specifically, the air distributor can be placed towards the entrance of the SHAD's A-frame so that the outlets in Rows 2, 3, and 4 are underneath the tallest section of the stockpile (center), as done in Chapter 4. Most importantly, the optimized

air distributor delivers air to the almond stockpile in relationship to their natural shape. Additional studies (Chapter 4) focused on evaluating the effect of the air-distributor when used along with the SHAD, as an alternative to conventional windrow drying.

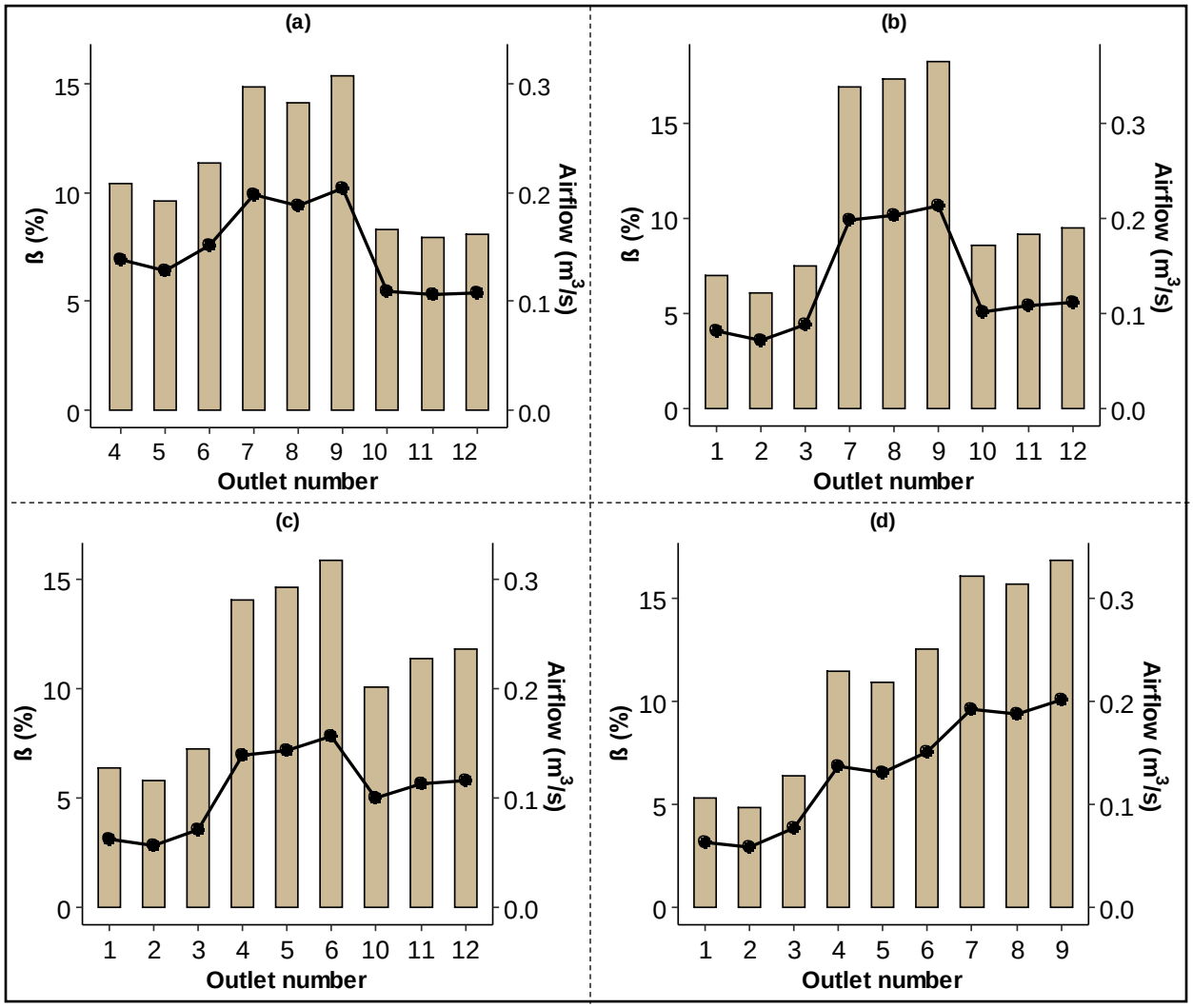

Figure 3.8. Percentage airflow distribution and airflow rate when sealing of outlets in rows (a) 1, (b) 2, (c) 3, and (d) (4).

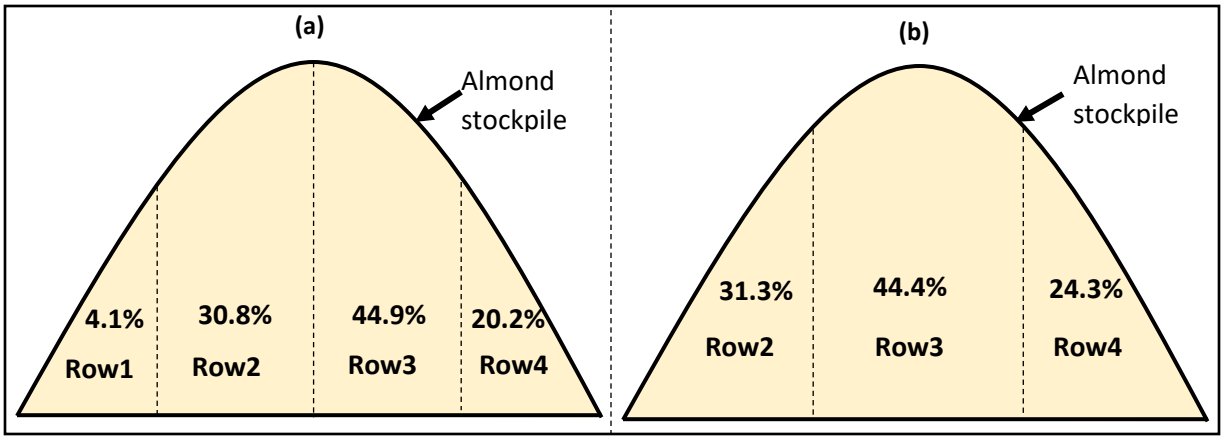

Figure 3.9. Schematic representation of an almond stockpile receiving air from an air distributor with a (a) 4-row configuration (a), and 3-row configuration and their corresponding β-values.

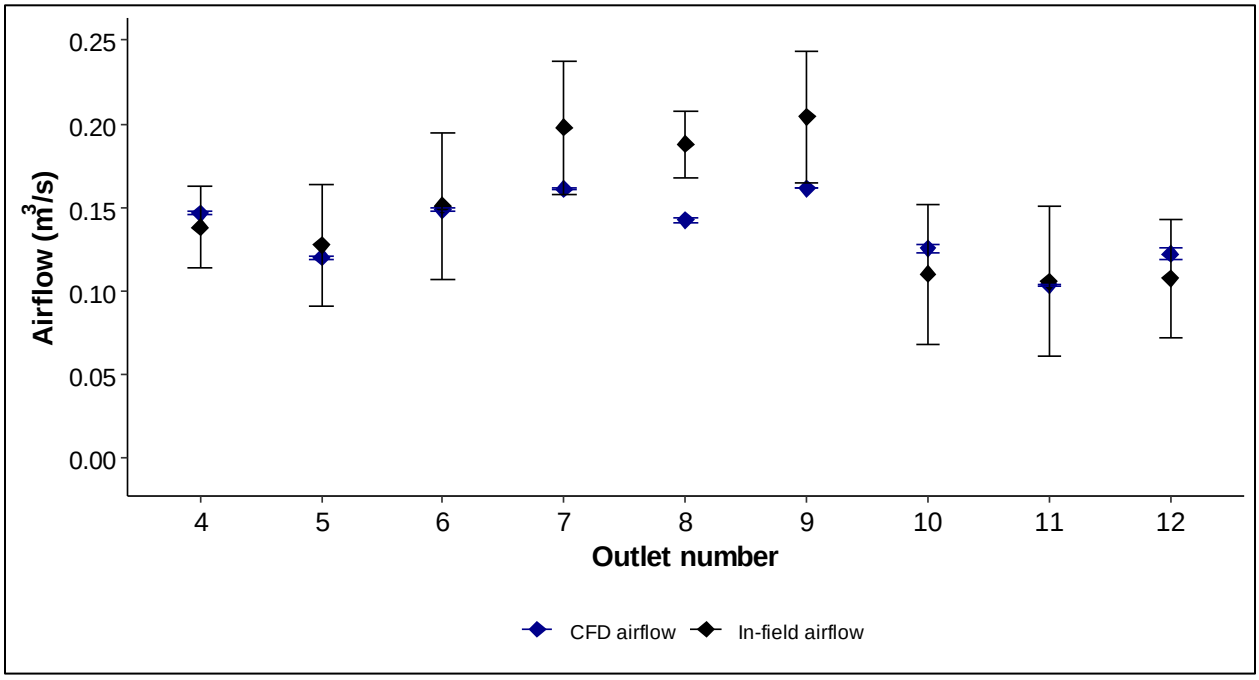

Figure 3.10. Airflow for in-field airflow and CFD airflow when outlets in row 1 are sealed off.

4.0 Conclusion

In-field airflow measurements from the 12-outlet air distributor yielded β-values equal to 4.1, 30.8, 44.9, and 20.2 % of the air distributed to outlets in rows 1, 2, 3, and 4, respectively. This leads to a low air distribution for almonds in the row 1 region. Therefore, optimization analysis showed that the air distributor can be transformed into a 3-row configuration when outlets in row 1 are sealed off. Sealing off outlets in row 1 leads to β-values of 31.3, 44.4, and 24.3% for outlets in

rows 2, 3, and 4, respectively. The 3-row air distributor configuration is desired, since the middle and tallest section of the stockpile, which contains the majority of the almonds, will receive the most airflow. Air distributor optimization showed that the %Error between the in-field airflow measurements and CFD airflow data was 31.21% and 14.72% for the initial model (4-row configuration) and optimized model (3-row configuration with outlets in row 1 sealed off), respectively. Comparison with other studies showed that the %Error of the 4-configuration model is beyond limits, but the optimized 3-configuration model is within acceptable limits. The optimized 3-row air distributor configuration yielded desirable β-values and can be used to enhance almond stockpile air distribution. Future work will focus on testing the effectiveness of the air distributor in stockpile drying. Also, an optimized 3-row configuration air distributor will be developed and evaluated to dehydrate larger almond stockpiles.

References

Allan Daly, P. E. (2002). Underfloor air distribution: lessons learned. ASHRAE journal, 44(5).

Ali, A. A., Elsafty, A. F., & Elsayed, A. A. (2012). CFD Investigation of indoor air distribution in marine applications. European Journal of Scientific Research, 88(2), 196-208.

Ameer, S. A., Chaudhry, H. N., & Agha, A. (2016). Influence of roof topology on the air distribution and ventilation effectiveness of wind towers. Energy and Buildings, 130, 733-746.

Antony, J., & Shyamkumar, M. B. (2016). Study on sand particles drying in a fluidized bed dryer using CFD. International Journal of Engineering, 8(2), 129-145.

Awbi, H. B. (1998). Energy efficient room air distribution. Renewable Energy, 15(1-4), 293-299.

Bistafa, S. R.. (2017). On the development of the Navier-Stokes equation by Navier. Revista Brasileira De Ensino De Física, 40(2). https://doi.org/10.1590/1806-9126-rbef-2017-0239

Bhatia, A. (2001). HVAC-How to Size and Design Ducts. PDH online Course, (M06-032), 22-25.

Camilleri, R., Howey, D. A., & Mcculloch, M. D.. (2015). Predicting the flow distribution in compact parallel flow heat exchangers. Applied Thermal Engineering, 90, 551–558. https://doi.org/10.1016/j.applthermaleng.2015.07.002

Celik, I., Karaismail, E., & Parsons, D. (2007, December). A reliable error estimation technique for CFD applications. In AVT-147 Symposium on Computational Uncertainty in Military Vehicle Design.

Cengel, Y. A., & Cimbala, J. M. (2017). Fluid mechanics: Fundamentals and applications (4th ed.). McGraw-Hill Education.

Delele, M. A., Ngcobo, M. E. K., Getahun, S. T., Chen, L., Mellmann, J., & Opara, U. L.. (2013). Studying airflow and heat transfer characteristics of a horticultural produce packaging system using a 3-D CFD model. Part II: Effect of package design. Postharvest Biology and Technology, 86, 546–555. https://doi.org/10.1016/j.postharvbio.2013.08.015

Deissler, R. G. (1976). Derivation of the Navier–Stokes equation. American Journal of Physics, 44(11), 1128-1130.

Drazin, P. G., & Riley, N. (2006). The Navier-Stokes equations: a classification of flows and exact solutions (Vol. 334). Cambridge University Press.

Fohimi, N. A. M., Asror, M. H., Rabilah, R., Mohammud, M. M., Ismail, M. F., & Ani, F. N. (2020). CFD Simulation on Ventilation of an Indoor Atrium Space. CFD Letters, 12(5), 52-59.

Hassan, J. M., Mohamed, T. A., Mohammed, W. S., Alawee, W. H. (2015). Experimental and Numerical Study on the Improvement of Uniformity Flow for Three-Lateral Dividing Manifold, 12(1), 29–37.

Hassan, J. M., Mohamed, T. A., Mohammed, W. S., Alawee, W. H. (2014). Modeling the Uniformity of Manifold with Various Configurations. Journal of Fluids, 2014, 1–8. https://doi.org/10.1155/2014/325259

Inoue, A., & Funaki, T.. (1979). On a new derivation of the Navier-Stokes equation. Communications in Mathematical Physics, 65(1), 83–90. https://doi.org/10.1007/bf01940961

Figliola, R. S., & Beasley, D. E. (2006). Theory and design for mechanical measurements. Hoboken, N.J: John Wiley.

Gandhi, M. S., Ganguli, A. A., Joshi, J. B., Vijayan, P. K. (2012). CFD simulation for steam distribution in header and tube assemblies. Chemical Engineering Research and Design, 90(4), 487–506. https://doi.org/10.1016/j.cherd.2011.08.019

Galdi, G. (2011). An introduction to the mathematical theory of the Navier-Stokes equations: Steady-state problems. Springer Science & Business Media.

Jin, H., Bauman, F., & Webster, T. (2006). Testing and modeling of underfloor air supply plenums.

Jones, W. P. (2019). Air Distribution. Air Conditioning Applications and Design, 231–259. https://doi.org/10.4324/9780080498935-5

Jonuskaite, A. (2017). Flow Simulation with SolidWorks, 1–52.

Konzo, S. (1953). Investigation of the pressure losses of takeoffs for extended-plenum type air conditioning duct systems. University of Illinois at Urbana Champaign, College of Engineering. Engineering Experiment Station..

Lawrence, J., & Maier, D. E. (2011). Three-dimensional airflow distribution in a maize silo with peaked, levelled and cored grain mass configurations. Biosystems engineering, 110(3), 321-329.

Lee, M., Park, G., Park, C., & Kim, C. (2020). Improvement of Grid Independence Test for Computational Fluid Dynamics Model of Building Based on Grid Resolution. Advances in Civil Engineering, 2020.

Leys, C., Ley, C., Klein, O., Bernard, P., & Licata, L.. (2013). Detecting outliers: Do not use standard deviation around the mean, use absolute deviation around the median. Journal of Experimental Social Psychology, 49(4), 764–766. https://doi.org/10.1016/j.jesp.2013.03.013

Lin, Z., Chow, T. T., Tsang, C. F., Fong, K. F., & Chan, L. S.. (2005). CFD study on effect of the air supply location on the performance of the displacement ventilation system. Building and Environment, 40(8), 1051–1067. https://doi.org/10.1016/j.buildenv.2004.09.003

Lombard, M. (2018). Mastering SolidWorks. John Wiley & Sons.

Łukaszewicz, G., & Kalita, P. (2016). Navier–Stokes Equations: An Introduction with Applications. Springer.

Misha, S., Mat, S., Rosli, M. A. M., Ruslan, M. H., Sopian, K., & Salleh, E. (2015). Simulation of air flow distribution in a tray dryer by CFD. In Recent Advances in Renewable Energy Sources, Proceedings of the 10th International Conference on Energy & Environment (EE'15) (pp. 126-135).

Mu, Z., Ren, Y., & You, S.. (2009). Experimental Research of Reversible Ventilation System Which Can Improve IAQ. https://doi.org/10.1109/icbbe.2009.5162816

Munson, B. R., Young, D. F., & Okiishi, T. H. (2006). Fundamentals of fluid mechanics. Hoboken, NJ: J. Wiley & Sons.

Nielsen, P. V. (2015). Fifty years of CFD for room air distribution. Building and Environment, 91, 78-90.

Nielsen, P. V. (2007). Analysis and design of room air distribution systems. HVAC&R Research, 13(6), 987-997.

Qin, R., Duan, C. (2017). The principle and applications of Bernoulli equation. *Journal of Physics: Conference Series*, *916*(1). https://doi.org/10.1088/1742-6596/916/1/012038

Riveros, H. G., Riveros-Rosas, D. (2010). Laminar and turbulent flow in water. Physics Education, 45(3), 288–291. https://doi.org/10.1088/0031-9120/45/3/010

Royapoor, M., & Roskilly, T. (2015). Building model calibration using energy and environmental data. Energy and buildings, 94, 109-120.

RSES. (2009). Refrigeration Service Engineers Society. Air flow Measurement. Sam Application Manual Chapter 630-104, Section 11A. Retrieved from http://www.rses.org/assets/serviceapplicationmanual/630-104.pdf

RSES. (2008). Refrigeration Service Engineers Society. The Principles of Air Flow , Air Pressure , and Air Filtration. National Air Filtration Association. Retrived from http://www.rses.org/assets/serviceapplicationmanual/630-156.pdf

SIEMENS (2021). SIEMENS Digital Industries Software CFD Simulation. Retrieved from https://www.plm.automation.siemens.com/global/en/our-story/glossary/cfd-simulation/67873

Sobachkin, A., & Dumnov, G. (2013, June). Numerical basis of CAD-embedded CFD. In NAFEMS World Congress (pp. 9-12).

SolidWorks. (2015). introducing solidworks Contents. Dassault Systèmes SolidWorks, 128.

SolidWorks. (2012). Solidworks Flow Simulation 2012 Tutorial, 266.

SolidWorks. (2011). An Introduction to Flow Analysis Applications with SolidWorks Flow Simulation, Student Guide.

Sonthikun, S., Chairat, P., Fardsin, K., Kirirat, P., Kumar, A., & Tekasakul, P.. (2016). Computational fluid dynamic analysis of innovative design of solar-biomass hybrid dryer: An experimental validation. Renewable Energy, 92, 185–191. https://doi.org/10.1016/j.renene.2016.01.095

Steven, W., (1979). Why n—1 in the Formula for the Sample Standard Deviation?. The Two-Year College Mathematics Journal, 10(5), 330-333.

Subramanian, R. S. (2011). Continuity equation. Encyclopedia of Earth Sciences Series, Part 4(July 2019), 153. https://doi.org/10.1201/9781315156637-3

Tórrez, N., Gustafsson, M., Schreil, A., & Martínez, J.. (1998). Modeling And Simulation Of Crossflow Moving Bed Grain Dryers. Drying Technology, 16(9-10), 1999–2015. https://doi.org/10.1080/0737393980891750

Van Leer, B., Powell, K. G. (2010). Introduction to Computational Fluid Dynamics. Encyclopedia of Aerospace Engineering, (December 2010). https://doi.org/10.1002/9780470686652.eae048

Versteeg, H. K., & Malalasekera, W. (2007). An introduction to computational fluid dynamics: The finite volume method. Harlow, England: Pearson Education Ltd.

Wan, X., Wang, W., Liu, J., & Tong, T.. (2014). Estimating the sample mean and standard deviation from the sample size, median, range and/or interquartile range. BMC Medical Research Methodology, 14(1), 135. https://doi.org/10.1186/1471-2288-14-135

Wang, C. C., Yang, K. S., Tsai, J. S., Chen, I. Y. (2011). Characteristics of flow distribution in compact parallel flow heat exchangers, part I: Typical inlet header. Applied Thermal Engineering, 31(16), 3226–3234. https://doi.org/10.1016/j.applthermaleng.2011.06.004

Wendt, J. F., Anderson, J. D., & Von Karman Institute for Fluid Dynamics. (1992). Computational fluid dynamics: An introduction. Berlin: Springer-Verlag.

Zhang, Y., Kacira, M., & An, L. (2016). A CFD study on improving air flow uniformity in indoor plant factory system. biosystems engineering, 147, 193-205.

Appendix: Engineering Drawings of Plenum (Appendix I) and Divider (Appendix II)

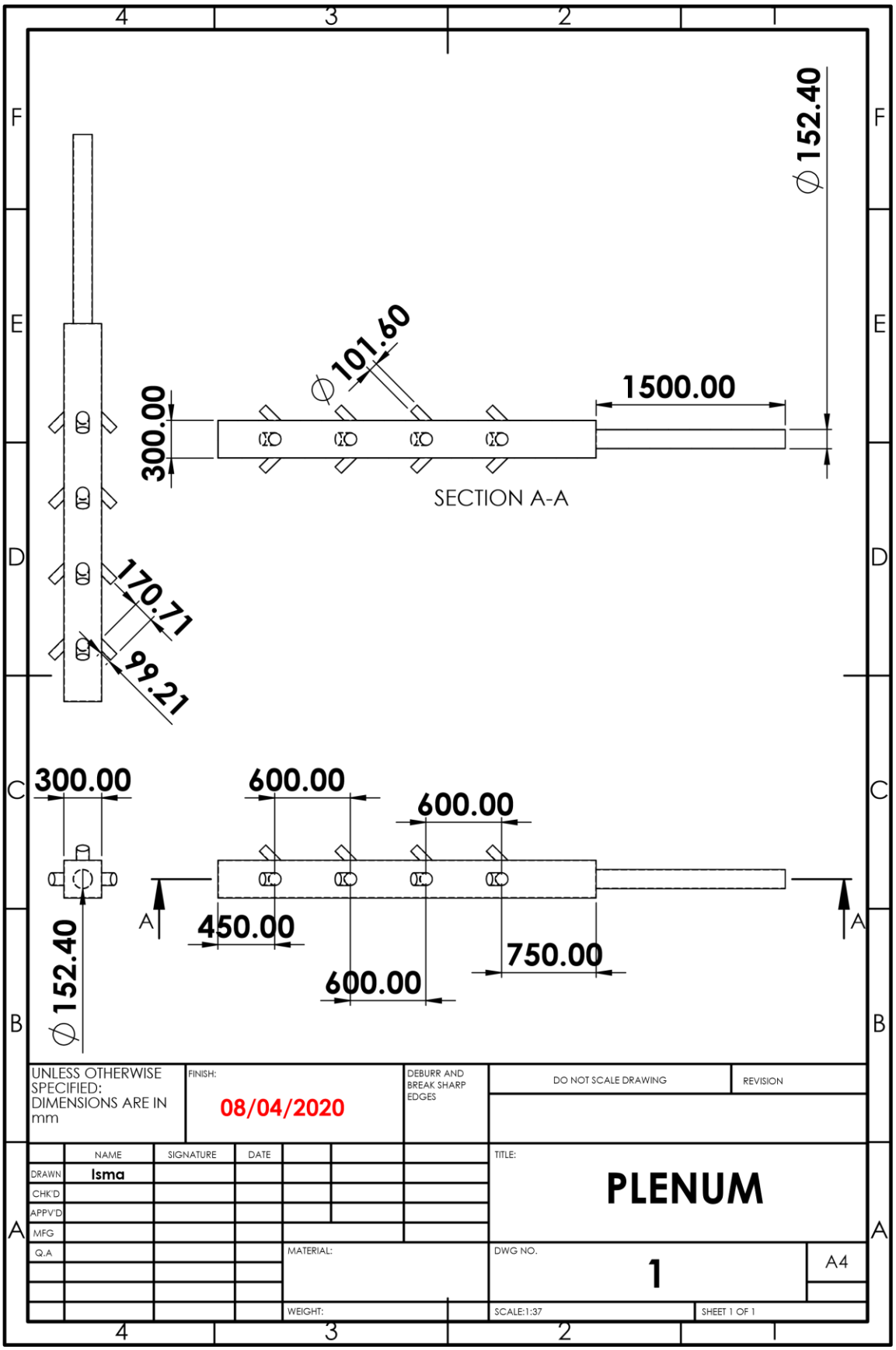
4
3
2
1
F
E
D
C
B
A
∅152.40
∅101.60
300.00
1500.00
SECTION A-A
170.71
99.21
300.00
600.00
600.00
A
A
450.00
750.00
600.00
∅152.40
UNLESS OTHERWISE SPECIFIED: DIMENSIONS ARE IN mm
FINISH:
08/04/2020
DEBURR AND BREAK SHARP EDGES
DO NOT SCALE DRAWING
REVISION
NAME
SIGNATURE
DATE
DRAWN
Isma
CHK'D
APPV'D
MFG
Q.A
TITLE:
PLENUM
MATERIAL:
DWG NO.
1
A4
WEIGHT:
SCALE:1:37
SHEET 1 OF 1

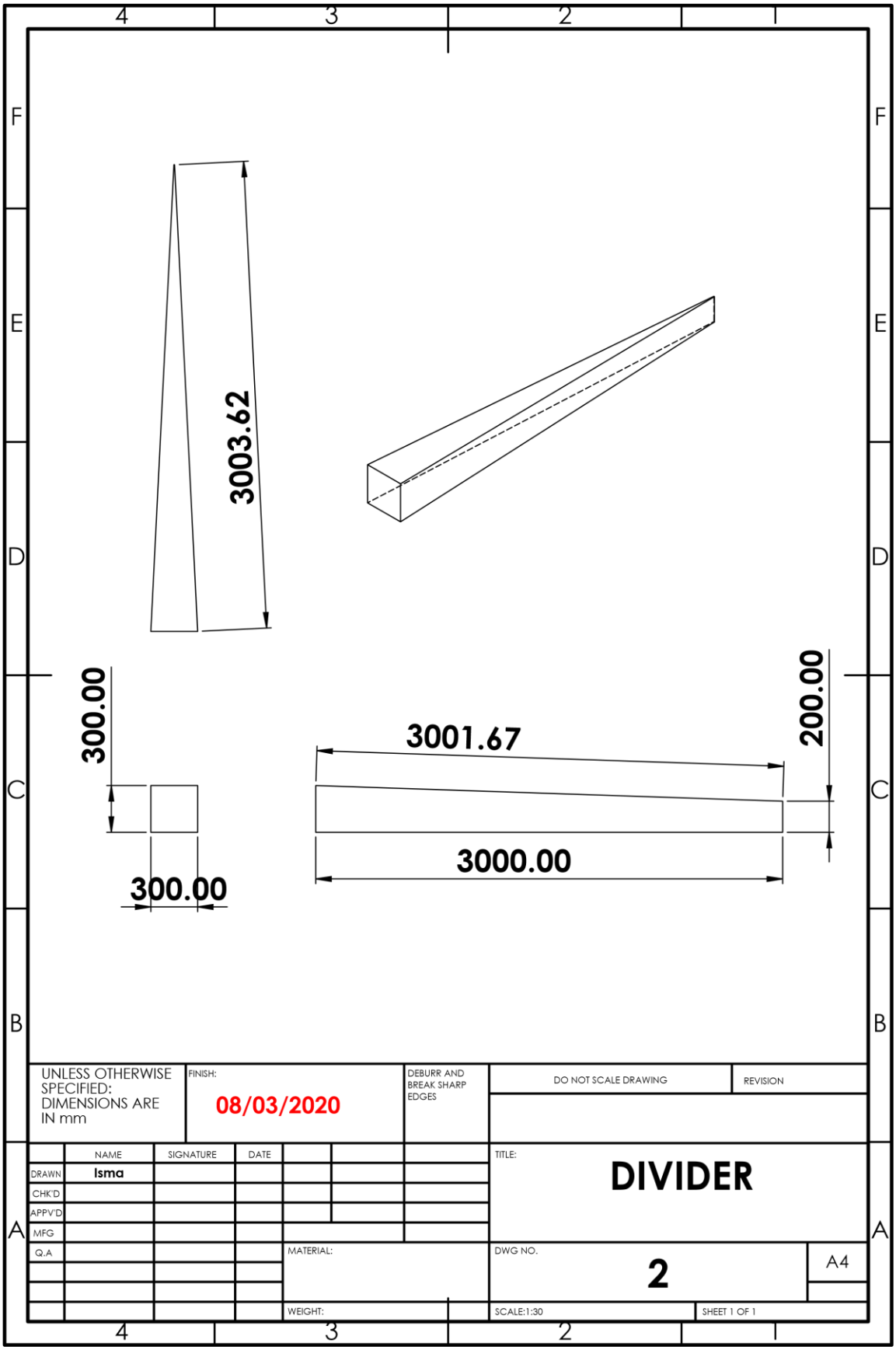
4
3
2
1
F
E
D
C
B
A
3003.62
300.00
300.00
3001.67
3000.00
200.00
UNLESS OTHERWISE SPECIFIED: DIMENSIONS ARE IN mm
FINISH:
08/03/2020
DEBURR AND BREAK SHARP EDGES
DO NOT SCALE DRAWING
REVISION
NAME
SIGNATURE
DATE
DRAWN
Isma
CHK'D
APPV'D
MFG
Q.A
TITLE:
DIVIDER
MATERIAL:
DWG NO.
2
A4
WEIGHT:
SCALE:1:30
SHEET 1 OF 1

CHAPTER 4

DRYING OF FRESHLY HARVESTED ALMONDS USING A STOCKPILE HEATED AND AMBIENT AIR DRYER (SHAD) WITH AN AIR DISTRIBUTOR

Abstract

A previous study indicated that an almond stockpile heated and ambient air dryer (SHAD) did not appropriately distribute air to the stockpile. Therefore, this project evaluated the effect of adding an air distributor within the SHAD A-frame as an alternative drying method to conventional windrow drying. Three almond stockpile drying experiments were performed on 'Nonpareil'(Np), 'Winter'(Wi), and 'Monterey'(Mo) varieties with different initial (fresh) weights and percentage kernel dry-basis moisture contents (MC_{db}) equal to 4,763 kg and 11.83 %, 2,585 kg and 11.46 %, and 6,849 kg and 21.49 %, respectively. All experiments were directly compared to conventional windrow drying. Almond quality parameters, including kernel Moisture Content dry-basis (MC_{db}), color, lipid oxidative stability, Peroxide Value (PV), Free Fatty Acid (FFA) content, internal cavities, and insect injury were measured before and after drying. Drying energy consumption, cost, and performance indicators which include Specific Moisture Extraction Rate (SMER), Moisture Extraction Rate (MER), and the Coefficient Of Performance (COP) were determined. Also, stockpile drying uniformity for the stockpile layers was evaluated. The SHAD with the air distributor uniformly dehydrated almonds in a maximum of 7-days to the desired MC_{db} of ≤ 6%, while conventional windrow drying took longer (up to 13.63), and the desired final MC_{db} was only reached during the 'Mo' trial. Drying cost, SMER, MER, and COP were directly related to the size of the stockpile equal to an average standard deviation of $ 9.5 ±5.2 per tonne of fresh almonds, 1.44 ±1.21 kg/kWh, 3.56 ±3.12 kg/h, and 4.73 ±2.58, respectively. All stockpile experiments generated desirable quality parameters. During the 'Np' and 'Mo' experiments, energy performance indicators were within or above acceptable limits when compared to other dryers in literature, and the SHAD dryer without an air distributor. Poor performance during the 'Wi' experiment is attributed to the underutilization of the SHAD, because of an undersized stockpile. Thus, the SHAD with an air distributor can be used to directly dehydrate almonds outdoors in stockpiles and can replace conventional windrow drying of almonds.

Keywords. Energy, Post-harvest, dehydration, Tree nuts

1.0 Introduction

Conventional windrow drying of almonds is prone to pest and human pathogen infestation. It affects timely irrigation and involves processes (picking and sweeping) that generate significant and undesirable dust (Perry et al., 1989; Schatzki and Ong, 2001; Martha et al, 2012; Downey et al., 2008; CARB, 2017; Goldhamer and Viveros, 2000). Therefore, a Stockpile heated and ambient air dryer (SHAD) was developed in Chapter 2 as an alternative that allows early harvest, timely irrigation, and eliminates dust-generating steps, such as the picking and sweeping of almonds (Mayanja et al., 2021). However, the SHAD did not properly distribute air to the stockpile, which resulted in a lack of drying uniformity through the stockpile layers. Additionally, the Coefficient Of Performance (COP) of the SHAD, equal to 1.33, was beyond the limits of other commercially available dryers (Chapter2; Mayanja et al., 2021). The latter suggests that the supplied air was not efficiently used to dehydrate almonds within the stockpile. Thus, showing the urgency to better distribute the drying air through the almond stockpile. Therefore, there is a need to develop an air distribution system that ensures uniform dispersion of drying air through the almond stockpile.

Air distribution systems are often used in dryers to deliver and uniformly distribute the drying air (heated or ambient) to achieve consistent drying of food under similar thermal conditions. The air distribution system mainly consists of: 1) A plenum chamber, which laminarizes the flow of the inlet air, before splitting it into multiple outlets; and 2) Outlets (air ducts, perforations, false floors), which are the drying air exit points aimed to dehydrate foods (IRRI, 2021). Numerous studies have documented the application of air distribution to the drying systems of various foods. Grain batch and continuous flow bin batch dryers for crops such as corn, rice, millet, and sorghum commonly contain a perforated plenum at the bottom of the drying bins (Bridge et al., 1986; Lawrence et al., 2015). Noyes (2006) used a horizontal configuration to distribute the drying air horizontally and

uniformly, where a perforated plenum containing multiple discharge ducts (outlets) was introduced in the centroid of the drying bin. The latter was based on the principle that a larger volume of air can be horizontally forced across a bin compared to vertically forcing the air while using the same fan power (Day and Nelson, 1962). A similar design, using the principle of horizontal air distribution was used by Alam et al. (2016), where a vertical concentric perforated plenum was introduced, and an axial fan placed at the top of the plenum to draw the drying air through a grain dryer.

In almonds, the air distribution concept is applied in almond bins or stadium dryers with a perforated bottom plenum (Chapter1). Chilka and Ranade (2019) developed an almond tray dryer with a centrifugal fan that draws ambient air into the dryer while perpendicularly exhausting the air through the outlet. The tray dryer has 6 heating coils that can regulate the temperature (T) of drying air. Further, Fielke and Coates (2017) conducted a study for on-farm mechanical drying of almonds and explored the use of: 1) Multiple equally spaced fans (total of 8 fans) blowing ambient air into the false floor of a shed drying facility; 2) Shipping container with a fan on the side, horizontally blowing air through the almonds; and 3) Open-ended triangular A-frame across the center of a stockpile with a fan on each end of the A-frame blowing ambient air into the stockpile. The latter doesn't control the direction of airflow especially in the middle section of the stockpile.

Thus, an air distributor comprising of 12 outlets using both vertical and horizontal air distribution was developed as an additional component of the SHAD. The air distributor was placed within the SHAD A-frame, underneath the almond stockpile aimed at improving drying uniformity in the stockpile. Hence, reducing energy consumption, and drying time while maintaining desirable almond quality.

This study focuses on evaluating the effect of an air-distributor when used along with SHAD, as an alternative for conventional windrow drying. To evaluate this, three almond stockpiles of three different varieties which include 'Nonpareil'(Np), 'Winter'(Wi), and 'Monterey'(Mo) containing an initial mass of 4,763, 2,585, and 6,849 kg, respectively were dehydrated from their initial kernel dry basis moisture content (MC_{db}) of 11.83 ± 1.99% ('Np'), 11.46 ± 0.60% ('Wi '), and 21.49 ± 2.11% ('Mo') to desired a storage condition of less than or equal to 6% MC_{db}. Windrow conventional drying experiments were held in parallel to the stockpile experiments for direct comparison. Measured quality parameters included kernel decay or mold damage, insect injury, presence of internal cavities, lipid oxidative stability, color, Peroxide Value (PV), and Free Fatty Acid (FFA) content. Also, energy cost and energy parameters including the Specific Moisture Extraction Rate (SMER), Moisture Extraction Rate (MER), and COP were calculated and compared with the previous study which did not use an air distributor in the SHAD and other commercially available dryers (Mayanja et al., 2018).

2.0 Materials and Methods

2.1 Sample preparation

Three drying experiments were conducted at NICKELS Soil Laboratory (Arbuckle, Calif.) for 'Np', 'Wi', and 'Mo' almond varieties. Each experiment comprised stockpile and windrow experiments conducted in parallel. Forty-two samples were prepared for each of the three experiments as described in Chapter 2 and Mayanja et al, (2021).

2.2 Drying equipment and ambient drying conditions

The mobile stand-alone SHAD drying system and weather station were the same as used in chapter 2 and Mayanja et al, (2021). In addition, an air distributor (Fig 4.1a) was placed within the SHAD A-frame. The air distributor is 3m long and contains twelve 101.6 mm diameter outlets. Each of

the three sides of the air distributor (left, right, and top) contains 4 outlets to ensure that the drying air supplied by SHAD, is evenly distributed through the stockpile. A high-T rigid 304 stainless steel duct of 152.40 mm diameter was used to connect the propane heated fan within the SHAD to the air distributor. The duct contains an embedded T and Relative Humidity (RH) sensor (HX94C, Omega Engineering Inc, Norwalk, CT) placed 2.2 m from the propane heated fan.

2.3 Almond drying and sample distribution

Almonds were directly deposited onto the A-frame from the conveyer cart until a third of the final stockpile height was achieved to form the bottom layer, 5 replicates of almond mesh bags weighing about 0.6 kg each containing T/RH sensors were placed on the partial almond stockpile. The procedure was repeated for the middle (two-thirds of final stockpile height) and top layers (final stockpile height). Also, the stockpile dimension for the 'Np', 'Wi', and 'Mo' drying experiments were 4.9 m x 3.6 m x 1.6 m (l x w x h), 3.6 m x 2.4 m x 1.5 m, and 7.3 m x 4.9 m x 1.6 m at a weight equal to 4,763, 2,585, and 6,849 kg respectively. An inbuilt weighing scale recorded the almond weight on the conveyer cart. In parallel, three side-by-side almond windrows were built (Fig 4.1b) within the almond field next to the stockpile experiments to monitor conditions during conventional windrow drying. Each windrow contained 5 almond mesh bags with T/RH sensors. After drying, samples from the stockpile and windrows (n=15 from each) were immediately transported to the post-harvest engineering laboratory at UC Davis to test for final MC_{db} and quality parameters.

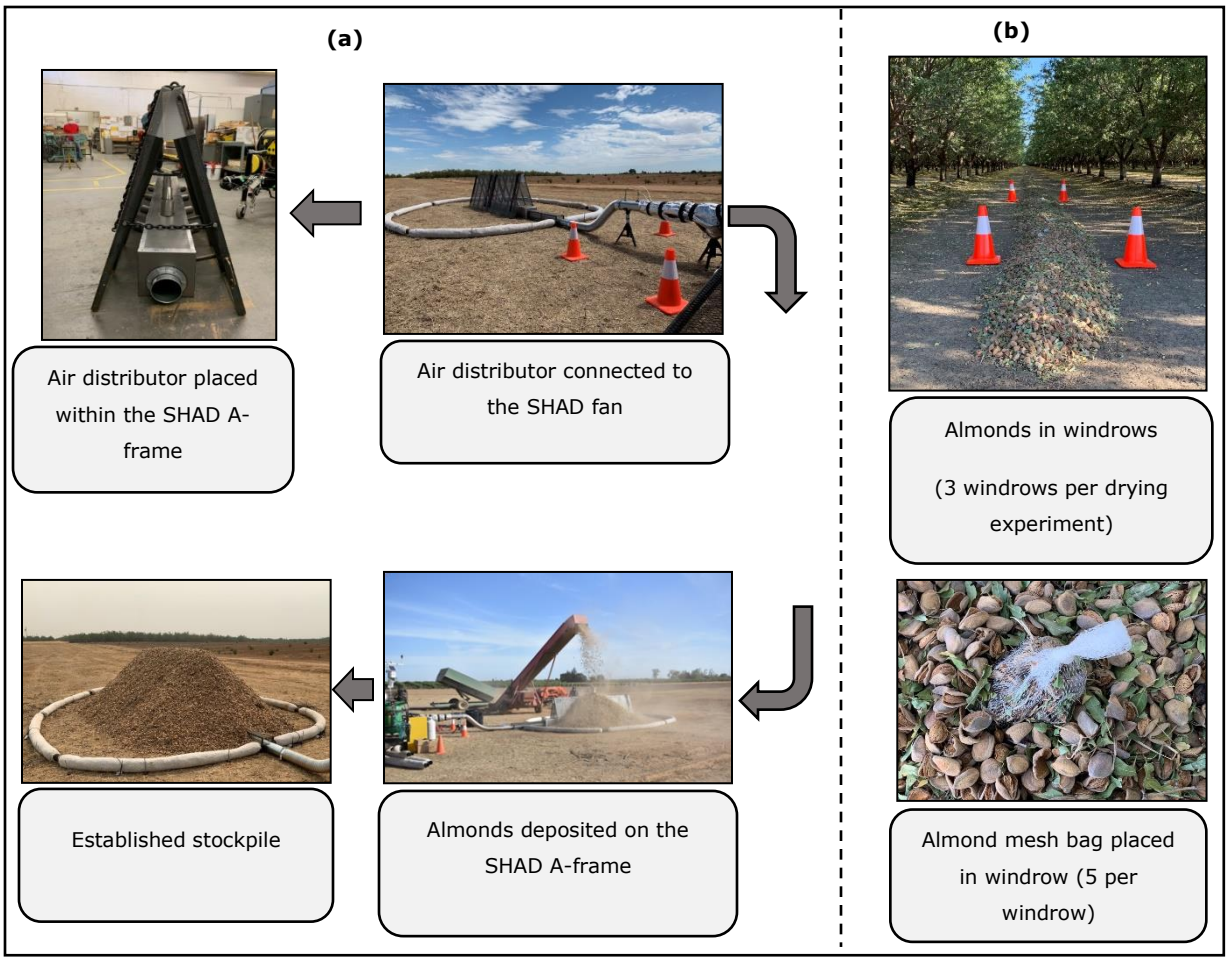

Figure 4.1(a). Steps to field set-up of SHAD and air distributor. (b) Windrow drying experiment held in parallel with stockpile drying.

2.4 Quality parameters determination

2.4.1 Sample Dry-basis moisture content (MC_{db})

Dry-basis moisture content (MC_{db}), damage by molds or decay, and presence of internal cavities were determined as described in Chapter 2 and Mayanja et al, (2021).

2.4.2 Color measurements

Color is a food quality sensory attribute that is essential to a consumer's judgment and food acceptability (Clydesdale, 1991; Corradini; 2019). Color affects the human perception of other food sensory attributes such as flavor, texture and can be used as a predictor for non-quality

attributes like moisture content, over-processing, and pigment content (Clydesdale, 1991). Further, color is applied in determining the quality grade of almonds. According to the U.S. Standards for Grades of Almonds in the Shell, a kernel having dark stains contrasting with the natural color of skin and brown spots greater than 3.2 mm is considered damaged (USDA, 2013). The color damage on almonds can partly be attributed to drying, especially at high T. Coates, (2018) indicated that drying almonds at T above 60 ^{o}C leads to skin flaking of the kernel pellicle. Skin flaking occurs when the pellicle of the almond detaches from the rest of the kernel mainly because of over-drying (Coates, 2018; Micke et al; 1966). Also, Rogel-Castillo et al, (2017) stated that drying almonds at above 75 ^{o}C leads to internal kernel brown discoloration. Kernel browning is typically caused by a chemical reaction (between reducing sugars and amino acids) known as milliard reaction, which is prevalent at high T (Davies and Labuza, 1997; Markowicz et al., 2012). Therefore, it is pertinent to ascertain internal and surface (pellicle) color changes in almond kernels due to drying.

In this study, color was measured with a spectrophotometer (Colorflex EZ, Hunter Associates Laboratory Inc, Reston, VA) using the three-dimensional CIE color space: lightness (L*), green/magenta (a*), and blue/yellow (b*) chromatic axes (CIE, 1986). Nine almond kernels were randomly selected from each sample mesh bag and longitudinally dissected using a sharp knife, then placed on the spectrophotometer to assess the kernel's internal color (kernel internal color). The procedure was repeated for the kernel’s pellicle (surface). Color difference parameter (AE) was used as a measure of the color change between freshly harvested almonds (initial) and the dehydrated almonds either by stockpile or windrow drying (final), as shown in Equation 1 (Minolta,1994).

$$\Delta E = \sqrt{(L_f{}^* - L_i^*)^2 + (a_f{}^* - a_i^*)^2 + (b_f - b_i^*)^2} \quad (1)$$

Where the subscript "i" indicates the color value of the initial freshly harvested almond and color values with an "f" subscript are for the dehydrated (final) almonds.

2.4.3 Oil extraction

Thirty almond kernels were randomly selected from each sample mesh bag, ground by hammering into particles of approximately less than 4 mm that were sorted using a 4 mm sieve (Gilson Company Inc, Lewis Center, OH). The ground almonds were then pressed for 5 minutes inside a stainless-steel oil extraction cylinder of size 57 mm diameter and 76 mm height using a hydraulic press (Model 3351 Carver Inc, Wabash, IN) at 5000 N to extract almond oil. The extracted oil was filtered using 11µm pore size filter paper (GE Healthcare systems, Chicago, IL). On average, 2 g of almond oil was collected per sample in a stainless-steel pan.

2.4.4 Lipid oxidative stability

Lipid oxidation occurs when there are a series of free radical reactions between fatty acids and oxygen, resulting in the oxidative degradation of lipids, known as rancidity (Addis, 1986; Mozuraityte et al., 2016). Rancid flavor and odor are detrimental to the quality of foods (Buransompob et al., 2003; Viera et al., 2017). Almonds are prone to rancidity due to their total fat content which is around 50 %, where 25 % of total fats are polyunsaturated fatty acids, and 63% are monounsaturated fatty acids (USDA, 2015; Lin et al., 2012). Rancidity in almonds can be determined using an oil oxidation stability test, which determines the time it takes for almond oil to resist oxidation, known as induction time (IT) (Läubli and Bruttel, 1986; Sewald and DeVries, 2015). The test was conducted using a Metrohm Rancimat Model 892 (Metrohm Ltd.,

Herisau, Switzerland). Almond oil equivalent to 1.5 g was added to a reaction vessel and heated to 120 °C, while 10 L-h^{-1} of filtered air was forced through the oil (Metrohm, 2017). This study used 1.5 g of almonds rather than the recommended 3g by the manufacture (Metrohm, 2017) due to a low oil yield from samples. Therefore, the focus of the IT analysis is meant to determine the relative difference between stockpile and windrow dying almonds, since samples were similarly treated.

2.4.5 Peroxide Value (PV) and Free Fatty Acid (FFA) content

Peroxides are the main breakdown products formed during lipid oxidation. Peroxide value (PV) represents the concentration of lipid peroxides. Ideally, a low PV value shows low levels of autooxidation (free radical reaction), but PV values can also rise and immediately decline as peroxides break down during the later stages of oxidation (Sewald and DeVries, 2015; Huang, 2014). This implies that PV is only valid at the early stages of oxidation and that a low PV is not often a representation of low rancidity. Nonetheless, PV can be informative if measured with other lipid oxidative quality parameters, such as the Free Fatty Acids (FFA) content. Also, PV is a typical industry measurement of rancidity (Paramount farms, 2000). PV is expressed as meq02/kg and was determined based on the CDR FoodLab protocol (2021a) using a CDR analyzer (CDR FoodLab, CDR s.r.l company, Salerno, Italy) with 25 µl of almond oil. PV of 2.0 meq02/kg is the upper limit for acceptable levels in almonds (Paramount farms, 2000; Buransompob et al, 2003).

FFAs are formed by the hydrolysis of lipids. The formed FFAs are unstable, making them prone to oxidation and thus becoming rancid. Therefore, FFA are used as indicators for hydrolytic rancidity (Mahesar et al.,2014). FFA content was determined following the CDR FoodLab procedure (2021b) using 10 µl of almond oil. FFA of 1 % oleic acid is the upper limit for acceptable levels of hydrolysis rancidity in almonds (Paramount farms, 2000; Buransompob et al, 2003).

2.5 Shad Airflow

Chapter 3 indicated that the air distribution percentage of the air distributor was 3.77 %, 30.65 %, 45.49 %, and 20.10 % for outlets in row1, row2, row3, and row4 respectively. This implied that the almonds in the region of outlets in row1 would receive a low air supply. Therefore, the air distributor was placed so that the outlets in row1 were at the edge of the SHAD A-frame as shown in Figure 4.2. The majority of almonds are in the middle of the stockpile, due to its cone shape. Therefore, it is ideal that most of the air is distributed in the middle section of the stockpile.

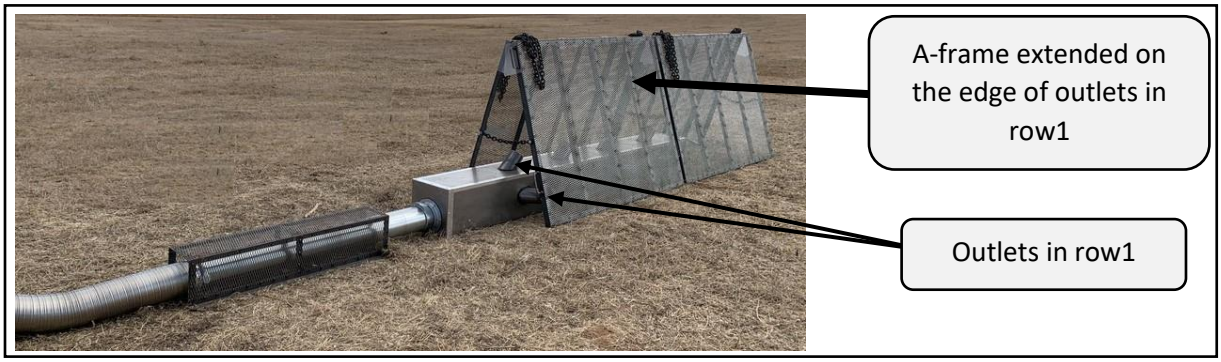

Figure 4.2: Picture showing the placement of the A-frame and SHAD

A pitot tube sensor (DS 300 flow sensors, Dwyer Instrument Inc, Michigan City, Indiana) was inserted inside the duct connecting the outlet of the fan to the air distributor, 2.5 m away from the fan to measure the airflow under approximate laminar flow (Cengel & Cimbala, 2017). A pressure sensor (Series MS Magnesense, Dwyer Instruments Inc, Michigan City, Ind) was connected to the pitot tube to record the static and total pressure. The difference between total and static pressure yields the velocity pressure (*Pv*). Ultimately, airflow (Q) was calculated in m^3/s using Equations 2 and 3 (Cengel & Cimbala, 2017)

$$V = \sqrt{\frac{2P_v}{\rho}} \qquad (2)$$

$$Q = AV \qquad (3)$$

Where

V is the velocity of airflow (m/s).

A is the area of the duct (m^2) or 0.018 m^2

ρ is the density of air (kg/m^3).

An average heated drying T of 57.23 ^oC ('Np'), 54.52 ^oC ('Wi'), and 56.46 ^oC ('Mo'), and ambient drying T of 30.20 ^oC ('Np'), 23.90 ^oC ('Wi'), and 26.69 ^oC ('Mo') were used to calculate the density of air ρ, as stated in Equation 4 (Dickerson et al., 1979).

$$\rho = \frac{P \times m}{n \times R \times T} \quad (4)$$

Where *P* is atmospheric pressure (101,325 Pa)

m is the molar mass of air (0.02896 kg/mol)

n is the number of moles (taken as 1 to match units of molar mass)

R is the gas constant (8.3145 J/Kmol)

2.6 Energy Usage and dryer performance indicators

Total energy utilized (electrical and propane), energy cost, and dryer performance indicators including Specific Moisture Extraction Rate (SMER), Moisture Extraction Rate (MER), and Coefficient of Performance (COP) were determined as stated in Chapter 2 and Mayanja et al, (2021).

2.7 Data Analysis and Visualization

Data analysis and visualization were conducted using R studio (version 1.4.1106) and SAS Enterprise 7.1. Data analysis was divided into three sections: 1) A split-plot design was used for

the stockpile (plot) drying experiments, which each was partitioned into three plots (bottom, middle, and top stockpile layers). One way Analysis-of-Variance (ANOVA) was conducted on MC_{db} and each of the quality parameters individually to ascertain whether they were a significant difference within the stockpile layers. When a significant main effect was found, a post hoc test using Tukey's Honest Significant Difference (HSD) test was conducted to ascertain where the difference of the means lies in the layers at a 95% confidence level ($p \leq 0.05$); 2) Similar to the stockpile experiment, the same design and analysis was used for the windrow experiments, except the three rows were considered as plots; and 3) A two-sample t-test analysis was conducted to ascertain whether the means of the MC_{db} and each of the quality parameters of stockpile and windrow drying experiments were significantly different. The latter included the calculation of the P-value using the Folded F method to assess whether the two-group had equal or unequal variances. When the P-value of the Folded F was greater than 0.05, it implied that the two groups had equal variances. Thereafter, the pooled method was used to determine whether the two groups were significantly different at P = 0.05 (Bhattacharyya, 2013). Otherwise, if unequal variances were observed, the Satterthwaite method was used to determine whether the two groups were significantly different at P = 0.05 (Allwood, 2008). In addition, data visualization of the mean T and RH data was plotted as conducted in Chapter 2 and Mayanja et al, (2021).

3.0 Results and Discussion

3.1 Drying Conditions and Time

Figures 4.3 and 4.4 show the RH and T profiles for the stockpile and windrow experiments. The setpoint for the heated fan was at 55 to 60 ^{o}C, which was running for 38% ('Np'), 15.30% ('Wi'), and 25.32% ('Mo') of the total drying time. This resulted in an average T of 54.52 ± 10.35 ^{o}C ('Wi'), and 56.46 ± 9.87 ^{o}C ('Mo'). The heated fan was deliberately turned off during day 6 ('Np'),

days 1 and 2 (‘Wi’), days 2, 3, and 4 (‘Mo’) due to the high fire risk in the region. During these days, the almonds were solely dehydrated with ambient air. Thus, the average recorded ambient RH was 40.37 ± 14.13% (‘Np’), 36.06 ± 15.09% (‘Wi’), 30.70 ± 12.46 % (‘Mo’), while the average ambient T was 30.20 ± 6.02 ^{o}C (‘Np’), 23.90 ± 5.76 ^{o}C (‘Wi’), and 26.69 ± 4.97 ^{o}C (‘Mo’).

The previous experiment (Chapter 2; Mayanja et al, 2021) with the SHAD removed 6.56% of MC_{db} in 11 days at 55 ^{o}C, under ambient drying T and RH of 18.47 ^{o}C, and 31.74 % respectively. The current stockpile experiment dehydrated 7.38% (‘Np’), 6.82 % (‘Wi’), and 17.46% (‘Mo’) MC_{db} in 6.21 days (‘Np’), 6 days (‘Wi’), and 7 days (‘Mo’). Therefore, the addition of the air distributor reduced the drying time by around half, partially attributed to a more even distribution of air through the stockpile. Even though the ambient T of these experiments was higher than the experiment without the air distributor, this effect can be considered negligible as the bottom and middle layers of the stockpiles are primarily dehydrated by the forced air generated by the SHAD, rather than the surrounding environmental air.

On contrary to the stockpile experiment, the windrow experiment solely relies on ambient air conditions to achieve dehydration. The windrow experiments took 13.63 days (‘Np’), 8.75 days (‘Wi’), and 12.33 days (‘Mo)’ to dehydrate the almonds. The windrow experiments drying time concurs with Micke, (1996) who indicated that drying almonds on the ground takes 1 to 2 weeks depending on the initial MC_{db}. Therefore, windrow drying of almonds takes a longer time than SHAD, for this case by a margin of 7.42 days (‘Np’), 2.75 days (‘Wi’), and 5.33 days (‘Mo’).

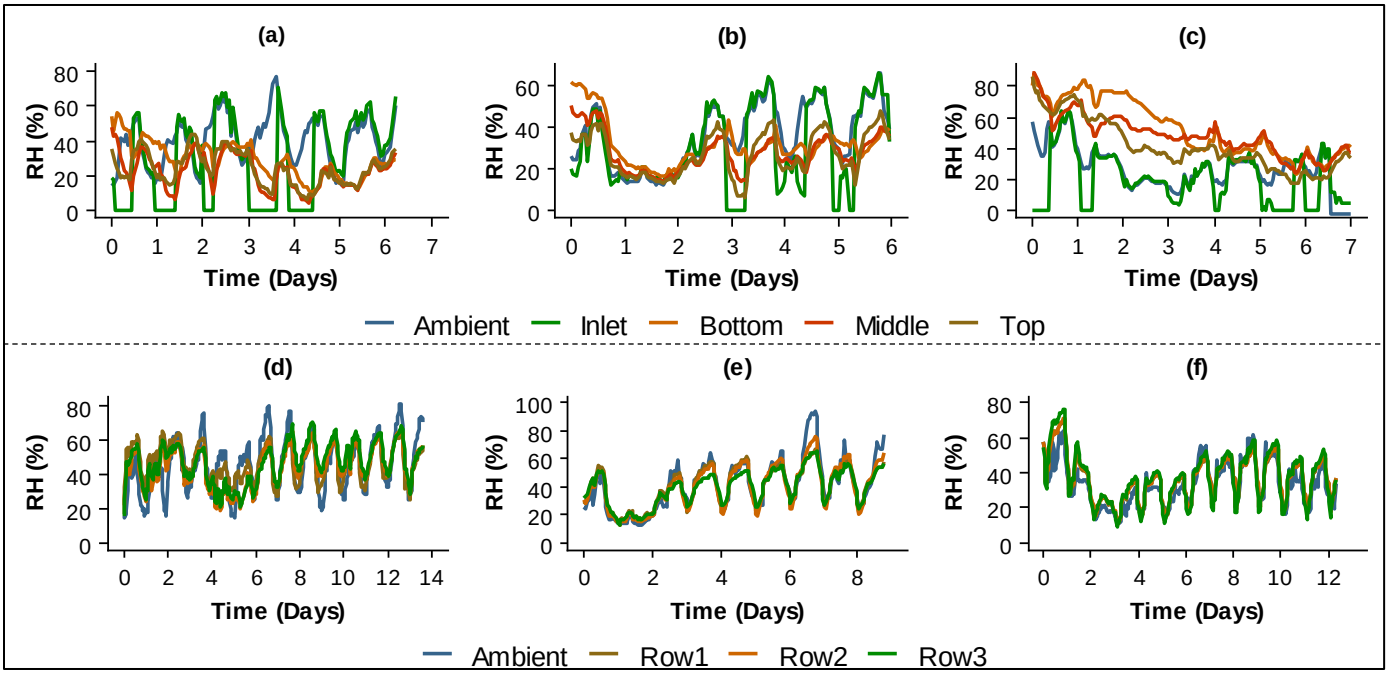

Figure 4.3 RH profile: (a) Stockpile ('Np'). (b) Stockpile ('Wi'). (c) Stockpile ('Mo'). (d) Windrow ('Np'). (e) Windrow ('Wi'). (f) Windrow ('Mo').

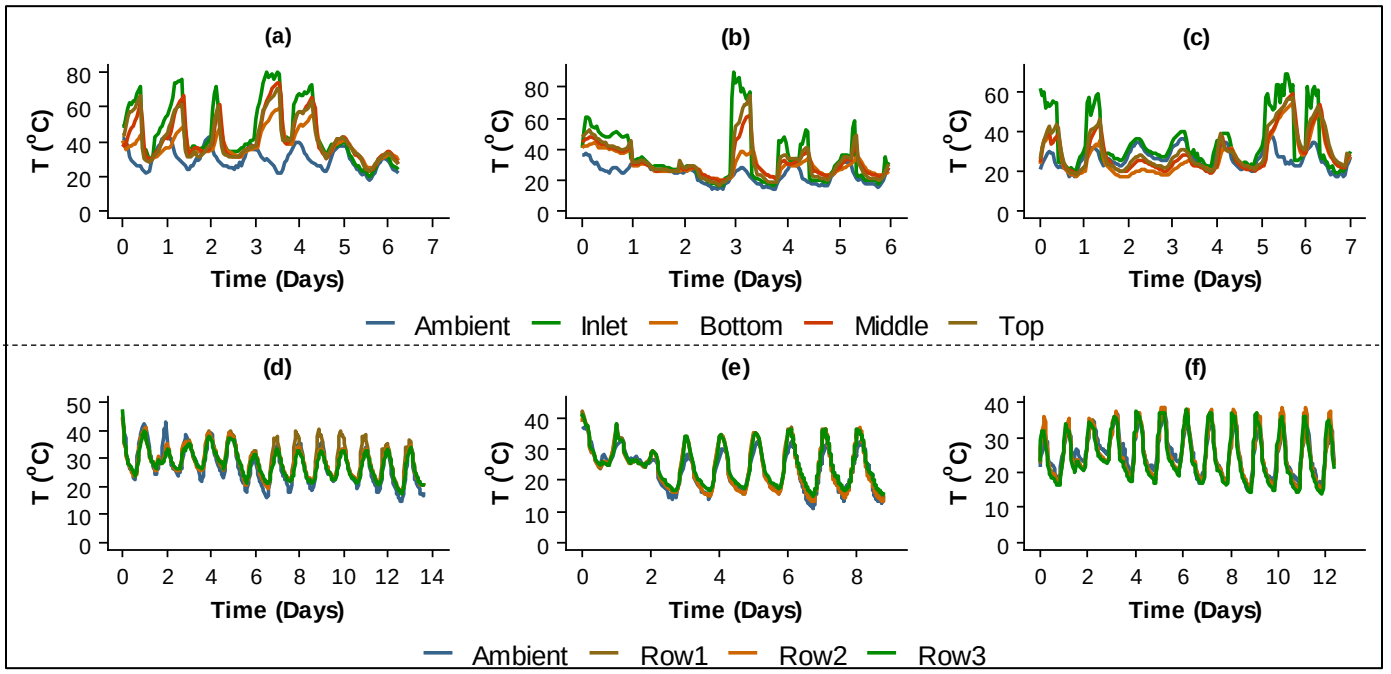

Figure 4.4 T (T) profile: (a) Stockpile ('Np'). (b) Stockpile ('Wi'). (c) Stockpile ('Mo'). (d) Windrow ('Np'). (e) Windrow ('Wi'). (f) Windrow ('Mo').

3.2 Moisture Content

The 'Mo' variety almonds contained the highest initial MC_{db} of 21.49 ± 2.12%, followed by 'Np' (11.83 ± 1.99%), and 'Wi' (11.46 ± 0.60%) which were then dehydrated by the stockpile and windrow drying methods.

Figure 3.5a shows the MC_{db} of the stockpile layers for each of the three experiments conducted. ANOVA test showed that the MC_{db} was significantly different between the stockpile layers at P = 0.5 for both 'Np', and 'Wi' varieties. Also, The Tukey HSD post-hoc test showed that the bottom and top layers are statistically different (p-value ≤ 0.05) for both 'Np', and the top layer for 'Wi' experiments. Regardless of the significant difference of MC_{db} between the stockpile layers, the MC_{db} attained for all stockpile experiments was desirable because it was below the desired 6%.

The average final MC_{db} across all the three varieties of the stockpile experiments was 4.03 ± 0.74%, 4.39 ± 0.88%, and 4.71 ± 0.73% for the bottom, middle, and top layers, respectively. Chen et al, (2020) dehydrated almonds in a column air dryer and indicated that almonds located at the point of entry of drying air will have a lower MC_{db}, which will increase proportional to the height. This concurs with the current stockpile experiments were the bottom layer had the lowest MC_{db} and increased to the middle, and top layers. On the other hand, the SHAD without an air distributor (Chapter 2; Mayanja et al., 2021) had a final MC_{db} of 7.12 ± 2.64% (bottom), 6.42 ± 3.27% (middle), and 4.59 ± 0.73% (top). In this case, the bottom and middle layers have MC_{db} higher than the desired 6%, and the bottom layer has the lowest MC_{db}, showing that the supplied drying air was not as effective as the ambient air which dehydrated the top layer that had the lowest MC_{db}. Thus, the use of the air distributor was effective and ensured that almonds across stockpile layers were all at the desired MC_{db}, once the drying experiments were finalized.

On contrary to the stockpile experiments, the windrow experiments yielded a more variable distribution of moisture, some at above 6% MC_{db} as shown in Figure 4.5b. The 'Np' windrow experiment had an overall average MC_{db} of 17.64 ± 1.52 % attributed to unwanted irrigation event, which accounts for the increase in the final MC_{db}, relative to the initial MC_{db}. The windrow experiment was conducted between almond rows on the ground of the orchard following conventional industry practices, which allows the almonds to be in contact with water, if the almond orchard is mistakenly irrigated. However, the previous occurrence is rare but can potentially affect the moisture of almonds while being conventionally dehydrated. The 'Wi' windrow experiment had an overall average MC_{db} of 6.79 ± 0.60%, which is above 6%. This can partly be attributed to a precipitation event that occurred leading to rehydration of the almonds (Uesugi and Harris, 2006). Differently to the 'Np', and 'Wi' windrow experiments, the final MC_{db} for all the rows in the 'Mo' windrow drying experiment were below 6%, which is desired. There was no significant difference between the MC_{db} across rows ($p \leq 0.05$) for all the windrow experiments, showing that drying occurs very similarly regardless of the row.

Further, Figure 3.5c shows the comparison between overall stockpile and windrow drying MC_{db} results. t-test showed that there was a significant difference between the stockpile and windrow MC_{db} for all the evaluated varieties. Therefore, the windrow drying is unreliable in terms of attaining desired MC_{db} since it is prone to adverse effects, including rain or unwanted irrigation events, as it was the case during the 'Np', and 'Wi' windrow drying experiment.

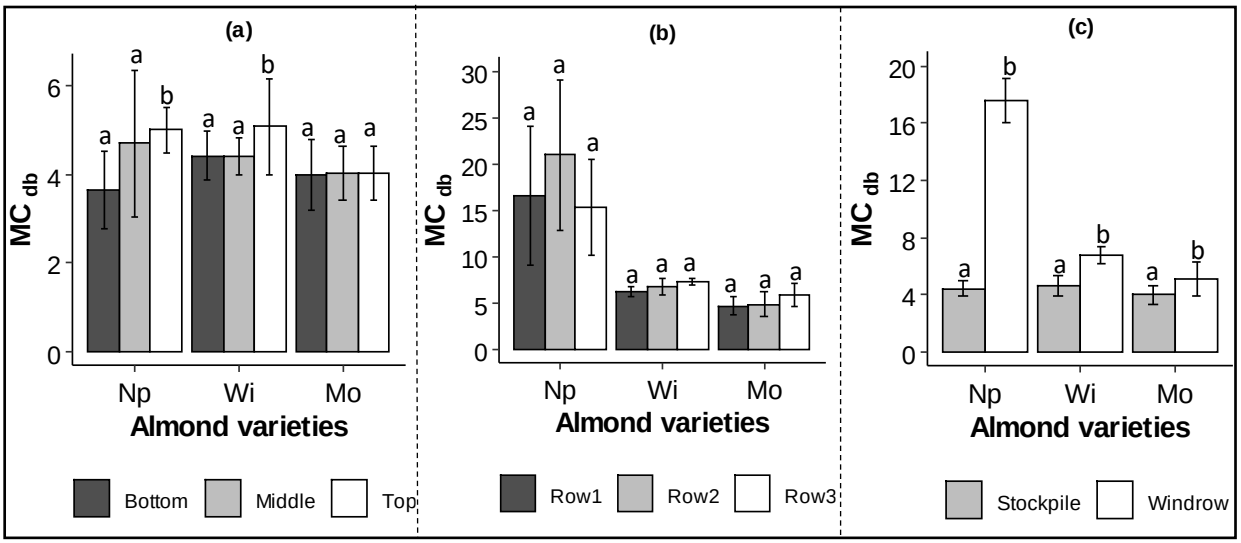

Figure 4.5 (a) Final MC_{db} for stockpile layers. (b) Final MC_{db} windrows. (c) Final MC_{db} for stockpile and windrow experiments. Appendix I shows the final MC_{db} for the almond components (kernel, Shell, hull, and whole) and II shows the corresponding bulk density.

3.3 Quality Parameters

3.3.1 Internal Cavities

The freshly harvested (initial) almonds had 0 % internal cavities. After drying, 0.13 ± 1.17 % ('Np') and 0% ('Wi' and 'Mo') were recorded for the stockpile experiment. Also, windrow drying showed 0 % internal cavities for all three varieties. Internal cavities are an indicator of fast-drying rate especially leading to the solidification of the outer surface of the almond kernel, hence causing the kernel to split (Coates, 2018). Further, Chen et al, (2021) dehydrated almonds at 40 – 60 oC in a column dryer and reported 0% internal cavities. Therefore, drying of almonds by both stockpile and windrow drying produced no or negligible kernel splitting. The previous SHAD experiment (Chapter 2; Mayanja et al., 2021) resulted in internal cavities of 1.77 ± 2.66%, which were higher than the SHAD experiment with air distributor but still considered low.

3.3.2 Decay or mold injury

Freshly harvested almonds contained 0% (‘Np’), and 0.33 ± 1.59% (‘Wi’), and 0.33 ± 0.38% (‘Mo’) decay or mold damage, which is considered negligible. After drying, the decay or mold injury for the ‘Np’ variety was 0.67 ± 1.87% and 1.33 ± 3.75% for the stockpile and windrow drying experiments, respectively. Results for the t-test of the ‘Np’ experiment showed that there was a significant difference (Satterthwaite P-value = 0.048, t-value = -0.62) in decay or molds between the stockpile and windrow experiment, mainly attributed to the irrigation event. Further, the decay or mold injury percentage for the ‘Wi’ variety after drying was 0.67 ± 1.38% (stockpile) and 1.11 ± 1.63% (windrow). Rain during the ‘Wi’ experiment could have contributed to the increase in the presence of decay or molds during the windrow experiment. Also, the ‘Mo’ variety had 0.89 ± 1.53 % and 0.44 ± 1.17 % for stockpile and windrow drying experiments. The wetness of almonds makes them susceptible to the development and growth of molds. This could be naturally when freshly harvested or due to irrigation and rain as evidenced in the ‘Np’, and ‘Wi’ experiments, respectively (King et al., 1983; Franz, 2012). Also, almonds are contaminated with molds and pathogens when mixed with the soil during windrow drying processes of sweeping and picking up (Fielke, 2019; Perry and Sibbett, 1998). Thus, the previous challenges are addressed in stockpile drying with SHAD since it eradicates sweeping and picking up of almonds.

The previous experiment where almonds were dehydrated with the SHAD without the air distributor (Chapter 2; Mayanja et al., 2021) yielded mold or decay damage at 1.81 ± 2.57%, which was low but can still be attributed to sections within the stockpile that are not receiving proper aeration. On the other hand, the SHAD experiment with the air distributors resulted in a less than 1 % decay or mold injury.

3.3.3 Insect damage

The insect damage of fresh almonds was 0 %. After drying, the SHAD stockpile experiment with and without the air distributor had 0 % insect damage. On the other hand, the insect damage for the windrow experiment was 0.44 ± 1.17% ('Np'), 0.22 ± 0.86 % ('Wi'), and 0% ('Mo'). Overall, the insect damage for the windrow experiment is low, at below 1 %. Thus, almonds in contact with the orchard ground can contribute to the presence of insect damage and its associated adverse effects such as aflatoxins (Campbell et al., 2003; King et al., 1970), which is not the case for almonds in a stockpile drying.

3.3.4 Colour analysis (ΔE parameter)

The average ΔE results of stockpile and windrow experiments for the inside and surface of the kernel are shown in Figure 4.6a and b, respectively. Relative comparison (t-test) indicates that ΔE of stockpile and windrow experiments are similar because there is no significant difference between the two groups. The same deduction is made when analyzing (ANOVA test) for the significant difference between the stockpile layers (fig 4.6d and e), and windrows (Fig 4.6 f and g) at $P \leq 0.05$. Further, the overall average ΔE results for the stockpile experiment were 3.66 ± 1.49 (inside), and 4.95 ± 1.97 (surface), while the ΔE values for the windrow experiment were 3.75 ± 1.42 (inside), and 4.77 ± 2.01 (surface). Coates, (2018) indicates that ΔE develops due to the exposure of the almond to heat when dehydrating. Thus, the surface results have higher ΔE values because they are exposed to more heat before it reaches the interior of the almonds.

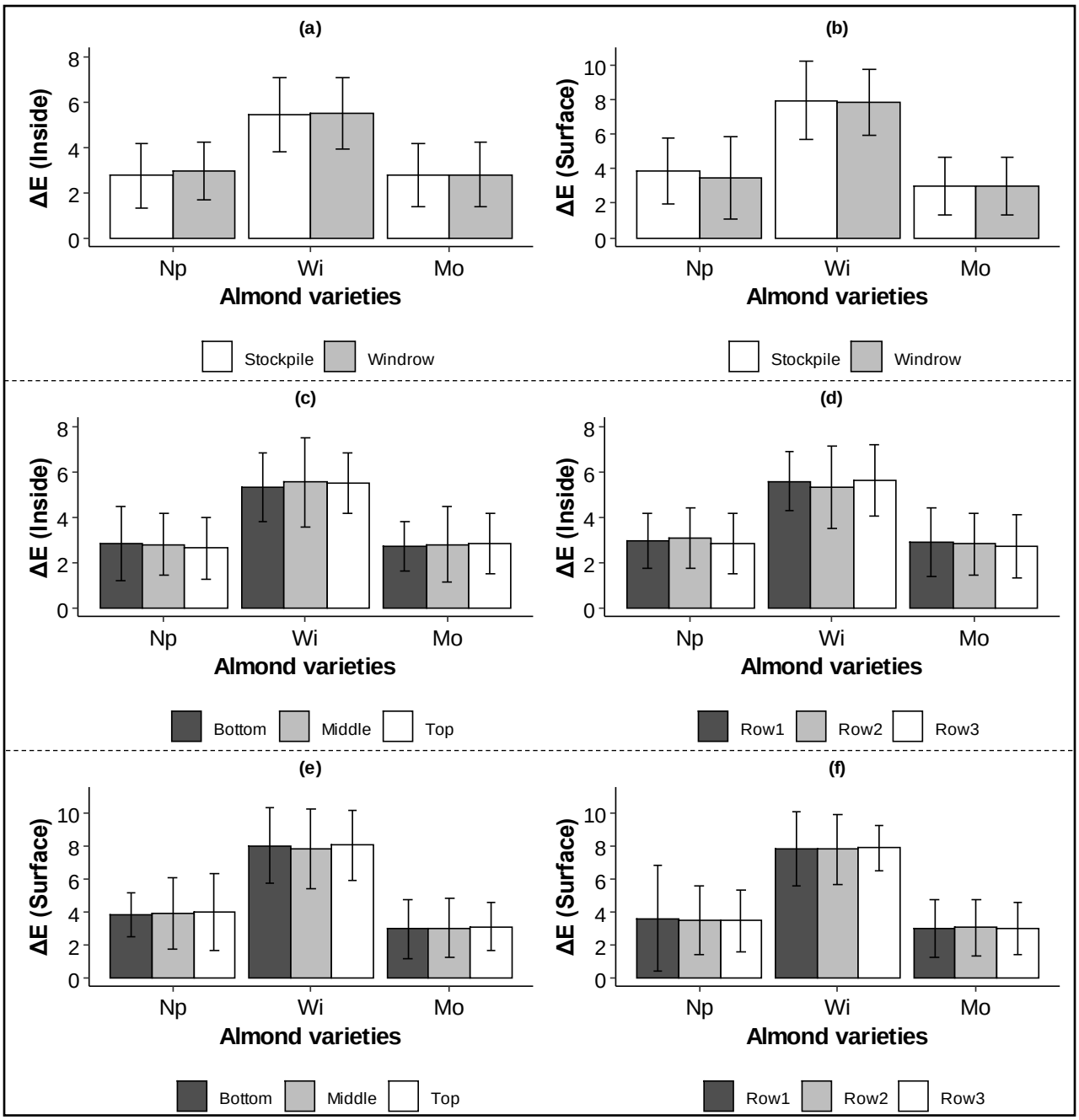

Figure 4.6. Bar plot showing average ΔE results for (a) Inside of stockpile and windrow experiments (b) Outside of stockpile and experiments. (c) Inside for each of the stockpile layers. (d) Outside for each of the windrows. (e) Surface for each of the stockpile layers. (f) Surface for each of the windrows.

Considering varieties, the average ΔE values of all the experiments were 2.86 ± 1.36 ('Np'), 5.48 ± 1.6 ('Wi'), and 2.78 ± 1.41 ('Mo') for the inside, while the surface values were 3.69 ± 2.22 ('Np'), 7.90 ± 2.11 ('Wi'), and 3.00 ± 1.66 ('Mo'). This difference of ΔE values shows that

different almonds varieties will react to heat differently due to the variability of physical properties (Dingke and Fielke, 2014), macro and micro-nutrients of almond varieties (Yada et al., 2011),

Ultimately, almond quality in terms of color effect was not concerning because statistics (t-test and ANOVA) conducted showed the effect was similar for the drying methods regardless of the existing difference between the inside and surface of almonds, and with the almond varieties. Appendices III and IV show the l*, a* and b* coordinates values used to derivate ΔE values for stockpile and windrow experiments, respectively.

3.3.5 Induction time (IT)

Figure 4.7a shows the IT for the stockpile and windrow experiments with t-test indicating that there is no significant difference in IT between the two groups for all the three varieties. Also, the ANOVA test showed no significant difference ($P \leq 0.05$) for the IT between the stockpile layers (Fig 4.7b) and windrows (Fig 4.7c). Metrohm, A. G. (2013) showed an IT of 4 hrs using an almond oil sample of 3g, while Capanoglu and Boyacioglu, (2008) used almond oil of 2.5g to generate IT of 4.16 hrs. This study had an overall IT of 5.38 ± 0.28 hrs (stockpile), and 5.29 ± 0.19 hrs (windrow) using 1.5g of almond oil. Therefore, the comparison of IT with other studies has a difference of about 1 hr can be partly attributed to the differences in the amount of almond oil used in the experiment. Additionally, the relative comparison showed that the effect of rancidity in dehydrating almonds was similar when compared with stockpile layers, windows, and the contrast between stockpile and windrow drying.

3.3.6 PV AND FFA values

The PV results for the stockpile and windrow experiments are shown in Figure 4.7d. Overall, the PV were less than 0.2 Meq02/kg. This concurs with other studies which have PV of 0.34 – 0.41

Meq02/kg (Li et al., 2018), 0.46 – 0.72 Meq02/kg (Chen et al., 2021), and 0.24 – 0.49 Meq02/kg (Gao et al., 2011). Therefore, negligible levels of autooxidation were generated for all the experiments. Further. recorded FFA values from all experiments were below 0.01 %, and other studies had FFA values of 0.18 – 0.24 (Li et al., 2018), 0.16 – 0.37 (Chen et al., 2021), 0.11 – 0.27 (Gao et al., 2011) implying negligible levels of hydrolytic rancidity. No statistical analysis was conducted for the PV and FFA results because there were all lower than the maximum acceptable limit of 2.0 Meq/kg (PV), and 1% oleic acid (Paramount farms, 2000; Buransompob et al, 2003), respectively.

3.4 Airflow

The average airflow of the SHAD was 1.18 ± 0.28 m^3/s ('Np'), 1.19 ± 0.33 m^3/s ('Wi'), and 1.14 ± 0.29 m^3/s ('Mo'). Therefore, the airflow per cubic meter of fresh almonds was 0.042 ± 0.01 ('Np'), 0.092 ± 0.03 ('Wi'), and 0.02 ± 0.005 ('Mo') m^3/s per m^3. The 'Wi' experiment had the highest airflow in relation to the quantity of dehydrated almonds, hence dehydrating almond is less time (6 days) compared to the 'Np' (6.21 days), and Mo (7 days) experiments. Coates, (2018) developed a cylindrical tower of 0.3 m diameter and 3 m height to determine the airflow rates necessary to aerate the almonds. The study showed that with drying conditions of 50 ^oC T and 40 % RH, that almonds should be dehydrated at an airflow of 0.19 m^3/s per m^3 to achieve equilibrium moisture content. The previously stated airflow is higher than the values achieved in the SHAD experiments. This is partly because the study was conducted in a closed environment, ignoring external factors such as wind gusts which also contribute to the dehydration of almonds in a stockpile. This therefore justifies the need for lesser airflow in a stockpile environment. Also, future work will ascertain whether the increase of airflow can potentially reduce the drying time of almonds.

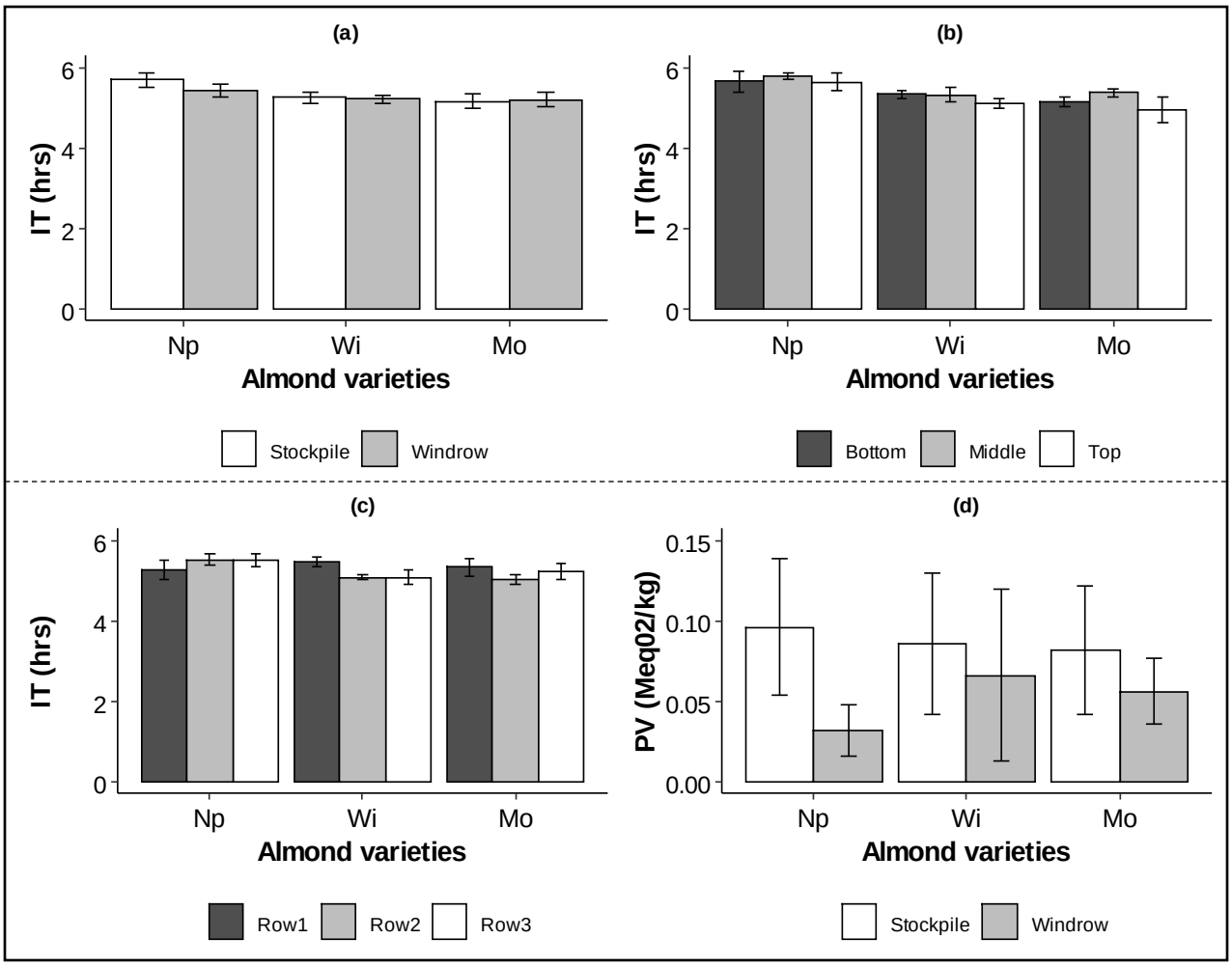

Figure 4.7. (a) Average IT of stockpile and windrow experiments. (b) Average IT for each of the stockpile layers. (c) Average IT for each of the windrows. (d) Average PV for stockpile and windrow experiments.

Further, the previous stockpile experiment that didn't contain an air distributor (Chapter 2; Mayanja et al., 2021) had an airflow of 0.078 m^3/s per m^3 of fresh almonds and drying was achieved in 11 days. Two of the SHAD experiments ('Np' and 'Mo') with the addition of the air distributor had a lower airflow per m^3 of almonds than the previous experiment, but still achieved drying in less time. Therefore, the reduction in drying time can be mainly attributed to the enhancement of air distribution through the stockpile, mainly due to the addition of the air distributor.

3.5 Air Usage, Cost, And Parameters

3.5.1 Energy usage and cost

The total energy consumption for the stockpile experiments was 1,130 MJ (‘Np’), 1,500 MJ (‘Wi’), and 1,543 MJ (‘Mo’). The specific energy required to dehydrate a tonne of water from the almond stockpile was 3,214 (‘Np’), 8,508 (‘Wi’), and 1,290 MJ/kg of water (‘Mo’). Thus, the specific energy was inversely proportional to the stockpile size, whereby the ‘Wi’ experiment used the most energy. This shows that a reduced stockpile size of 2,585 kg is below the operation capacity of the SHAD. On the other hand, the largest stockpile (‘Mo’) utilized the lowest amount of energy. The previous SHAD drying experiment without an air distributor (Chapter 2; Mayanja et al., 2021) yielded specific energy of 5,623 MJ/kg of water, demonstrating that the SHAD utilized more energy than the current ‘Np’ and ‘Mo’ experiments due to the lack of proper air distribution.

The cost of dehydrating a tonne of fresh almonds was 6.5 (‘Np’), 15.47 (‘Wi’), and 6.44 $ per kg of almonds (‘Mo’). The ‘Wi’ experiment reflected the highest energy cost, mainly due to the underutilization of the SHAD. Also, the previous experiment, without the air distributor yielded a cost of 11.65 $ per kg, which is higher than the ‘Np’ and ‘Mo’ experiments but not the underutilized ‘Wi’ experiment.

3.5.2 Energy parameters

The SMER for the stockpile experiment was 1.12 kg/kWh (‘Np’), 0.42 kg/kWh (‘Wi’), and 2.78 kg/kWh (‘Mo’). SMER describes the effectiveness of energy used during drying (Prasertsan and Saen-Saby, 1998). Therefore, a comparison with existing dryers (Fig 4.8a) showed that the supplied energy was effectively used to achieve drying, since these values are in the upper limit of energy efficiency. The ‘Wi’ experiment was on the lower limit due to the stockpile's reduced size, showing that some of the drying air was escaping the stockpile before it removed moisture from

the almonds. Also, comparisons show that the average SMER of SHAD experiments with an air distributor (1.44 ± 1.21 kg/kWh) was higher than the previous experiment (0.64 kg/kWh) with a 125% increase in energy efficiency (Chapter 2; Mayanja et al., 2021).

Further, the stockpile experiment had MER of 2.36 kg/h ('Np'), 1.22 kg/h ('Wi'), and 7.11 kg/hr ('Mo'). MER is used to measure the dryer capacity (Prasertsan and Saen-Saby, 1998). Therefore, a comparison with existing dryers (Fig 4.8b) showed that the 'Wi' experiment was dehydrating almonds below its capacity. 'Np' and 'Mo' experiments where larger stockpiles showed high values of MER. The average MER for the SHAD experiments with the air distributor (3.56 ±3.12 kg/h) was higher than the previous experiment (1.02 kg/h) with a 249% increase (Chapter 2; Mayanja et al., 2021).

Additionally, the COP for the stockpile experiment was 5.47 ('Np'), 1.84 ('Wi'), and 6.86 ('Mo'). Oktay and Hepbasli, (2003) stated that COP is used to evaluate the efficiency of the propane-heated fan. Therefore, comparison with existing dryers (Fig 4.8c) showed that the fan for the 'Wi' experiment was not efficient, as it utilized more energy than required to dehydrate the almonds. Thus, 'Np' and 'Mo' experiments are more efficient. The average COP for the SHAD experiments with the air distributor (4.73 ± 2.59) was greater than the previous experiment (1.33) with a 255% increase (Chapter 2; Mayanja et al., 2021).

The addition of the air distributor improved the energy efficiency of the SHAD, but only for the 'Np' and 'Mo' experiments compared to exiting dryers and the SHAD without an air distributor (Chapter 2; Mayanja et al., 2021). Future studies will be performed to determine the maximum drying capacity of the SHAD with an air distributor, as well as the effect of increasing the fan size and covering the stockpile to recirculate and better distribute the air through the stockpile.

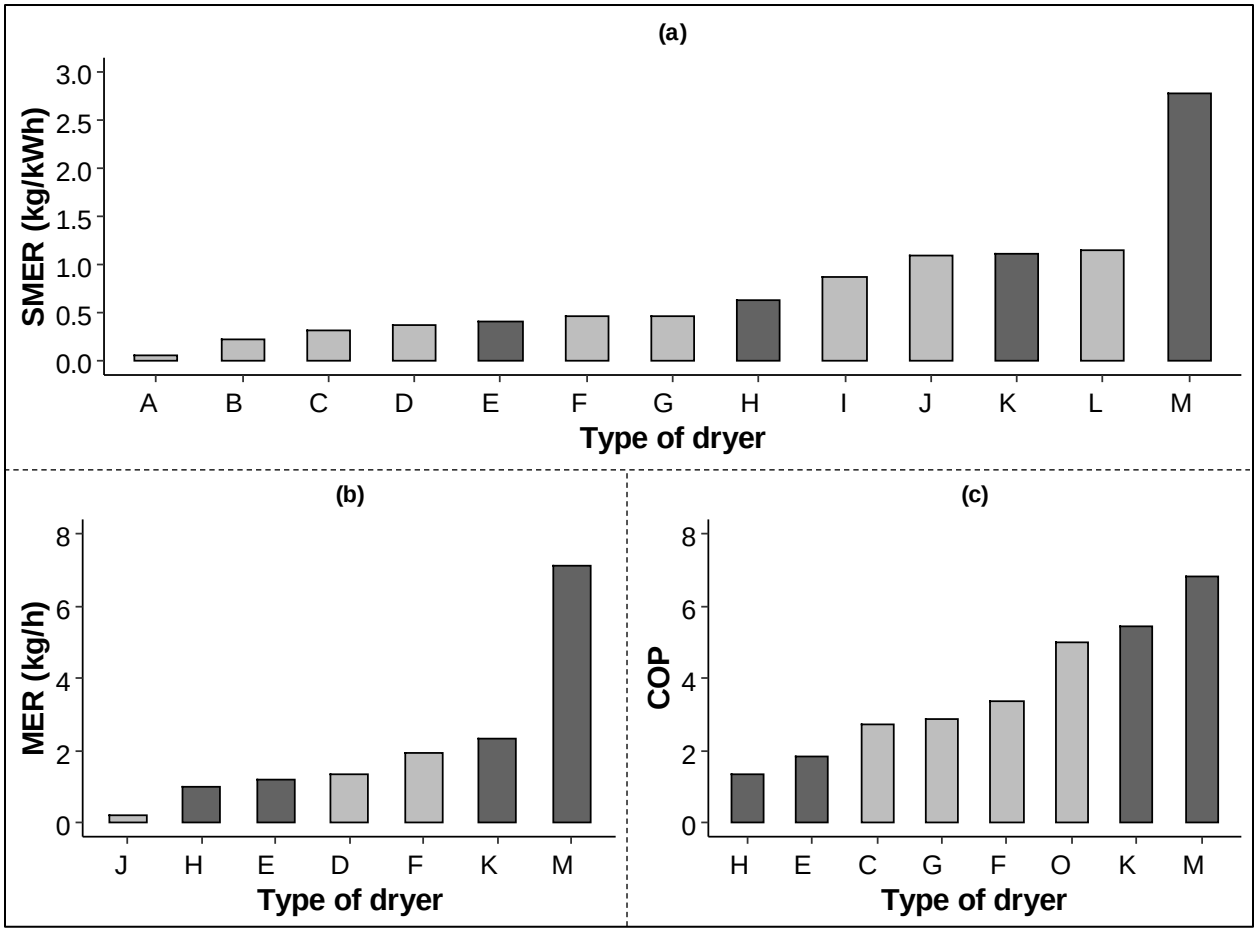

Figure 4.8. (a). Bar plot comparing SMER of different dryers. (b) Bar plot comparing MER of different dryers. (c) Bar plot comparing COP of different dryers. [A] Closed system heat pump dryer for ginger at 50°C (Chapchaimoh et al., 2016), [B] Convection solar dryer for bitter gourd (Vijayan et al., 2016), [C] Heat pump dryer for tomato slices at 45°C (Coşkun et al., 2017), [D] Solar dryer for cassava at 40°C (Yahya et al., 2016), [E] Stockpile heated and ambient air dryer for almonds 'Wi ' at 59ºC (this study),[F] Solar assisted heat pump dryer for cassava at 45°C (Yahya et al., 2016), [G] Solar assisted heat pump for mushrooms at 45°C (Şevik et al., 2013), [H] Stockpile heated and ambient air dryer for almond, previous experiment (Mayanja et al., 2021), [I] Solar dryer for chili at 50°C (Mohanraj and Chandrasekar, 2009), [J] Heat pump dryer for sweet pepper at 40°C (Pal and Khan, 2010), [K] Stockpile heated and ambient air dryer for almonds 'Np' (this study) [L] Heat pump assisted hybrid photovoltaic thermal solar dryer for saffron at 45°C (Mortezapour et al., 2012), [M] Stockpile heated and ambient air dryer for almonds 'Mo' at 55ºC (this study) **[**0] Heat pump for mint leaves at 45°C (Ceylan and Gürel, 2016)

3.6 Conclusion

Drying of almonds with a combination of SHAD and air distributor achieved drying in a shorter time (maximum of 13.63 days), compared to the previous experiment without an air distributor which took 11 days (Chapter 2; Mayanja et al., 2021). Also, the desirable MC_{db} (< 6%), internal cavities (0.2 %), decay or mold injury (< 0.9 %), PV (<0.2 Meq02/kg), and FFA ((<0.01 % Oleic acid) were achieved across all stockpile experiments. Further, relative comparison (t-test) of the

ΔE values and IT of stockpile with windrow experiment showed no significant difference which was also considered desirable. On the other hand, the conventional windrow drying took longer drying periods (up to 9.5-days), and the desired final MC_{db} was only reached during the 'Mo' experiment. The Np' and 'Wi' experiments were compromised by irrigation and rain, respectively. Further, the addition of the air distributor improved the energy parameters by a percentage increase of 125% (SMER), 249% (MER), and 255% (COP). Comparison of the energy parameters with dryers in the literature showed that the 'Np' and 'Mo' experiments were either within or above limits. However, the 'Wi' experiment poorly performed due to the underutilization of the SHAD because of its small size. Thus, SHAD and air distributors should be used to dehydrate almonds in the range of 4,763 (0.042 ± 0.01 m3/s per m3 of fresh almonds) and 6,849 kg (0.02 ± 0.005 m3/s per m3) for satisfactory results. Future work will evaluate the effectiveness of utilizing the SHAD with the air distributor to properly dehydrate larger almond stockpiles, as well as the effect of incorporating larger fans, and the addition of stockpile covers to augment air recirculation.

References

Addis, P. B. (1986). Occurrence of lipid oxidation products in foods. Food and Chemical Toxicology, 24(10-11), 1021–1030. https://doi.org/10.1016/0278-6915(86)90283-8

Alam, M. A., Saha, C. K., Momin, M. A., Alam, M. M., Bala, B. K. (2016). Spatial Distribution of Temperature and Moisture in Grain Bin and Grain Bin Size Effect on STR Dryer Performance in Bangladesh. Journal of Agricultural Machinery and Bioresource Management, 7(1), 1–8

Allwood, M. (2008). The Satterthwaite formula for degrees of freedom in the two-sample t-test. The College Board.

Bhattacharyya, M. (2013). To pool or not to pool: A comparison between two commonly used test statistics. International Journal of Pure and Applied Mathematics, 89(4), 497-510.

Bridge, T. C., White, G. M., Loewer, O., Jr. (1986). Batch-ln-Bin grain drying. Retrieved from https://www.uky.edu/bae/sites/www.uky.edu.bae/files/AEN-57.pdf

Buransompob, A., Tang, J., Mao, R., & Swanson, B. G. (2003). Rancidity of walnuts and almonds affected by short time heat treatments for insect control. Journal of food processing and preservation, 27(6), 445-464.

Campbell, B. C., Molyneux, R. J., & Schatzki, T. F. (2003). Current Research on Reducing Pre- and Post-harvest Aflatoxin Contamination of U.S. Almond, Pistachio, and Walnut. Journal of Toxicology: Toxin Reviews, 22(2-3), 225–266. https://doi.org/10.1081/txr-120024093

CDR FoodLab. (2021a). Peroxide Value Test in Fats and Oils. Retrieved from https://www.cdrfoodlab.com/foods-beverages-analysis/peroxide-value-oils-fats/

CDR FoodLab. (2021b). Free Fatty Acids Test in Fats and Oils. Retrieved from https://www.cdrfoodlab.com/foods-beverages-analysis/ffa-fats-oils/

Cengel, Y. A., & Cimbala, J. M. (2017). Fluid mechanics: Fundamentals and applications (4th ed.). McGraw-Hill Education.

Ceylan, I., & Gurel, A. E. (2016). Solar-assisted fluidized bed dryer integrated with a heat pump for mint leaves. Appl. Thermal Eng., 106, 899-905. https://doi.org/10.1016/j.applthermaleng.2016.06.077

Chapchaimoh, K., Poomsa-ad, N., Wiset, L., & Morris, J. (2016). Thermal characteristics of heat pump dryer for ginger drying. Appl. Thermal Eng., 95, 491-498. https://doi.org/10.1016/j.applthermaleng.2015.09.025

Chen, C., Liao, C., Wongso, I., Wang, W., Gebreil, R. K. A. E., Ning, Z., Huang, G., Niederholzer, F., Wang, L., & Pan, Z. (2021). Drying and disinfection of off-ground harvested almonds using step-down temperature hot air heating. https://doi.org/10.13031/aim.202100267

Chen, C., Gebreil, R. K. A. E., Shen, Y., Wu, X., Ning, Z., Niederholzer, F., & Pan, Z.. (2020). Energy and Quality Analyses of Off-ground Harvested Almonds under Hot Air Column Drying. https://doi.org/10.13031/aim.202000193

Chilka, A. G., & Ranade, V. V..(2019). CFD modelling of almond drying in a tray dryer. The Canadian Journal of Chemical Engineering, 97(2), 560–572. https://doi.org/10.1002/cjce.23357

Commission Internationale de l'Eclairage (CIE) (1986) Colorimetry. 2nd Edition, Publication CIE No. 15.2. Commission Internationale de l'Eclairage, Vienna.

Coates, M. C. (2018). Defining and modeling the boundaries for mechanized dehydration to produce high quality almonds. PhD diss. University of South Australia, School of Engineering.

Capanoglu, E., & Boyacioglu, D. (2008). Improving the quality and shelf life of Turkish almond paste. Journal of food quality, 31(4), 429-445.

Corradini, M. G.. (2019). Synthetic Food Colors (pp. 291–296). https://doi.org/10.1016/b978-0-08-100596-5.21606-5

Coskun, S., Doymaz, Ä., Tunckal, C., & Erdogan, S. (2017). Investigation of drying kinetics of tomato slices dried by using a closed loop heat pump dryer. Heat Mass Transfer, 53(6), 1863-1871. https://doi.org/10.1007/s00231-016-1946-7

Clydesdale, F.M., 1991. Color perception and food quality. Journal of Food Quality 14, 61–74.. doi:10.1111/j.1745-4557.1991.tb00047.x

Das, S., Das, T., Srinivasa Rao, P., & Jain, R. K.. (2001). Development of an air recirculating tray dryer for high moisture biological materials. Journal of Food Engineering, 50(4), 223–227. https://doi.org/10.1016/s0260-8774(01)00024-3

Davies C. G. A., Labuza T. P. (1997). The Maillard Reaction Application To Confectionery Products. Confectionery Science, 33, 35–66. Retrieved from https://pdfs.semanticscholar.org/561f/5d0292e2cec1752430e2df3966204bab9a28.pdf

Day, D.L., Nelson, G.L., 1962. Predicting performances of crossflow systems for drying grain in storage in deep cylindrical bins. American Society of Agricultural Engineers, Paper No. 62-925.

Dickerson, Richard E. and Gray, Harry B. and Haight, Gilbert P. (1979) Chemical principles. Third edition. The Benjamin/Cummings Publishing Company, Inc. , Menlo Park, CA. ISBN 0805323988.

Dingke, Z., & Fielke, J. (2014). Some physical properties of Australian Nonpareil almonds related to bulk storage. International Journal of Agricultural and Biological Engineering, 7(5), 116-122.

Franz Niederholzer. (2012). Coping with rain at harvest. Retrieved from https://www.almonds.com/sites/default/files/coping_with_rain_at_harvest%5B1%5D.pdf

Fielke, J. M.. (2019). On-farm evaluation of a new paradigm for almond drying and storage: Australia 2019 harvest. https://doi.org/10.13031/aim.201900210

Fielke, J. M., & Coates, M. C. (2017). Lessons learnt from on-farm mechanical drying of almonds in 2017. In VII International Symposium on Almonds and Pistachios 1219 (pp. 273-280).

Gao, M., Tang, J., Villa-Rojas, R., Wang, Y., & Wang, S.. (2011). Pasteurization process development for controlling Salmonella in in-shell almonds using radio frequency energy. Journal of Food Engineering, 104(2), 299–306. https://doi.org/10.1016/j.jfoodeng.2010.12.021

Huang, G. (2014). Almond Shelf Life Factors. Almond Board of California, (July), 1–4. Retrieved from https://www.almonds.com/sites/default/files/content/attachments/2014aq0007_shelf_life_factors.pdf

IRRI (2021) International Rice Research Institute. Rice Knowledge Bank. Air Distribution System. Retrieved from http://www.knowledgebank.irri.org/step-by-step-production/postharvest/drying/dryer-components/item/air-distribution-system

King Jr, A. D., Miller, M. J., & Eldridge, L. C. (1970). Almond harvesting, processing, and microbial flora. Applied Microbiology, 20(2), 208-214.

Läubli, M.W., Bruttel, P.A., 1986. Determination of the oxidative stability of fats and oils: Comparison between the active oxygen method (AOCS Cd 12-57) and the rancimat method. Journal of the American Oil Chemists' Society 63, 792–795.. doi:10.1007/bf02541966

Lawrence, J., Atungulu, G. G., Siebenmorgen, T. J. (2015). Modeling in-bin rice drying using natural air and controlled air drying strategies. Transactions of the ASABE, 58(4), 1103–1111. https://doi.org/10.13031/trans.58.10911

Li, R., Kou, X., Zhou, X., Zhang, L., & Wang, S.. (2018). Application of radio frequency pasteurization process to almond kernels: Heating uniformity improvement. https://doi.org/10.13031/aim.201800526

Lin, X., Wu, J., Zhu, R., Chen, P., Huang, G., Li, Y., Ye, N., Huang, B., Lai, Y., Zhang, H., Lin, W., Lin, J., Wang, Z., Zhang, H., Ruan, R., 2012. California Almond Shelf Life: Lipid Deterioration During Storage. Journal of Food Science 77, C583–C593.. doi:10.1111/j.1750-3841.2012.02706.x

King, A. D. J., Halbrook, W. U., Fuller, G., & Whitehand, L. C.. (1983). Almond Nutmeat Moisture and Water Activity and its Influence on Fungal Flora and Seed Composition. Journal of Food Science, 48(2), 615–617. https://doi.org/10.1111/j.1365-2621.1983.tb10802.x

Mahesar, S. A., Sherazi, S. T. H., Khaskheli, A. R., & Kandhro, A. A. (2014). Analytical approaches for the assessment of free fatty acids in oils and fats. Analytical Methods, 6(14), 4956-4963.

Markowicz, D., Monaro, E., Siguemoto, E., & Sefor, M. (2012). Maillard Reaction Products in Processed Food: Pros and Cons. https://doi.org/10.5772/31925

Mayanja, I. K., Coates, M. C., Niederholzer, F., & Donis-González, I. R. (2021). Development of a Stockpile Heated and Ambient Air Dryer (SHAD) for Freshly Harvested Almonds. Applied Engineering in Agriculture, 37(3), 417-425.

Metrohm. (2017). 892 Professional Rancimat. Retrieved from https://www.metrohm.com/en-my/documents/88928001

Metrohm, A. G. (2013). Oxidative stability of oils and fats-Rancimat method. Metrohm application bulletin No, 204, 1-4. Retrieved from https://partners.metrohm.com/GetDocumentPublic?action=get_dms_document&docid=1184905

Micke W, Kester D, Rizzi A, Carlson C. 1966. Early harvesting of almonds. Calif Agr 20(12):14-16.

Minolta, 1994. Precise Colour Communication: Color Control from Feeling toInstrumentation, Minolta report, Japan.

Mohanraj, M., & Chandrasekar, P. (2009). Performance of a forced convection solar drier integrated with gravel as heat storage material for chili drying. J. Eng. Sci.Technol., 4(3), 305-314

Mortezapour, H., Ghobadian, B., Minaei, S., & Khoshtaghaza, M. H. (2012). Saffron drying with a heat pump-assisted hybrid photovoltaic-thermal solar dryer. Drying Technol., 30(6), 560- 566. https://doi.org/10.1080/07373937.2011.645261

Mozuraityte, R., Kristinova, V., & Rustad, T.. (2016). Oxidation of Food Components (pp. 186–190). https://doi.org/10.1016/b978-0-12-384947-2.00508-0

Noyes, R. T. (2006). Development of a new low-energy environmentally compatible grain and seed drying and storage technology. Proceedings of the 9th International Working Conference on Stored-Product Protection, ABRAPOS, Passo Fundo, RS, Brazil, 15-18 October 2006, 1285–1294. Retrieved from http://bru.gmprc.ksu.edu/proj/iwcspp/pdf/9/kp11.pdf%0Ahttps://www.cabdirect.org/cabdirect/abstract/20103006857

Oktay, Z., & Hepbasli, A. (2003). Performance evaluation of a heat pump assisted mechanical opener dryer. Energy Convers. Manag., 44(8), 1193-1207. https://doi.org/10.1016/S0196-8904(02)00140-1

Pal, U. S., & Khan, M. K. (2010). Performance evaluation of heat pump dryer. J. Food Sci. Technol., 47(2), 230-234. https://doi.org/10.1007/s13197-010-0031-3

Paramount Farms. 2000. Product data sheet: Natural whole supreme almonds. Bakersfield, CA.

Perry, E., & Sibbett, G. S. (1998). Harvesting and Storing Your Home Orchard's Nut Crop: Almonds, Walnuts, Pecans, Pistachios, & Chestnuts.

Prasertsan, S., & Saen-Saby, P. (1998). Heat pump drying of agricultural materials. Drying Technol., 16(1-2), 235-250. https://doi.org/10.1080/07373939808917401

Rogel-Castillo, C., Luo, K., Huang, G., & Mitchell, A. E. (2017). Effect of drying moisture exposed almonds on the development of the quality defect concealed damage. Journal of agricultural and food chemistry, 65(40), 8948-8956.

Sampedro, F., Fan, X., & Rodrigo, D. (2010). High hydrostatic pressure processing of fruit juices and smoothies: research and commercial application. In Case studies in novel food processing technologies (pp. 34-72). Woodhead Publishing.

Sewald, M., & DeVries, J. (2003). Food product shelf life. Medallion Laboratories Analytical Progress, 1-10.

Sevik, S., Aktas, M., Dogan, H., & Kocak, S. (2013). Mushroom drying with solar assisted heat pump system. Energy Conversion Manag., 72, 171-178. https://doi.org/10.1016/j.enconman.2012.09.035

Simpson, E. S. C., & Weiner, J. A. (Eds.) (1989). The Oxford Encyclopaedic English Dictionary. Oxford: Clarendon Press

Uesugi, A. R., & Harris, L. J. (2006). Growth of Salmonella Enteritidis phage type 30 in almond hull and shell slurries and survival in drying almond hulls. Journal of food protection, 69(4), 712-718.

USDA. (2013). United States Standards for Grades of Almonds in the Shell. USDA-Agricultural Marketing Service. Retrieved from https://ucfoodsafety.ucdavis.edu/sites/g/files/dgvnsk7366/files/inline-files/175432.pdf

U.S. Department of Agriculture, Agricultural Research Service, Nutrient Data Labratory. USDA National Nutrient Database for Standard Reference, Release 28. Version Current: September 2015. http://www.ars.usda.gov/nea/bhnrc/ndl.

Vieira, S.A., Zhang, G. & Decker, E.A. Biological Implications of Lipid Oxidation Products. J Am Oil Chem Soc 94, 339–351 (2017). https://doi.org/10.1007/s11746-017-2958-2

Vijayan, S., Arjunan, T. V., & Kumar, A. (2016). Mathematical modeling and performance analysis of thin layer drying of bitter gourd in sensible storage based indirect solar dryer. Innovative Food Sci. Emerg. Technol., 36, 59-67. https://doi.org/10.1016/j.ifset.2016.05.014

Yada, S., Lapsley, K., & Huang, G.. (2011). A review of composition studies of cultivated almonds: Macronutrients and micronutrients. Journal of Food Composition and Analysis, 24(4-5), 469–480. https://doi.org/10.1016/j.jfca.2011.01.007

Yahya, M., Fudholi, A., Hafizh, H., & Sopian, K. (2016). Comparison of solar dryer and solar-assisted heat pump dryer for cassava. Sol. Energy, 136, 606-613. https://doi.org/10.1016/j.solener.2016.07.049

Appendix

Appendix I: Final MC_{db} of almond components

Kernel							
Stockpile				Windrow			
Variety	Bottom	Middle	Top	Variety	Bottom	Middle	Top
Np	3.64 ±0.88	4.70 ±1.64	5.02 ±0.51	Np	16.57 ±7.55	21.01 ±8.14	15.34 ±5.26
Wi	4.43 ±0.56	4.42 ±0.42	5.08 ±1.09	Wi	6.24 ±0.51	6.82 ±0.91	7.31 ±0.40
Mo	4.01 ±0.79	4.03 ±0.59	4.04 ±0.60	Mo	4.72 ±1.03	4.89 ±1.28	5.82 ±1.25
Shell							
Stockpile				Windrow			
Variety	Bottom	Middle	Top	Variety	Bottom	Middle	Top
Np	5.87 ±1.14	5.77 ±1.15	5.40 ±0.35	Np	25.50 ±14.97	36.48 ±12.70	22.10 ±10.33
Wi	5.85 ±0.48	5.73 ±0.12	6.65 ±0.63	Wi	7.22 ±0.57	8.08 ±0.88	8.09 ±0.63
Mo	6.75 ±2.68	7.60 ±1.10	8.43 ±0.79	Mo	7.39 ±1.51	7.26 ±1.56	8.14 ±1.86
Hull							
Stockpile				Windrow			
Variety	Bottom	Middle	Top	Variety	Bottom	Middle	Top
Np	23.78 ±1.04	24.75 ±4.38	26.62 ±1.53	Np	104.05±66.81	131.63±40.47	85.76±43.72
Wi	17.89 ±0.87	17.61 ±0.68	19.45 ±1.82	Wi	23.15 ±0.60	24.02 ±1.94	24.56 ±1.13
Mo	14.54 ±4.30	13.13 ±4.72	12.11 ±1.84	Mo	18.35 ±6.79	20.13 ±7.37	23.88 ±5.37
Whole							
Stockpile	Windrow						
Variety	Bottom	Middle	Top	Variety	Bottom	Middle	Top
Np	14.52 ±0.68	15.37 ±2.96	16.39 ±1.14	Np	68.59 ±51.43	83.72 ±41.83	56.76 ±35.46
Wi	10.10 ±0.77	9.90 ±0.76	11.54 ±1.82	Wi	13.95 ±1.05	14.87 ±1.16	15.31 ±1.31
Mo	9.25 ±2.97	8.20 ±1.45	7.98 ±1.11	Mo	10.16 ±3.17	11.24 ±3.55	13.03 ±2.30

Appendix II: Initial and final bulk density for almonds

Initial (Kg/m^3)							
Np	338.00 ±12.99		Wi	333.63 ±5.36		Mo	334.87 ± 8.55
Stockpile (final)				Windrow (final)			
Variety	Bottom	Middle	Top	Variety	Bottom	Middle	Top
Np	343.55±7.05	340.37±12.15	341.56±12.06	Np	414.67±48.73	440.72±36.43	395.84±42.48
Wi	346.95±5.68	342.38±5.31	339.16±1.68	Wi	339.79±11.55	340.28 ±4.92	342.4 ±5.14
Mo	358.21±8.19	349.79±12.67	337.73±5.93	Mo	353.61±9	341.9±12.64	329.59±8.15

Appendix III: l*, a* and b* coordinates values for stockpile experiments

l* (inside)				l* (surface)			
Variety	**Bottom**	**Middle**	**Top**	**Variety**	**Bottom**	**Middle**	**Top**
Np	52.94 ±1.34	52.27 ±1.61	51.99 ±1.22	**Np**	29.51 ±1.70	29.48 ±1.38	29.37 ±1.91
Wi	52.91 ±1.32	52.67 ±1.75	52.27 ±1.29	**Wi**	26.73 ±1.32	27.00 ±1.61	26.67 ±1.16
Mo	53.34 ±1.47	53.79 ±1.17	54.20 ± 0.95	**Mo**	27.83 ±1.25	28.23 ±1.14	27.88 ±1.16
a* (inside)				**a* (surface)**			
Variety	**Bottom**	**Middle**	**Top**	**Variety**	**Bottom**	**Middle**	**Top**
Np	1.63 ±0.49	1.66 ±0.49	1.72 ±0.51	**Np**	8.77 ±0.51	8.57 ±0.64	8.39 ±0.78
Wi	1.09 ±0.27	1.20 ±0.33	1.18 ±0.22	**Wi**	7.03 ±0.64	7.19 ±0.79	7.30 ±0.55
Mo	1.12 ±0.36	1.05 ±0.31	0.97 ±0.28	**Mo**	7.57 ±0.60	7.46 ±0.59	7.26 ± 0.58
b* (inside)				**b* (surface)**			
Variety	**Bottom**	**Middle**	**Top**	**Variety**	**Bottom**	**Middle**	**Top**
Np	12.73 ±2.21	12.57 ±1.98	12.81 ±1.85	**Np**	13.74 ±1.93	12.93 ±1.79	12.64 ±1.90
Wi	10.34 ±1.32	10.76 ±2.05	10.81 ±1.44	**Wi**	10.42 ±1.39	10.63 ±1.34	10.20 ±1.24
Mo	11.19 ±1.74	10.42 ±1.37	10.13 ±1.30	**Mo**	11.31 ±1.40	11.08 ±1.13	10.49 ±1.13

Appendix IV: l*, a* and b* coordinates values for windrow experiments

l* (inside)				l* (surface)			
Variety	**Row1**	**Row2**	**Row3**	**Variety**	**Row1**	**Row2**	**Row3**
Np	50.29 ±2.63	49.09 ±2.42	50.59 ±2.26	**Np**	30.79 ±1.78	30.17 ±1.41	30.23 ±1.60
Wi	51.57 ±1.53	52.34 ±1.37	51.83 ±1.59	**Wi**	26.93 ±1.06	27.17 ±1.19	27.34 ±1.17
Mo	53.68 ±1.21	53.77 ±1.06	53.90 ±1.17	**Mo**	28.25 ±1.08	28.90 ±1.10	28.50 ±1.22
a* (inside)				**a* (surface)**			
Variety	**Bottom**	**Middle**	**Top**	**Variety**	**Bottom**	**Middle**	**Top**
Np	1.80 ±0.52	1.76 ±0.62	1.70 ±0.46	**Np**	9.08 ±0.76	9.09 ±0.53	9.02 ±0.55
Wi	1.13 ±0.32	1.16 ±0.29	1.11 ±0.33	**Wi**	6.96 ±0.58	7.25 ±0.55	7.24 ±0.53
Mo	1.05 ±0.38	0.99 ±0.36	1.03 ±0.34	**Mo**	7.49 ±0.56	7.54 ±0.73	7.40 ±0.60
b* (inside)				**b* (surface)**			
Variety	**Bottom**	**Middle**	**Top**	**Variety**	**Bottom**	**Middle**	**Top**
Np	14.44 ±2.50	14.32 ±2.37	14.14 ±2.28	**Np**	15.58 ±2.06	15.29 ±1.70	15.08 ±1.87
Wi	10.43 ±1.62	10.85 ±1.82	10.20 ±1.75	**Wi**	10.58 ±1.15	10.73 ±1.11	11.06 ±1.19
Mo	10.54 ±1.76	10.71 ±1.87	10.65 ±1.42	**Mo**	11.21 ±1.05	11.60 ±1.21	11.41 ±1.20

CHAPTER 5

FINAL REMARKS AND FUTURE WORK

Almond is the most produced nut, accounting for 31% of the World nut production (INC, 2020). The majority of the almonds are produced in California (USA) with a 77% World share, followed by Australia (8%), and Spain (6%) (INC, 2020). As it was described in Chapter 1, conventional harvest and post-harvest handling of almonds in California involves: 1) Shaking the almonds to the orchard ground, with a mechanical shaker when nearing 100% hull split; 2) Drying almonds on the orchard ground for up to 21 days, from a typical 10% to 25% kernel dry basis moisture content (MC_{db}) to an industry storage standard of 6% MC_{db} or less; 3) Sweeping the almonds into windrows, with a mechanical sweeper; 4) Picking-up almonds from the orchard ground, with a mechanical harvester; and 5) Transporting the almonds to stockpiles for storage, and/or fumigation, then to the hulling and shelling facility. However, shaking, sweeping, and picking-up processes produce nearly 16.7 million kg of microscopic dust particles (CARB, 2017). Dust production is a growing point of contention within the community because it is a human hazard, which reduces visibility and aggravates allergies. The rapid growth of the almond acreage in California from 525,000 to 1,180,000 acres, in a span of 2 decades (2001 to 2021) reflects a high potential for the continuous rise in dust emission if conventional harvest and post-harvest handling methods are maintained (CDFA, 2020).

Further, almonds in the orchard are typically consumed by birds (e.g., Scrub Jays), rodents, and infested with insects such as the Navel Orange Worm (NOW) leading to loss of almond growers' revenue (Perry et al., 1989). In addition, almonds are susceptible to contamination with human pathogenic microorganisms (e.g. *Salmonella Enteritidis)* when exposed to the orchard ground, especially during windrow drying (Schatzki and Ong, 2001; Martha et al, 2012). Also, almond

windrow drying delays irrigation and can reduce yield by as much as 77% (Goldhamer and Viveros, 2000).

Therefore, this research evaluated stockpile drying as an alternative technique to dehydrate almonds because it: 1) Eradicates the sweeping and picking processes during conventional harvesting; 2) Allows early harvesting, which reduces human pathogen infestation and pests; and 3) Doesn't interfere with irrigation, since it's not conducted directly on the almond orchard. The concept of stockpiling almonds is not alien to the almond industry. Currently, stockpiles are used to store almonds before being transferred to the processing facilities, and fumigation mainly for NOW. Thus, adopting the proposed stockpile drying technique is practical mainly due to the existing infrastructures in place.

Chapter 2 describes the development and testing of an almond Stockpile Heated Air Dryer (SHAD) to dehydrate almonds outdoors, but away from the orchard. Almonds are deposited onto an A-frame within the SHAD, from the harvesting conveyor cart to form a stockpile. The A-frame acts as a plenum where drying air is supplied before distributing it to the almond stockpile. The SHAD uses a combination of heated and ambient air to achieve almond dehydration. SHADs can potentially be installed in a designated area adjacent to the almond orchard, or during commercial almond stockpiling within the hulling and processing (shelling) facilities. The effectiveness of the SHAD was tested on dehydrating a 4,155 kg 'Monterey'('Mo') variety almond stockpile. Almonds were dried for 11 days from an average MC_{db} equal to 12.6 % to the desired storage MC_{db} of or below 6 %. However, a lack of moisture uniformity throughout the stockpile was observed, mainly attributed to the inability of the SHAD to properly distribute and deliver the drying air to the almonds. Comparison with other commercially available dryers showed that the SHAD yielded a low and undesirable Coefficient of Performance (COP) of 1.33. A low COP equates to a poor

SHAD's efficiency, high-energy consumption, and thus higher operational costs. Hence, there was a need to develop a means of improving the distribution of the supplied drying air to the almond stockpile by the SHAD.

Therefore, an air distributor comprising of 12 outlets, arranged in 4 rows with 3 outlets in each row was developed to address the challenge of non-uniform air distribution in a stockpile, as described in Chapter 3. The air distributor is placed within the A-frame and under the stockpile, ensuring that supplied air is uniformly diverted to all sections of the stockpile. In-field airflow measurements showed that the percentage airflow distribution (*β-value*) was 4.1, 30.8, 44.9, and 20.2% for rows 1, 2, 3, and 4, respectively, when all outlets are open. Thus, almonds located in the region of row 1 would not receive sufficient airflow. So, an optimized 3-row air distributor configuration was developed, which involved sealing off all outlets in row 1. The optimized air distributor 3-row configuration *β-values* from in-field airflow measurements were equal to 31.3%, 44.4%, and 24.3% for rows 2 through 4. Due to the typical cone-shape of the almond stockpile, it is desirable for the middle section to receive the highest airflow (44.4%) since it has the most almonds. Alternatively, it is possible for a 4-row air distributor configuration to properly distribute air through the stockpile if it is placed in accordance with the stockpile shape. However, this implies that airflow percentage equal to around 4.1 % would be lost to the environment, which would otherwise be utilized by the other open outlets. Possible modifications of the developed and optimized 3-row air distributor configuration design include increasing its length, modifying the placement of the outlets, and increasing the number of outlets. The latter then has the potential of including more than 4-rows of outlets, as potentially required to dehydrate larger stockpiles. Also, the use of more than one air distributor within the same stockpile can allow efficient dehydrating

of larger stockpiles. However, there is a need to evaluate the efficiency, energy usage, and cost for alternative air-distributor designs.

In Chapter 4, the effect of incorporating the developed air distributor as a SHAD component was evaluated. This was compared with the effectiveness of dehydrating almonds with the SHAD without the air distributor (Chapter 2), and with conventional windrow drying. Stockpile dehydration experiments with the SHAD and the air distributor were conducted on 'Nonpareil'('Np'), 'Winter'('Wi'), and 'Mo' varieties weighing 4,763 kg, 2,585 kg, and 6,849 kg, respectively. In terms of energy performance indicators, adding the air distributor to SHAD outperformed the experiment without the air distributor by a percentage increase of 125% (Specific Moisture Extraction Rate (SMER)), 249% (Moisture Extraction Rate (MER), and 255% (COP). Comparison with other commercially available dryers showed that the 'Np' and 'Mo' experiments were either within or above limits. However, the 'Wi' experiment underperformed mainly attributed to the underutilization of the SHADs drying air, due to the stockpile's small size. Hence, the SHAD and air distributor can be used to effectively dehydrate fresh almond stockpiles in the range of 4,763 kg (0.04 ± 0.01 m^3/s per m^3 of almonds) to 6,849 kg (0.02 ± 0.005 m^3/s per m^3 of almonds). There is still a need to determine the upper limit of the SHAD and air distributor, which can only be achieved by testing it on larger stockpiles (> 6849 kg) until unsatisfactory energy performance indicators are observed. Further, the drying time using the SHAD with air distributor was shorter (maximum of 7.0 days) compared to windrow drying (up to 13.6 days). It was observed that the quality of almonds (decay or mold injury, insect damage, internal cavities, color, Induction time, Peroxide Value, and Free Fatty Acid content) conventionally dehydrated can be compromised. For example, the 'Np' and 'Wi' conventional windrow drying experiments were affected by irrigation and rain, respectively. Ultimately, the SHAD and air distributor reduced the

challenges of conventional windrow drying including dust emission, pest, and human pathogen infestation, and irrigation timing. Also, there is no evidence that the almond quality of the stockpile-dried almonds was affected.

Furthermore, comparing the weight of almonds accommodated per unit area between the conventional windrow and stockpile drying will also influence the almond growers' decision on which drying method to adapt. Casanova-Gascón et al., (2019) stated that conventional planting at 278 trees/ha (6 x 6 m spacing) yields fresh almond whole fruit weight of 53 kg per tree, which translates to 14,734 kg/ha. For conventional windrow drying, almonds are swept with a mechanical sweeper to form windrows in between the almond trees (6 m spacing) as illustrated in Figure 5.1a, and windrows accommodate the almond yield generated from that specific almond orchard. Thus, 14,734 kg is accommodated per ha in windrows, whilst using the conventional windrow drying method. In contrast, the previous experiments (Chapter 4) were conducted on stockpiles of weights 4,763 kg, 2,585 kg, and 6,849 kg with corresponding ground coverages of 4.9 x 3.6 m, 3.6 x 2.4 m, and 7.3 x 4.9 m for 'Np', 'Wi', and 'Mo' experiments, respectively as shown in Figure 5.1b. Therefore, the weight of almonds accommodated for stockpile drying is 2,700,113 kg/ha ('Np'), 2,991,898 kg/ha ('Wi'), and 1,914,733 kg/ha ('Mo'), which translates to an average of 2,535,581 kg/ha (without accounting for the space of the drying equipment). Hence, the use of SHAD to dehydrate almonds in stockpiles allows to dehydrate larger quantities of almonds, in less space, when compared to the conventional windrow drying (around 18,323 kg/ha).

Thus, the positive results generated in this study highlight the possibility, feasibility, and applicability of drying off-ground freshly harvested almonds in a stockpile, as an alternative to the existing conventional windrow drying.

Future work will evaluate the SHAD and air distributor as a feasible method to dehydrate larger stockpiles (> 10,000 kg), by incorporating a larger fan and further optimizing the design of the air distributor. Also, future studies will explore the effect of air recirculation, which would otherwise be lost to the environment, on the effectiveness of the SHAD. Air recirculation in a stockpile can be achieved by adding covers, such as a tarp, which can create backpressure that doesn't allow the air to directly escape through the top of the stockpile. With an appropriate cover, the drying air can be redirected to escape through the bottom of the stockpile, instead of the top.

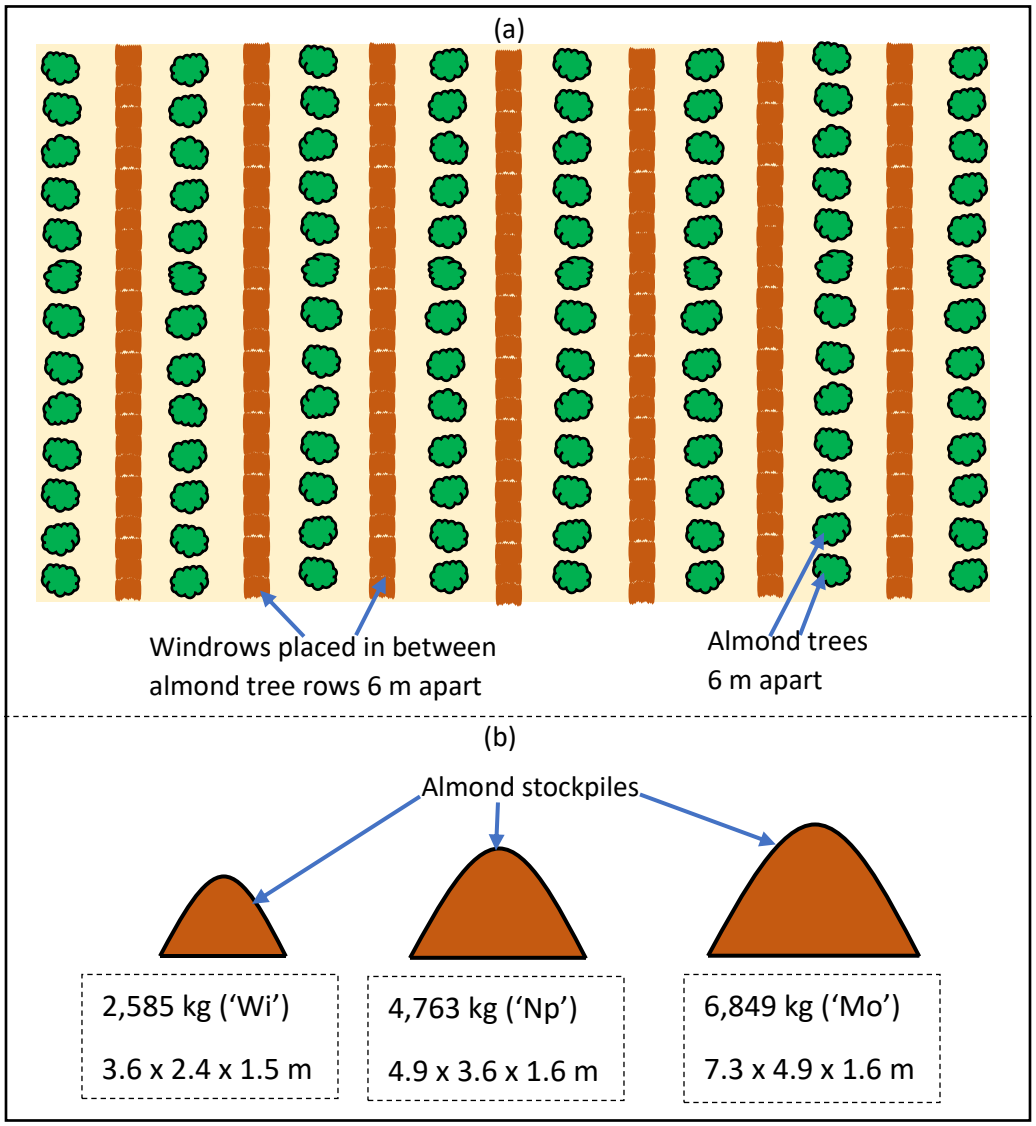

Figure 5.1. Schematic of: (a) Almond orchard showing almond trees and windrows placed in between the tree rows. (b) Almond stockpiles of three different sizes

Currently, the SHAD is powered by propane, which is a non-renewable fuel source. Propane is used to heat the air (heater) and to power the generator for the electrical components, such as the fan, and sensors. There is a need to investigate alternative energy sources, which involve capitalizing on the available solar energy during the almond harvest season (August through October). To compare with other alternative energy sources, the Energy Cost parameter (EC) is used, which is expressed as the ratio of the cost utilized in the generation of the energy ($) to the energy utilized (MJ). Thus, the EC for the electrical and propane energy for SHAD was 0.044 $/MJ and 0.025 $/MJ, respectively, averaged from the previous experiments conducted in Chapter 4. The EC for electrical energy was higher than the propane energy. Electrical energy can be provided by using photovoltaic (PV) modules or solar panels to harness the solar energy, which can power the SHAD's electrical components. Feldman et al., (2021) showed that the EC for commercialized PV including storage is $ 0.0202/ MJ. Also, a thermal rock bed may be used to store the heat during the day in form of thermal energy and utilize it to heat the SHAD's drying air during the night and cooler days. Allen et al., (2016) stated that the energy cost for a thermal rock bed can be less than $ 0.02/MJ. The SHAD may be powered by either; 1) A dual propane-solar system, which uses propane to power the heater and solar energy (PV or thermal rock bed) to power the electrical components and store heat, or 2) A solely solar-powered system. A comprehensive cost comparison and a life cycle analysis is needed to ascertain the best option that optimizes the available resources while reducing drying energy usage and the cost.

The availability of land to cultivate almonds and other crops is diminishing partly due to urbanization, this creates a need for a High-Density Planting (HDP) system. HDP is a cultivation technique in which a higher number of plants are planted within a unit area in comparison to

conventional planting. The purpose of HDP is to obtain the maximum crop yield per unit area (Mishra and Goswami, 2016; Choudhary et al, 2015).

On one hand, conventional planting of 238 trees per ha with a 6 x 7 m spacing yielded a dry kernel weight of 2,508.4 kg/ha (López-López et al., 2018). On the other hand, HDP of 2190 trees per ha with 3.8 x 1.2 m spacing yielded a dry inshell weight of 5,410 kg/ha (Maldera et al., 2021).

Thus, increasing on the planting densities increases the almond yield. Furthermore, reducing the space between rows in an HDP system doesn't allow sufficient space for mechanical shakers and sweepers to properly operate. Therefore, Over-The-Row (OTR) harvesters can be potentially used to harvest almonds, which are driven within the almond rows. OTR harvesters engulf the whole almond tree through an opening that contains swaying bow-rods on both ends to shake the almond tree canopy and detach the almonds are collected, then conveyed to a trailer, as shown in Figure 5.2. The almond industry has not yet adopted the use of OTR, but this harvesting method has been successfully implemented in harvesting grapes (Morris, 1999), blueberries (Sargent et al., 2021), and olives (Pérez-Ruiz et al., 2018).

At harvest, hulls account for 55% of the total weight of almonds (Dingke and Fielke, 2014). Thus, removing the almond hull (dehulling) prior to drying will significantly reduce the weight and bulk of almonds during transport, and will reduce the drying energy by 60 %, which is the typical requiered eneryg to dehydrate hulls (Chen et al., 2021). OTR harvesters with an add-on dehulling mechanism can be potentially used to harvest and dehull almonds prior to stockpile drying, but the technology is still not commercially available. Fielke (2018) developed a prototype that has the potential to be adapted to an OTR harvest. The previous, uses forced air to impact the fresh almonds, while being conveyed, and therefore detaching them from their hull. Ultimately, as

almond production evolves, a combination of HDP, OTC harvesters, on-farm hulling, and SHAD with proper air distribution can offer a feasible solution to efficiently harvest and dry almonds.

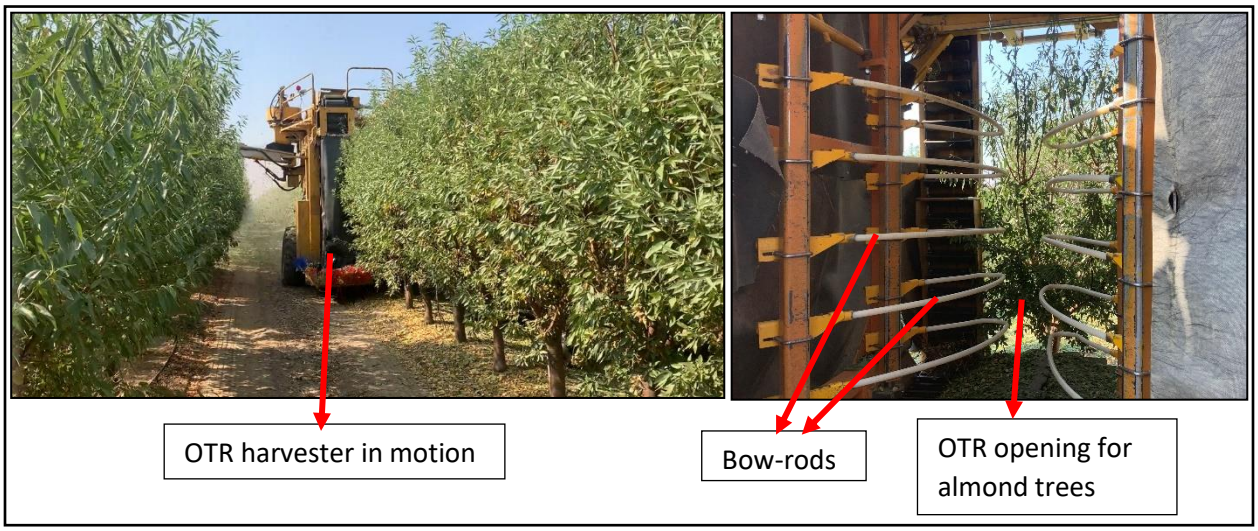

Figure 5.2. Pictures showing Over-The-Row (OTR) harvester

References

Allen, K., von Backström, T., Joubert, E., & Gauché, P. (2016, May). Rock bed thermal storage: Concepts and costs. In AIP Conference Proceedings (Vol. 1734, No. 1, p. 050003). AIP Publishing LLC.

CARB. (2017). Agricultural harvest operations. California Air Resources Board: Emission Inventory Source Category. Retrieved from https://ww3.arb.ca.gov/ei/areasrc/fullpdf/full7-5_2017.pdf

Casanova-Gascón, J., Figueras-Panillo, M., Iglesias-Castellarnau, I., & Martín-Ramos, P.. (2019). Comparison of SHD and Open-Center Training Systems in Almond Tree Orchards cv. 'Soleta'. Agronomy, 9(12), 874. https://doi.org/10.3390/agronomy9120874

CDFA. (2020). California almond acreage report. California Department of Food and Agriculture. Retrieved from https://www.nass.usda.gov/Statistics_by_State/California/Publications/Specialty_and_Other_Releases/Almond/Acreage/202004almac.pdf

Chen, C., Khir, R., Shen, Y., Wu, X., Zhang, R., Cao, X., ... & Pan, Z. (2021). Energy consumption and product quality of off-ground harvested almonds under hot air column drying. LWT, 138, 110768.

Choudhary, H. D., Khandelwal, S. K., Choudhary, M. K., Gadawal, O. P., & Choudhary, M. R. (2015). High density and meadow orchard planting system in fruit crops. Horticulture Research Report of SKN College of Agriculture, Jobner, 1-5.

Dingke, Z., & Fielke, J. (2014). Some physical properties of Australian Nonpareil almonds related to bulk storage. International Journal of Agricultural and Biological Engineering, 7(5), 116-122.

Fielke, J. (2018). Advanced processing of Almonds. Hort Innovation. Retrieved from https://www.horticulture.com.au/globalassets/laserfiche/assets/project-reports/al12003/al12003---final-report-complete.pdf

Goldhamer, D. A., Viveros, M. (2000). Effects of preharvest irrigation cutoff durations and postharvest water deprivation on almond tree performance. Irrigation Science, 19(3), 125–131. https://doi.org/10.1007/s002710000013

INC. (2020). Nuts and dried fruits. Statistical yearbook 2019/2020. International Nut, and Dried Fruit Council. Retrieved from https://www.nutfruit.org/files/tech/1587539172_INC_Statistical_Yearbook_2019-2020.pdf

López-López, M., Espadafor, M., Testi, L., Lorite, I. J., Orgaz, F., & Fereres, E.. (2018). Yield response of almond trees to transpiration deficits. Irrigation Science, 36(2), 111–120. https://doi.org/10.1007/s00271-018-0568-x

Maldera, F., Vivaldi, G. A., Iglesias-Castellarnau, I., & Camposeo, S.. (2021). Two Almond Cultivars Trained in a Super-High Density Orchard Show Different Growth, Yield Efficiencies and Damages by Mechanical Harvesting. Agronomy, 11(7), 1406. https://doi.org/10.3390/agronomy11071406

Martha A.K, Harbir. K, Luxin. W, Michelle D.D, Linda J. H; Survival of Salmonella, Escherichia coli O157:H7, and Listeria monocytogenes on Inoculated Almonds and Pistachios Stored at −19, 4, and 24°C. J Food Prot 1 August 2012; 75 (8): 1394–1403. doi: https://doi.org/10.4315/0362-028X.JFP-12-023

Mishra, D. S., & Goswami, A. K. (2016). High density planting in fruit crops. HortFlora Research Spectrum, 5(3), 261-264.

Morris, J. R. (1999). Developing mechanized systems for producing, harvesting, and handling brambles, strawberries, and grapes. Horttechnology, 9(1), 22-31.

Perry, E., Sibbett, G. S. (1998). Harvesting and Storing Your Home Orchard ' s Nut Crop : 8005, 1–9. Retrieved from http://homeorchard.ucdavis.edu/8005.pdf

Sargent, S. A., Takeda, F., Williamson, J. G., & Berry, A. D.. (2021). Harvest of Southern Highbush Blueberry with a Modified, Over-the-Row Mechanical Harvester: Use of Soft-Catch Surfaces to Minimize Impact Bruising. Agronomy, 11(7), 1412. https://doi.org/10.3390/agronomy11071412

Schatzki, T. F., Ong, M. S. (2001). Dependence of aflatoxin in almonds on the type and amount of insect damage. Journal of Agricultural and Food Chemistry, 49(9), 4513–4519. https://doi.org/10.1021/jf010585w